APPLICATIONS OF SINGULARITY THEORY

TO NEUROBIOLOGY

by

Isabel Salgado Labouriau

Being a thesis submitted to the University of Warwick for the degree of Doctor of Philosophy in August 1983.

To Melody = {Zé, Leo, Ricardo, Laura, Bev, Tom, Guillermo, Esteban, Des, Tony, Marcelo, Margarida, Isabel, Becky, Eduardo, Giorgio}.

CONTENTS

CHAPTER I : INTRODUCTION

1. BIOLOGY.

The nervous system of animals contains certain specialized cells, called nerve cells or neurones, that are responsible for the transmission of information within the animal's body. Those cells consist of an enlarged part containing the nucleus, and cytoplasmatic processes extending from if (Fig. I.1). The processes are classified by hystological and physiological criteria as axons or dendrites. Neurones of vertebrates usually have only one axon, and it rarely branches except at its termination.

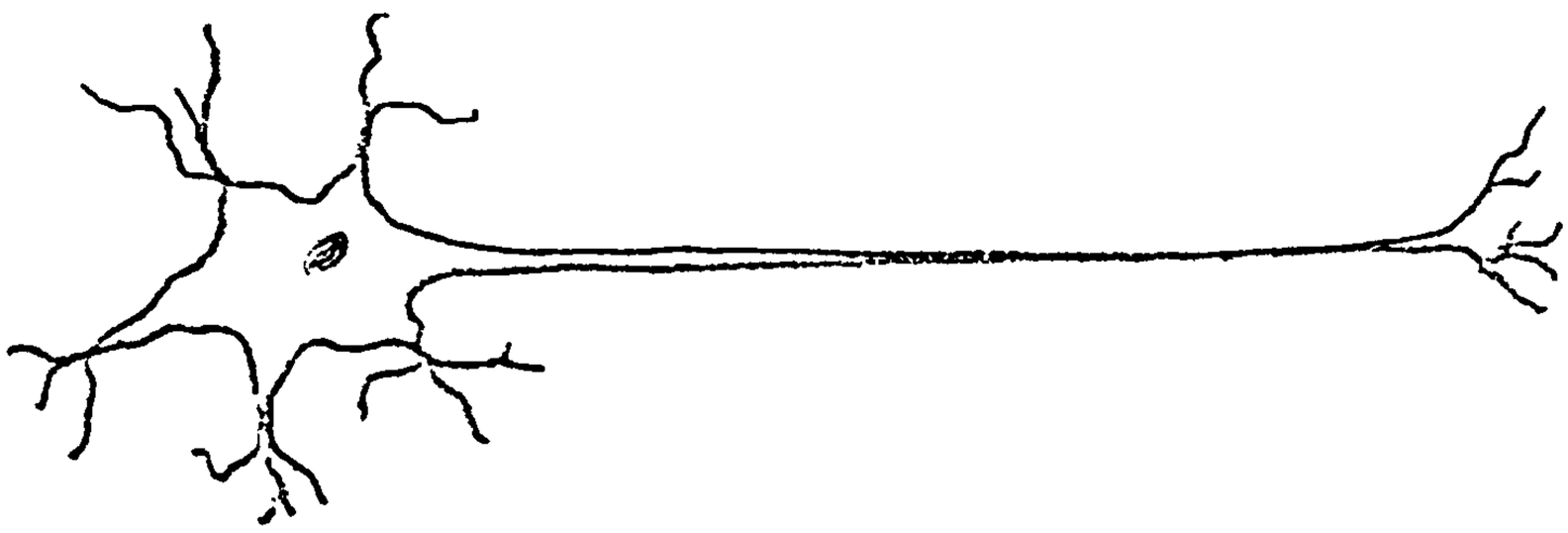

Fig. I.1 A "typical" neurone . The axon is the process extending to the right.

It has been known since the beginning of this century that the activity of neurones (and muscle fibres as well) is always accompanied by electrical changes. In 1952 Hodgkin, Huxley and Katz published a series of articles in which they used a new experimental technique of studying the electric activity of nerve cells, called *current* clamp. Using this technique they established a mechanism for the electrical activity of giant neurones of the squid [14] [15] [16] [17] [18] [19].

It is generally accepted that the same mechanism describes (qualitatively) the behaviour of nerve cells in other animals, and this has been extensively confirmed by experiments.

The physico-chemical model can be summarized as follows:

(1.1) The neurone is surrounded by a thin membrane which is selectively permeable to ions present in the physiological environment.

(1.2) The cell uses energy to keep the concentration of some of these ions, like Na^+, K^+, Cl^-, away from thermo-dynamical equilibrium, giving rise to a difference of electric potential across the membrane of the order of -70 mV, the inside of the cell being electronegative with respect to the outside. At this steady state the cell concentrates K^+ in its interior and pumps out Na^+.

(1.3) The activity of other nerve cells and other external factors, can induce fluctuations on the membrane potential. Depolarization of the membrane over a certain threshold value induces a quick increase of its permeability to Na^+, leading to further depolarization. After reaching a definite value the conductance of sodium decreases slowly.

(1.4) Depolarization also starts a slow increase in permeability to K^+ that moves out of the neurone, bringing the membrane potential back to rest.

(1.5) The depolarization flows as a capacitance current to nearby parts of the membrane, starting the same process at another point. This causes the depolarization wave to travel along the axon.

(1.6) These events take place uniformly around the circumference of the axon.

The series of events is called the nerve impulse. A quantitative version of this model was formulated in [17], and is known as the Hodgkin and Huxley equations. It consists of a reaction diffusion equation for the electrical potential V, coupled with three temperature dependent equations for ionic conductances.

Numerical solutions of the Hodgkin and Huxley equations fit the experimental results remarkably well. The main objection they find among biologists is due to the fact that there is no physiological interpretation for the ionic conductances m, n and h, and the equations they satisfy.

Although some general form of explanation is suggested in [17], direct experimental measurement of these variables is not possible. The only observable variable is V. For a discussion of this point see, for instance, [10] Chapter 2, and bibliography quoted there.

In a current clamp experiment V is made uniform over a length of axon. The response to suprathreshold stimulation is a stationary pulse. As the spatial dependence of V is eliminated the experiments are discribed by a system of autonomous differential equations, depending on the parameter I (stimulus intensity), and called the clamped Hodgkin and Huxley equations (see Section IV.0). From now on we shall omit the word clamped, and call them Hodgkin and Huxley equations or nerve impulse equations.

Under some circumstances, current clamped squid axoms respond to maintained stimulation with a train of voltage pulses that lasts until stimulation is withdrawn. This response, called repetitive firing was observed in other types of excitable cells. An example of particular importance is the activity of heart pace-makers.

Again in this case the Hodgkin and Huxley equations are in qualitative agreement with experiments - it can be shown [13], that they have periodic solutions for certain values of the parameter I. The periodic solutions have been studied numerically by Rinzel and Miller [25], whose

results are compared to experimental data in [11]. They appear as a pair of I-parametrized families of periodic solutions bifurcating off the steady state solution. We are concerned here with the topology of these solution branches, and their temperature dependence. We provide a topological explanation for Rinzel and Miller's numerical results by finding a hidden organizing centre for the recurring behaviour of the equations. We also obtain evidence of the existence of periodic solution branches not previously described in the literature.

The topology of periodic solution branches of the nerve impulse equations is highly sensitive to changes in the coefficients present in the equations, like the average ion permeabilities $\bar{g}_{Na}$, $\bar{g}_{k}$ (see IV.0). These numbers are obtained from experimental data, and therefore are necessarily likely to vary from cell to cell. As is the case for any set of phenomenological equations, the analysis of the sensitivity of the Hodgkin and Huxley equations to changes in the coefficients is relevant for an adequate comparison of theoretical prediction and experiment. This is critical in the case of nerve impulse, since the equations are expected to hold, with minor adaptation, for neurones of animals other than the squid, as well as for different types of excitable tissue. A suitable mathematical instrument for the analysis of perturbations of the nerve impulse equations is provided by singularity theory.

2. MATHEMATICS

A C^K version of the Hopf bifurcation theorem [20], [13] (IV.5) can be used to show that the Hodgkin and Huxley equations have periodic solutions for values of the control parameter I, and temperature T in some suitable intervals [12] [25]. For any temperature in that range, there exist two branches of periodic solutions that bifurcate from the equilibrium as I is varied.

Although the hypotheses in the Hopf theorem are generic [24], i.e. invariant under small perturbations and true for most choices of maps, when the differential equations depend on extra parameters, like the temperature in the nerve impulse equations, it is possible for some of these hypotheses to fail in a stable way. This is the case for the Hodgkin and Huxley equations. The present work aims at obtaining a qualitative description of those I-parametrized families of periodic solutions, when the equations are subject to small perturbations and imperfections.

The keyword in the last paragraph is *qualitative*. We take it to have the usual singularity theory interpretation of "invariant under appropriate changes of coordinates", in this case, changes of coordinares that preserve the topology of the I-parametrized periodic solution branches. This can be achieved by first restricting the problem to a Hilbert space of periodic functions, and then changing variables on each I-fibre, so that

the changes of variables depend smoothly on I.

The algebraic machinery of singularity theory can be used to describe in finite dimensional terms an arbitrary perturbation of a 1-parameter family of equations. In the case of parametrized families of germs†, under changes of variables that preserve a distinguished parameter, the singularity theory results have been developed in [8], [9], and in a more general setting, in [5]. The results can be applied to the case of germs of differential equations that satisfy some (but not necessarily all) of the hypotheses in the Hopf theorem [6]. In most cases, it allows us to determine the maximum number of parameters needed to describe all possible perturbations of a given problem, as well as the way in which the parameters should be inserted into the equations. In this way we can obtain a list of all possible inequivalent problems that may arise through perturbation of the original equations. This list can be determined if we know the numerical value of a finite number of derivatives of the right hand side of a differential equation.

The complexity of the nerve impulse equations (see IV.0!) rules out the possibility of obtaining the above mentioned

---

† The germ of a map f is the class of all maps that coincide with f in a neighbourhood of the origin.

information on its derivatives by direct calculation. For classification purposes, however, it is not necessary to compute their actual value. In all cases the equivalence classes are characterized by a set of derivatives that equal zero, and also by the sign of some of the non-zero derivatives. This information can be obtained numerically, with the zeros appearing as points where the derivative changes sign as some parameter in the equations is varied. We use FORTRAN programs to obtain estimates of those derivatives that are relevant for the classification.

3. ORGANIZATION

The results of [5], [6], [7], [8], that form the mathematical framework of generalized Hopf bifurcation germs, are stated without proof in Chapter II. We discuss the way the Liapunov-Schmidt reduction and singularity theory techniques can be used to obtain a classification of perturbations of local Hopf bifurcation problems that fail to satisfy some of the hypotheses in the classical Hopf theorem [20]. Chapter III contains a complete characterization of these problems under symmetry preserving equivalence, and up to codimension three. This taxonomy of low codimension germs includes, for each germ f, the defining conditions for f, the normal form of its universal unfolding, as well as a description of the critical set of unfolding parameters that correspond to the structurally unstable germs in the unfolding of f. We draw the critical set

near the origin, and bifurcation diagrams for an open dense subset of the set of all perturbations of f.

The defining conditions for equivalence to a given germ are computable, and in Appendix 1 we state the formulae, adapted from [6], that relate them to the derivatives of the original problem.

The mathematical machinery developed in Chapters II and III is applied to the nerve impulse in Chapter IV. We use FORTRAN programs (Appendix 1) to evaluate the formulae of Appendix 2, and find an organizing centre for the recurrent behaviour of the Hodgkin and Huxley equations. The effects of temperature are discussed and the equations are perturbed by varying the weight of sodium conductance. As a result, the perturbed Hodgkin and Huxley equations are shown to satisfy the defining conditions for equivalence to a member of a one-parameter family of generalized Hopf bifurcation germs. We have found a hidden organizing centre for the nerve impulse equations.

The concept of an organizing centre is discussed in Chapter V, where universal unfoldings are used to obtain diagrams for the bifurcation of periodic solutions of the perturbed Hodgkin and Huxley equations. Finally, we compare the results of Chapters IV and V to experiments and numerical tracings of periodic solutions by other authors.

All the results in this thesis are original, except where otherwise explicitly stated.

4. ACKNOWLEDGEMENTS

I am greatly indebted to Martin Golubitsky for suggestions, encouragement, and for granting me access to his manuscripts (literally), as well as to Ian Stewart for invaluable assistance in the process that changed a spectator's view of mathematics into that of an actor.

Thanks are also due to Maria Suzana de Carvalho for discussions on the Hopf theorem, to José Basto Gongalves who taught me FORTRAN, and to Ian Lidell who was always ready to show how to make a better use of the B6700.

Terri Moss performed the miracle of transforming a mass of handwriting into a thesis in almost no time.

This work was done with financial support from the Conselho Nacional de Desenvolvimento Científico e Tecnológico (CNPq) of Brazil. Additional support was provided by a grant from the Ministério das Relações Exteriores of Brazil, and sometimes by the Fundação Apolodoro Plausonio.

CHAPTER II : GENERALIZED HOPF BIFURCATION GERMS

0. INTRODUCTION

In this chapter we look at germs of vector fields, satisfying some of the hypotheses in the Hopf bifurcation theorem [20].

A germ

$$(0.1) \qquad F:\mathbb{R}^{n+1},(0,\lambda_0) \to \mathbb{R}^n,0$$

of a parametrized family of differential equations:

$$(0.2) \qquad \dot{v} = F(v,\lambda)$$

will be called a *generalized Hopf bifurcation germ* on $\mathbb{R}^n$ when

$$(0.3) \qquad F(0,\lambda) \equiv 0$$

and $d_vF(0,\lambda)$ has a pair of simple complex eigenvalues $\sigma(\lambda) \pm i\theta(\lambda)$ crossing the imaginary axis at λ_0, i.e.

$$(0.4) \qquad \sigma(\lambda_0) = 0, \ \theta(\lambda_0) = \theta_0 \neq 0.$$

We also require the derivative $d_vF(0,\lambda_0) = A$ to have no other eigenvalues of the form $ik\theta_0$ for integer k (non-resonance condition). This is part of the hypotheses in the Hopf theorem. We denote by H_n the class of all generalized Hopf bifurcation germs on $\mathbb{R}^n$, and when no ambiguity can arise we call such germs *Hopf bifurcation germs.*

In this chapter we outline the way Golubitsky and Langford [6] use the implicit function theorem to reduce the problem of finding periodic orbits of

$$\dot{v} = F(v,\lambda)$$

to the study of the bifurcation of the zeros of a map $r(F) : \mathbb{R}^2 \to \mathbb{R}$. The reduction is summarized in Table II.2.13. We give the usualy singularity theory definitions in a symmetry preserving context: equivalence, unfolding, codimension, etc., for the germs $r(F):\mathbb{R}^2 \to \mathbb{R}$, and we discuss the way these definitions can be pulled back to the original problem.

We are interested in periodic orbits of (0.2) with periods $\frac{2\pi}{\theta_0(1+\tau)}$ for small τ, that may appear near the *bifurcation point* $(0,\lambda_0)$. Rescaling time as

$$(10.5) \qquad t' = (1+\tau)t$$

we obtain orbits with period $\frac{2\pi}{\theta_0}$ in t'.

We can restrict our attention to the Banach spaces $C^1_{2\pi/\theta_0}$ and $C^o_{2\pi/\theta_0}$ of $\frac{2\pi}{\theta_0}$-periodic C^1 and C^o maps $u:\mathbb{R} \to \mathbb{R}^n$ (or $\mathbb{C}^n$), with the inner product:

$$(0.6) \qquad \langle u,v \rangle = \frac{\theta_0}{2\pi} \int_0^{2\pi/\theta_0} v^*(t)u(t)dt$$

where v^* is the (conjugate) transpose of v.

II.1. THE LIAPUNOV-SCHMIDT REDUCTION

A periodic solution of

$$(1.1) \qquad (1+\tau)\,\frac{dx}{dt'} = F(x,t')$$

is a zero of the non-linear operator

$$(1.2) \qquad F: C^1_{2\pi/\theta_0} \times \mathbb{R}^2 \to C^0_{2\pi/\theta_0}$$

$$F(u;\lambda,\tau) = (1+\tau)\,\frac{du}{dt} - F(u,\lambda).$$

Given $c,d \in \mathbb{C}^n$, eigenvectors of $A = d_v F(0,0)$ and A^* respectively, and chosen so that $dc = 2^{(\dagger)}$, define:

$$(1.3) \qquad \phi(t) = ce^{i\theta_0 t} \qquad \psi(t) = de^{i\theta_0 t}$$

$$(1.4) \qquad P: C^0_{2\pi/\theta_0} \to \text{kernel } (d_u F(0,\lambda_0,0)) = \text{span}_{\mathbb{R}} \{\text{Re}\,\phi\,, \text{Im}\phi\}$$

$$P(u) = \text{Re}\,[\langle u,\psi\rangle\phi]$$

(†) This normalization does not determine c and d, but it is enough to guarantee that P and Q are projections. We leave the choice of c to Chapter IV. The consequences of having this degree of freedom on c and d are discussed in Appendix 1.

(1.5) $$Q: C^{o}_{2\pi/\theta_0} \to \text{Image } [d_u F(0,\lambda_0,0)] =$$

$$= [\text{span}_{\mathbb{R}} \{\text{Re } \psi, \text{ Im } \psi\}]^{\perp}$$

$$Q = Id - P$$

(1.6) $$W = \{w \in C^{\perp}_{2\pi/\theta_0} : \langle w, \text{Re } \psi\rangle = \langle w, \text{Im}\psi\rangle = 0\} =$$

$$= Q(C^{1}_{2\pi/\theta_0}).$$

We notice that $C^{1}_{2\pi/\theta_0} = \text{span}_{\mathbb{R}} \{\text{Re } \phi, \text{ Im } \phi\} \oplus W$

and

$$C^{o}_{2\pi/\theta_0} = \text{span}_{\mathbb{R}} \{\text{Re}\phi, \text{Im}\phi\} \oplus [\text{span}_{\mathbb{R}} \{\text{Re } \psi, \text{ Im}\psi\}]^{\perp}.$$

Therefore we can decompose $v \in C^{o}_{2\pi/\theta_0}$, $u \in C^{\perp}_{2\pi/\theta_0}$ as

(1.7) $$u = x \text{ Re } \phi + y \text{ Im } \phi + w, \quad w \in W$$

$$v = \tilde{x} \text{ Re } \phi + \tilde{y} \text{ Im } \phi + \tilde{w}, \quad \langle \text{Re } \psi, \tilde{w}\rangle = 0$$

$$\langle \text{Im } \psi, \tilde{w}\rangle = 0.$$

The derivative $d_w(QF)(0,\lambda_0,0) = d_u F(0,\lambda_0,0)/W$ is invertible, so the implicit function theorem guarantees the existence of a unique map $w(x,y;\lambda,\tau)$ defined near $(0,0;\lambda_0,0)$ satisfying:

(1.8) $$QF(x \text{ Re } \phi + y \text{ Im } \phi + w(x,y;\lambda,\tau),\lambda,\tau) \equiv 0$$

and

(1.9) $$w(0,0;\lambda,\tau) \equiv 0.$$

This has reduced the problem of solving

$$F(u,\lambda,\tau) = 0,$$

an infinite-dimensional problem, to that of solving the finite dimensional equation:

$$f(x,y,\lambda,\tau) = jPF(x \text{ Re } f + y \text{ Im } f + w(x,y;\lambda),\tau),\lambda,\tau) = 0 \tag{1.10}$$

for x and y near 0, where j is the isomorphism:

$$j:\text{span}_{\mathbb{R}} \{\text{Re } \phi , \text{Im}\phi\} \to \mathbb{R}^2 \tag{1.11}$$

$$j(x \text{ Re } \phi + y \text{ Im } \phi) = (x,y).$$

II.2 ROTATIONAL SYMMETRY

If $u(t)$ is any solution of $\dot{u} = F(u,\lambda)$ for some λ, then $v_s(t) = u(t+s)$ is also a solution. Moreover if u is periodic, v_s will also be periodic of the same period p, and

$$v_p(t) = u(t) \quad \forall t. \tag{2.1}$$

Therefore, if we define, for each $\alpha \in \mathbb{R}$ the shift operator:

$$S_\alpha : C^i_{2\pi/\theta_0} \quad , \ i = 0,1$$

$$[S_\alpha u](t) = u(t-\alpha/\theta_0) \tag{2.2}$$

we have:

$$(2.3) \qquad F(u,\lambda,\tau) = 0 \iff F(S_\alpha u,\lambda,\tau) = 0.$$

It is easy to see that the operators S_α induce a representation of the group SO(2) of plane rotations on $C^i_{2\pi/\theta_0}$. Each S_α commutes with the projections P and Q, and satisfies

$$(2.4) \qquad \langle S_\alpha u, S_\alpha v\rangle = \langle u,v\rangle$$

thus leaving invariant the subspaces spanned by {Re ϕ, Im ϕ} and by {Re ψ, Im ψ}, as well as their orthogonal complements in $C^o_{2\pi/\theta_0}$ and $C^1_{2\pi/\theta_0}$.

The action of S_α on $\mathrm{span}_{\mathbb{R}}$ {Re ϕ, Im ϕ} induces the standard representation of SO(2) on $\mathbb{R}^2$. The map w defined in (1.8) commutes with the rotations S_α, as can be seen using a uniqueness argument. Therefore, for each λ and τ, we have:

$$(2.5) \qquad f(S_\alpha(x,y);\lambda,\tau) = S_\alpha f(x,y;\lambda,\tau).$$

Golubitsky and Schaeffer [7] use a result of Schwarz [27] to show that f can be written as:

$$(2.6) \qquad f(x,y,\lambda,\tau) = \binom{x}{y} p(x^2+y^2;\lambda,\tau) + \binom{-y}{x} q(x^2+y^2;\lambda,\tau),$$

and also that any periodic solution of (1.1) near the origin has the form:

$$(2.7) \qquad S_\alpha[x(\lambda,\tau)\ \mathrm{Re}\ \phi + w(x(\lambda,\tau),0;\lambda,\tau)]$$

where $x(\lambda,\tau)$ is a solution of

$$(2.8) \qquad f(x(\lambda,\tau),0;\lambda,\tau) = 0,$$

$$x(\lambda,\tau) > 0,$$

or, in coordinates:

$$(2.9) \qquad \begin{cases} x\ p(x^2;\lambda,\tau) = 0 \\ x\ q(x^2;\lambda,\tau) = 0 \end{cases}$$

The derivatives of the functions p and q with respect to τ can be computed from the definitions to be:

$$(2.10) \qquad \frac{\partial p}{\partial \tau}(0;0,0) = 0 \qquad \frac{\partial q}{\partial \tau}(0;0,0) = -1$$

A second application of the implicit function theorem yields a unique solution $\tau(x^2,\lambda)$ to the equation

$$(2.11) \qquad q(x^2;\lambda,\tau(x^2,\lambda)) \equiv 0.$$

Writing $a(x^2,\lambda) = p(x^2;\lambda,\tau(x^2,\lambda))$, the problem is now reduced to solving:

$$(2.12) \qquad [r(F)](x,\lambda) \overset{\text{def}}{=\!=} x\ a(x^2,\lambda) = 0.$$

A summary of the reduction process is given in Table II. 2.13.

TABLE II.2.13.

$F:\mathbb{R}^{n+1} \longrightarrow \mathbb{R}^n$		solve: $\dot{u} = F(u,\lambda)$, u periodic
$\downarrow$ $t' = (1+\tau)t$, $\tau \sim 0$		$\downarrow$
$F:C^1_{2\pi/\theta_0} \times \mathbb{R}^2 \to C^0_{2\pi/\theta_0}$	$F(u,\lambda,\tau) = (1+\tau)\frac{du}{dt} - F(u,\lambda) =$	$F(u,\lambda,\tau) = 0$
$\downarrow$ Liapunov-Schmidt reduction ($QF \equiv 0$)	$= PF + QF.$	$\downarrow$
$f:\mathbb{R}^4 \longrightarrow \mathbb{R}^2$	$f(x,y;\lambda,\tau) = jPF(x\ \mathrm{Re}\ \phi + y\ \mathrm{Im}\ \phi + w(x,y,\lambda,\tau),\lambda,\tau)$	$f(x,y;\lambda,\tau) = (0,0)$
$\downarrow$ SO(2) symmetry		$\downarrow$
$p,q:\mathbb{R}^2 \longrightarrow \mathbb{R}$	$f(x,y;\lambda,\tau) = \binom{x}{y} p(x^2+y^2,\lambda,\tau) + \binom{-y}{x} q(x^2+y^2,\lambda,\tau)$	$\begin{cases} x\ p(x^2,\lambda,\tau) = 0 \\ x\ q(x^2,\lambda,\tau) = 0 \end{cases}$
$\downarrow$ implicit function theorem ($q \equiv 0$)		$\downarrow$
$r(F):\mathbb{R}^2 \longrightarrow \mathbb{R}$	$a(x,\lambda) = p(x,\lambda,\tau(x,\lambda)$, $rF(x,\lambda) = xa(x^2,\lambda)$	$(rF)(x,\lambda) = 0$

II.3 $\mathbf{Z}_2$-EQUIVARIANT GERMS

The reduced germ r(F) constructed in Sections 1 and 2 is an odd function in x - this is what remains of the SO(2) symmetry. We reproduce here definitions and results from [7], [8] and [5] on the ring $\mathcal{E}^{\mathbb{Z}_2}$ of germs of odd functions:

$$(3.1) \qquad G:\mathbb{R}^2,0 \longrightarrow \mathbb{R},0$$

$$G(x,\lambda) = xa(x^2,\lambda)$$

also called $\mathbf{Z}_2$-*equivariant germs*. Those are standard results from singularity theory, adapted to the situation when there is one distinguished parameter λ [8], and $\mathbb{Z}_2$ symmetry [5] and [7]. The basic idea is to show that a large class of germs in $\mathcal{E}^{\mathbb{Z}_2}$ can be represented as polynomials in x and λ, and that all perturbations of germs in this class are represented by the universal unfolding, also a polynomial. In this context, represented means equivalent, under the following relation:

(3.2) Definition Two $\mathbb{Z}_2$ equivariant germs G and F are $\mathbf{Z}_2$-*equivalent* (denoted $F \sim_{\mathbb{Z}_2} G$) if and only if, for representatives $\tilde{G}$ and $\tilde{F}$ of G and F respectively we have

$$(3.2.1) \qquad \tilde{F}(x,\lambda) = T(x^2,\lambda)\ G(X(x^2,\lambda)x,\Lambda(\lambda)\lambda)$$

where $\quad T(0,0) \neq 0,\ X(0,0) > 0$ and $\Lambda(0) > 0$

with T, X and Λ C^∞ maps.

In what follows we shall often identify a germ and its representatives

(3.3) Definition A n-parameter $\mathbb{Z}_2$ *unfolding* of $\tilde{G} \in E^{\mathbb{Z}_2}$ is the germ of a function $F(x,\lambda,\alpha)$ satisfying:

(3.3.1) $F(x,\lambda,0) = G(x,\lambda)$

where G is a representative of $\tilde{G}$, and for each $\alpha \in \mathbb{R}^n$.

(3.3.2) $F_\alpha(x,\lambda) = F(x,\lambda,\alpha) \in E^{\mathbb{Z}_2}$.

(3.4) Definition Given F and H two $\mathbb{Z}_2$ unfoldings of $G \in E^{\mathbb{Z}_2}$ with m and n parameters respectively, F *is induced from* H if and only if there is a smooth map $A:\mathbb{R}^m \to \mathbb{R}^n$ such that, for each $\alpha \in \mathbb{R}^m$ fixed, near the origin, we have:

(3.4.1) $F_\alpha(x,\lambda) \sim_{\mathbb{Z}_2} H_{A(\alpha)}(x,\lambda)$.

(3.5) Definition An n-parameter $\mathbb{Z}_2$ unfolding F of $G \in E^{\mathbb{Z}_2}$ is *versal* if and only if every $\mathbb{Z}_2$ unfolding of G is induced from F. It is *universal* if and only if it is versal, and n is the smallest number of parameters for which a versal unfolding of G exists.

In order to obtain a universal $\mathbb{Z}_2$ unfolding of a germ G we remark, first, that the tangent space TG to the equivalence class

(3.6.1) $\mathcal{O}_G = \{\tilde{G} \in E^{\mathbb{Z}_2} : \tilde{G} \sim_{\mathbb{Z}_2} G\}$

is given by:

(3.6.2) $TG = \tilde{T}G + \{\Lambda(\lambda) \cdot \frac{\partial G}{\partial \lambda}\}$

where

$$\tilde{T}G = \{d_x G(X(x,\lambda)) + T(x,\lambda)G\}$$

with Λ, X and T as in Definition (3.2).

(3.7) Definition The $\mathbb{Z}_2$ *codimension* of a germ $G \in E^{\mathbb{Z}_2}$ is the dimension of $E^{\mathbb{Z}_2}/TG$ as a vector space over $\mathbb{R}$.

(3.7.1) Remark Golubitsky and Schaffer [7] [8] define a finite codimension germ as a germ G such that $E^{\mathbb{Z}_2}/\mathcal{O}_{TG}$ is finitely generated over $\mathbb{R}$, and define codimension for germs in this class, only. This distinction is made in order to prove Theorems (3.8) and (3.10). In a recent paper by Damon [5], however, both results are obtained without the extra assumption on G.

(3.8) Theorem [7] If $G \in E^{\mathbb{Z}_2}$ has finite codimension and $F(x,\lambda,\alpha)$ is an n-parameter unfolding of G, then F is a universal unfolding of G if and only if

(3.8.1) $$TG \oplus \operatorname{span}_{\mathbb{R}} \{\frac{\partial F}{\partial \alpha_i}(x,\lambda,0)\}_{i=1,\ldots,n} = E^{\mathbb{Z}_2}.$$

In this case n = codimension of G.

(3.9) Definition A germ $G \in \mathcal{E}^{\mathbb{Z}_2}$ is k-*determined* if every germ whose Taylor expansion at the origin of order k coincides with the Taylor expansion of order k of G is $\mathbb{Z}_2$ equivalent to G. It is *finitely determined* if it is k-determined for some k.

Clearly every finitely determined germ can be represented as a polynomial. What we need now is a characterization of finitely determined germs.

(3.10) Theorem If $G \in \mathcal{E}^{\mathbb{Z}_2}$ has finite codimension then G is finitely determined. In particular both G and its universal unfolding F_α are $\mathbb{Z}_2$-equivalent to polynomials in x and λ, and x, λ and α respectively.

(3.11) Theorem [6] If $G \in \mathcal{E}^{\mathbb{Z}_2}$ has $\mathbb{Z}_2$-codimension < 3, then G is $\mathbb{Z}_2$-equivalent to one of the germs H listed in Table II. 3.12 below:

Table II.3.12. Classification of $\mathbb{Z}_2$ equivariant germs.
Here ε, δ and $\phi = \pm 1$ and $V \subset E^{\mathbb{Z}_2}$ is such that $\text{span}_{\mathbb{R}} V + TG = E^{\mathbb{Z}_2}$.
Numbers in brackets (right) refer to the description in Chapter III.

H	cod H	V	No. in Ch. III
εx	0		(1.0)
$\varepsilon x^3 + \delta\lambda x$	0		(1.1)
$\varepsilon x^3 + \delta\lambda^2 x$	1	x	(1.2)
$\varepsilon x^5 + \delta\lambda x$	1	x^3	(1.3)
$\varepsilon x^3 + \delta\lambda^3 x$	2	λx, x	(1.4)
$\varepsilon x^7 + \delta\lambda x$	2	x^3, x^5	(1.5)
$\varepsilon x^3 + \delta\lambda^4 x$	3	$x, \lambda x, \lambda^2 x$	(1.6)
$\varepsilon x^9 + \delta\lambda x$	3	x^3, x^5, x^7	(1.7)
$\varepsilon x^5 + 2b\lambda x^3 + \delta\lambda^2 x$, $b^2 \neq \varepsilon\delta, b \neq 0$	3*	$x, x^3, \lambda x^3$	(2.1)
$\varepsilon x^5 + \delta\lambda^2 x$	3	$x, x^3, \lambda x^3$	(2.4)
$\phi x^7 + \varepsilon(x^5 + \lambda^2 x) + 2\delta\lambda x^3$	3	$x, x^3, \lambda x^3$	(2.6)
$\varepsilon x^5 + 2\delta\lambda x^3 + \phi\lambda^3 x$	3	$x, \lambda x, \lambda^2 x$	(2.7)
$\varepsilon x^7 + \delta\lambda x^3 + \phi\lambda^2 x$	3	x, x^3, x^5	(2.8)

(3.13) The hierarchy of $\mathbb{Z}_2$ equivariant germs of codimension < 3 is better illustrated by diagram II.3.14, where the germs appear arranged in codimension *strata*. The arrow F → G indicates that F is $\mathbb{Z}_2$ equivalent to a germ in the unfolding of G. Numbers in brackets refer to the pictures and more detailed description in Chapter III.

Diagram II.3.14. $\mathbb{Z}_2$-equivariant germs of low codimension. Numbers in brackets refer to Ch. III. See (3.16).

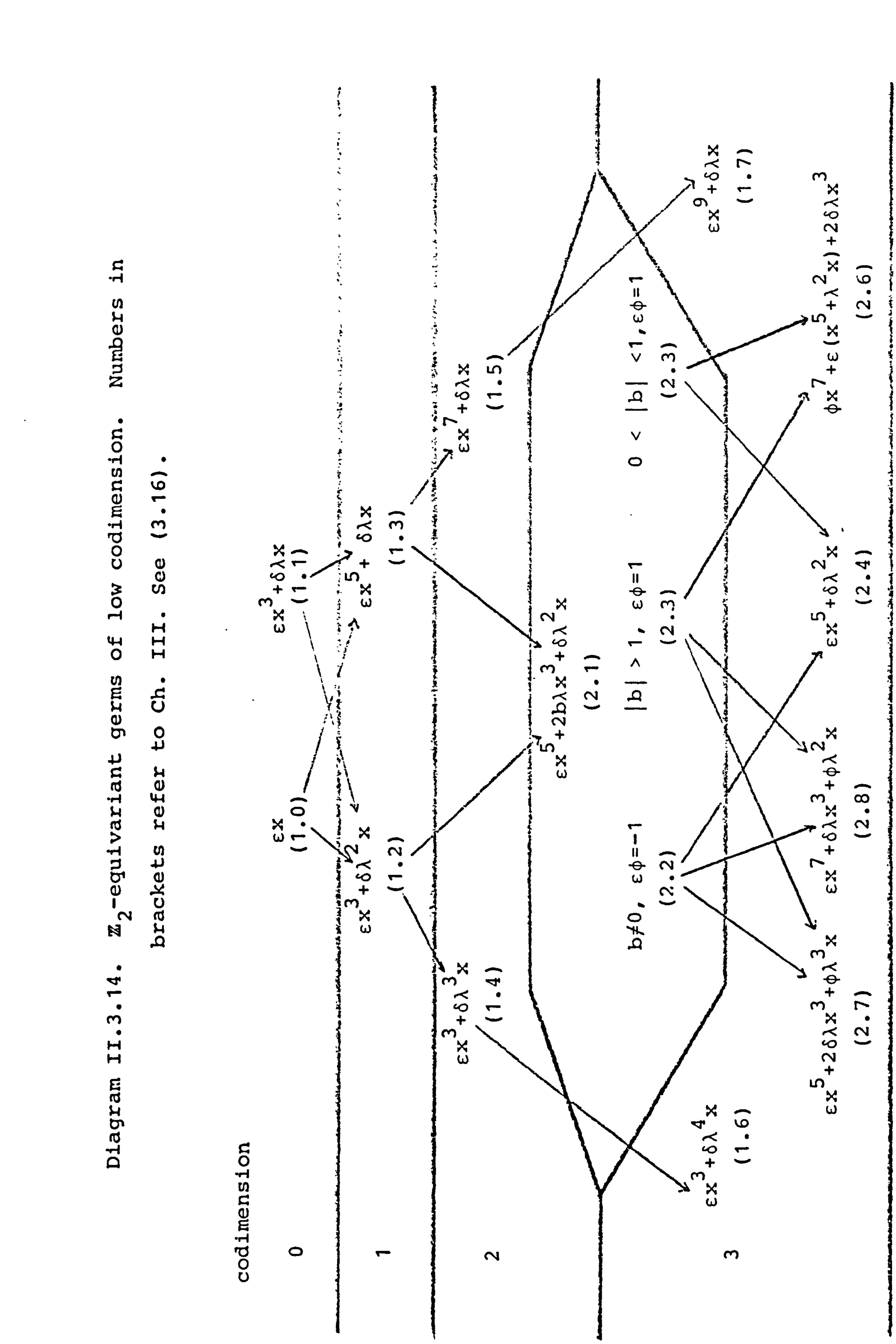

II.4. STRUCTURAL STABILITY

(4.1) Definition A germ $G \in E^{\mathbb{Z}_2}$ is *structurally stable* when its $\mathbb{Z}_2$ codimension is zero or, equivalently, when, for any n-parameter unfolding $F(x,\lambda,\alpha)$ of G there is a neighbourhood U of 0 in $\mathbb{R}^n$ such that $F_\alpha(x,\lambda) \sim_{\mathbb{Z}_2} G(x,\lambda)$ for all $\alpha \in U$.

There are only three examples of structurally stable $\mathbb{Z}_2$-equivariant germs, *viz.* cases (1.0) and (1.1) of Table II.3. When seen as reduced Hopf bifurcation germs, cases (1.1) represent the situation in the classical Hopf bifurcation theorem.$^{\oplus}$ In case (1.0) no bifurcation takes place.

(4.2) Definition A *bifurcation diagram* for a map $\tilde{G}:\mathbb{R}^2 \to \mathbb{R}$ is the set

$$(4.2.1) \qquad \{(x,\lambda):\tilde{G}(x,\lambda) = 0\}.$$

We shall also call the set (4.2.1) a bifurcation diagram for the germ of $\tilde{G}$.

$\oplus$ The hypotheses in the Hopf theorem are stable in a broader sense. See [24].

(4.3) Example: All bifurcation diagrams for the structurally stable germs in E^{Z_2} look like:

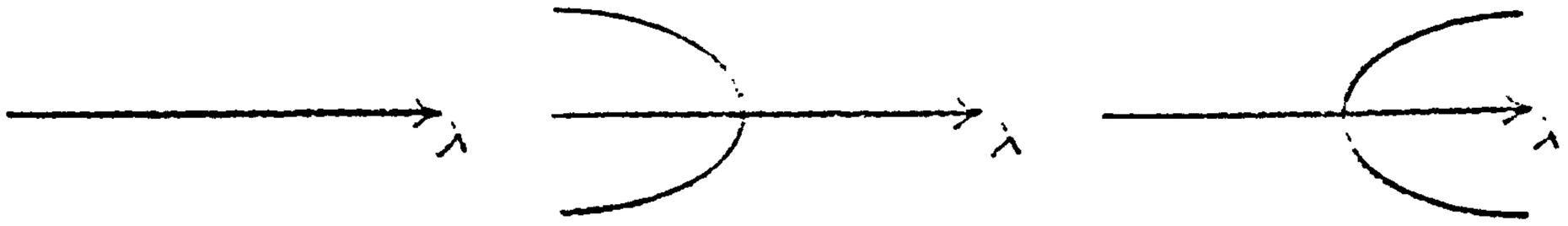

(1.0) (1.1), $\varepsilon\delta = 1$ (1.1) $\varepsilon\delta = -1$

where the ordinate is x and the abscissa is λ.

In order to study the bifurcation diagrams for unstable germs and their unfoldings, we shall shift our attention from germs to their representatives. The first step is to extend the definition of Z_2-equivalence to the new class:

(4.4) Definition. Let $v \subset \mathbb{R}^2$ be a neighbourhood of 0. Two Z_2-*equivariant maps* g and $h:U \to \mathbb{R}$ (i.e. two maps satisfying (3.1) for all $(x,\lambda) \in U$) are Z_2 *equivalent on* U (denoted $f \underset{U}{\sim} Z_2$ g) when they satisfy (3.2.1) for all $(x,\lambda) \in U$.

(4.5) Definition. If $F(x,\lambda,\alpha)$ is an n-parameter unfolding of $G \in E^{Z_2}$, $U \subset \mathbb{R}^2$, $V \subset \mathbb{R}^n$ are neighbourhood of zero, $f:U \times V \to \mathbb{R}$ is a representative of F, and $U' \subset U$, we say that $\alpha \in V$ is (f,U')-*stable* when $f_\alpha \underset{U'}{\sim} Z_2 f_\beta$ for all β near α. Otherwise α is said to be (f,U') *unstable*. The bifurcation diagram f_α is U'-*stable* when α is (f,U')-stable.

The problem of describing all the different U-stable bifurcation diagrams for a representative of an unfolding of a Z_2-equivariant germ is simplified by the following result:

(4.6) Theorem [9]

Let F be an n parameter unfolding of $G \in \mathcal{E}^{Z_2}$, and $f(x,\lambda,\alpha) = x\,A(x^2,\lambda,\alpha)$; $A: U \times V \to \mathbb{R}$ a representative of F, where $U \subset \mathbb{R}^2$, $V \subset \mathbb{R}^n$ are neighbourhoods of the origin. Then there exist neighbourhoods S, L and V' of the origin in $\mathbb{R}$, $\mathbb{R}$ and $\mathbb{R}^n$ respectively such that α is $(f, S \times L)$-stable for all $\alpha \in V' - \Sigma$, where Σ is the union of the 6 critical sets below:

$$H_0 = \{\alpha: \exists\, \lambda : A(0,\lambda,\alpha) = A_u(0,\lambda,\alpha) = 0\}$$

$$B_0 = \{\alpha: \exists\, \lambda : A(0,\lambda,\alpha) = A_\lambda(0,\lambda,\alpha) = 0\}$$

$$DL_0 = \{\alpha: \exists\, \lambda,\ \exists\, u > 0 : A_u(0,\lambda,\alpha) = A(u,\lambda,\alpha) = A_u(u,\lambda,\alpha) = 0\}$$

$$H_1 = \{\alpha: \exists\, \lambda,\ \exists\, u > 0 : A(u,\lambda,\alpha) = A_u(u,\lambda,\alpha) = A_{uu}(u,\lambda,\alpha) = 0\}$$

$$B_1 = \{\alpha: \exists\, \lambda,\ \exists\, u > 0 : A(u,\lambda,\alpha) = A_u(u,\lambda,\alpha) = A_\lambda(u,\lambda,\alpha) = 0\}$$

$$DL_1 = \{\alpha: \exists\, \lambda,\ \exists\, w > u > 0 : A(u,\lambda,\alpha) = A(w,\lambda,\alpha) = A_u(u,\lambda,\alpha) = A_u(w,\lambda,\alpha) = 0\}.$$

Here $u = x^2$, $A_u = \frac{\partial A}{\partial u}$, $A_\lambda = \frac{\partial A}{\partial \lambda}$ and $A_{uu} = \frac{\partial^2 A}{\partial u^2}$.

The proofs of (4.6) and (4.7) follow closely those of the analogous results in [8], where germs of maps $g:\mathbb{R}^{n+1} \to \mathbb{R}^n$ are studied without the assumption of $\mathbb{Z}_2$-equivariance. The introduction of symmetry only modifies the stability conditions at $x = 0$.

The sets $B_0 \cup B_1$, $H_0 \cup H_1$ and $DL_0 \cup DL_1$ are called, respectively, *bifurcation*, *hysteresis* and double *limit* sets. Their union, Σ, is sometimes called *the* critical set.

(4.7) Corollary. Let $f_\alpha: U \times V \to \mathbb{R}$, S, L and V' be as in Theorem (4.6). If α and β are in the same connected component of $V' - \Sigma$ then f_α is $\mathbb{Z}_2$-equivalent to f_β on $S \times T$.

Typical bifurcation diagrams for f_α when α is (f,U)-unstable are shown in Fig. II.4.8. Those for stable maps, however, are subject to less variation. Indeed, for any representative $f: U \to \mathbb{R}$ of an unfolding of a $\mathbb{Z}_2$-equivariant germ, we can write

$$f_\alpha(x,\lambda) = x\, a_\alpha(x^2,\lambda),$$

and if α is (f,U)-stable there are four possibilities for a solution (u_0,λ_0) of $f_\alpha = 0$, where $u = x^2$:

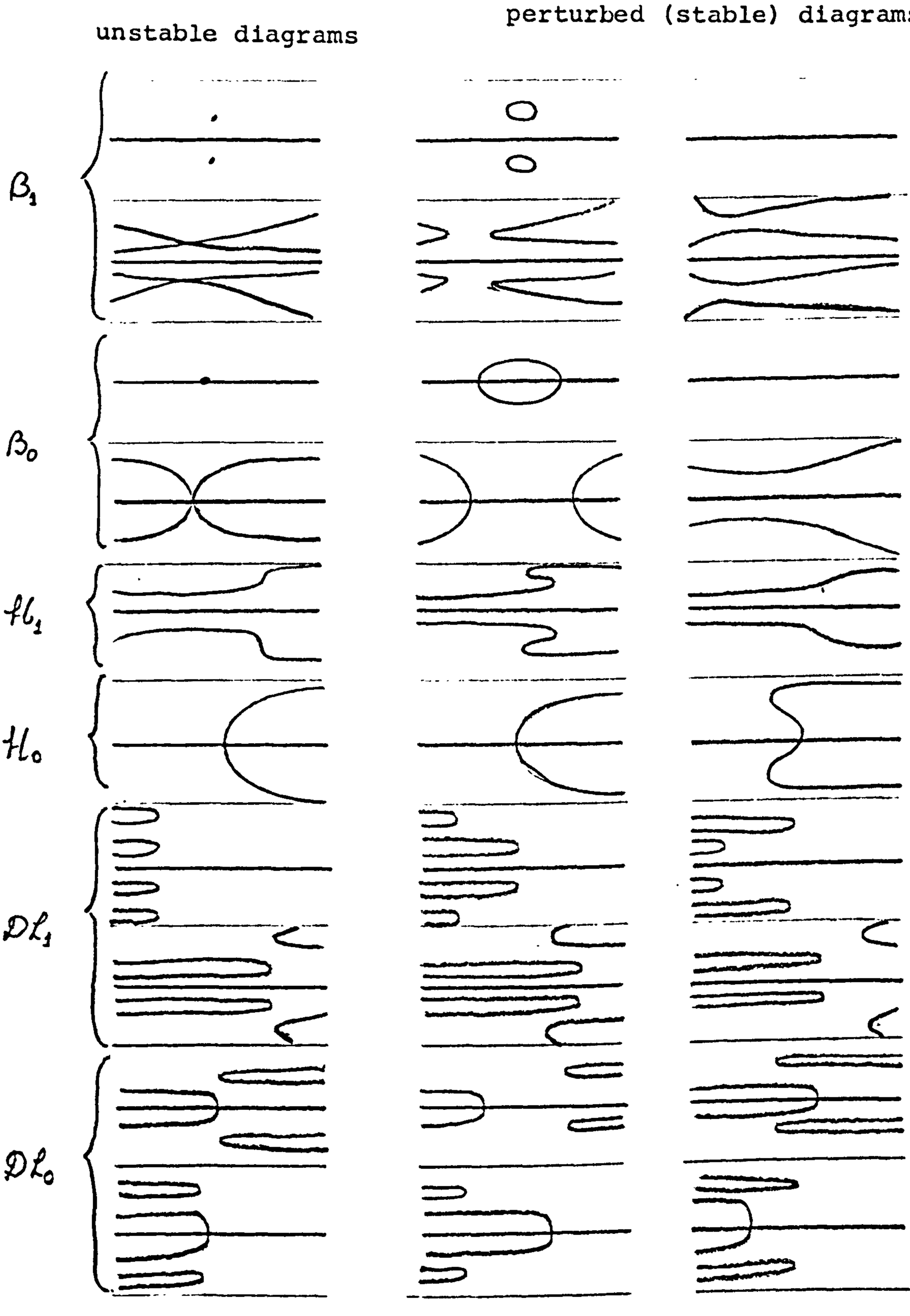

Fig. II.4.8 Bifurcation diagrams for f_α, when α is in a critical set (II. 4.6). Ordinate = x, abcissa = λ.

(4.9.1) $u_0 = x_0^2 = 0$, $a_\alpha(0,\lambda_0) \neq 0$. In some suitable neighbourhood of (x_0,λ_0) the only solution of $f(x,\lambda) = 0$ is $x = 0$. Locally the bifurcation diagram looks like (1.0) (see (4.3)).

(4.9.2) $u_0 = x_0^2 = 0$, $a_\alpha(0,\lambda_0) = 0$. Because α is (f,U)-stable we have

$$\frac{\partial a_\alpha}{\partial u}(0,\lambda_0) \neq 0 \text{ and } \frac{\partial a_\alpha}{\partial \lambda}(0,\lambda_0) \neq 0.$$

The implicit function theorem guarantees the existence of a unique solution $u(\lambda)$ for $a(u(\lambda),\lambda) = 0$ in some neighbourhood of $(0,\lambda_0)$, with $u(\lambda_0) = 0$. Moreover, $u'(0) \neq 0$, and thus the solution $u(\lambda)$ is positive for λ in some interval $(\lambda_0,\lambda_0 + \varepsilon)$ or $(\lambda_0-\varepsilon,\lambda_0)$, with $\varepsilon > 0$ small, and $x(\lambda) = \pm\sqrt{u(\lambda)}$ are two well defined solutions of $f_\alpha = 0$ in one of the intervals mentioned above, with a common vertical tangent at $\lambda = \lambda_0$. In this case the point $(0,\lambda_0)$ is called a *stable branching point*. Around $(0,\lambda_0)$ the bifurcation diagram for f_α looks like one of cases (1.1) (see (4.3)).

(4.9.3) $u_0 = x_0^2 \neq 0$, $a_\alpha(u_0,\lambda_0) = 0$ and $\frac{\partial a_\alpha}{\partial u}(u_0,\lambda_0) \neq 0$.

Again, there exists locally a unique solution $u(\lambda)$ for $a_\alpha(u(\lambda),\lambda) = 0$, with $u(\lambda_0) = x_0^2$. Since $x_0^2 > 0$, $u(\lambda)$ remains positive in some interval $(\lambda_0-\varepsilon,\lambda_0+\varepsilon)$, where the solutions $x(\lambda) = \pm\sqrt{u(\lambda)}$ are well defined.

(4.9.4) $u_0 = x_0^2 \neq 0$, $a_\alpha(u_0,\lambda_0) = 0 = \frac{\partial a_\alpha}{\partial u}(u_0,\lambda_0)$,

and since α is (f,U)-stable, both $\frac{\partial a_\alpha}{\partial \lambda}(u_0,\lambda_0) \neq 0$ and $\frac{\partial^2 a_\alpha}{\partial u^2}(u_0,\lambda_0) \neq 0$. The unique solution is $\lambda(x^2)$ with $\lambda(x_0^2) = \lambda_0$ and $\lambda'(u_0) = 0$. We call (x_0,λ_0) a *stable fold point*. Bifurcation diagrams near a stable fold point look like:

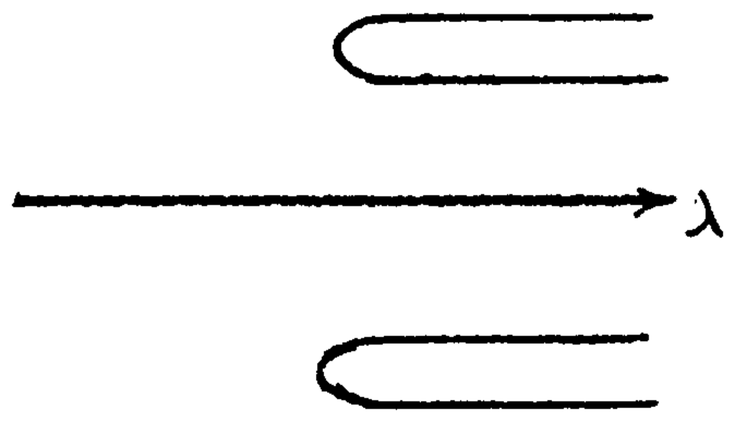

Thus we have established:

(4.10) Proposition. Let $f:U \times V \to \mathbb{R}$, $U \subset \mathbb{R}^2$, $V \subset \mathbb{R}^n$ be a representative of the universal unfolding of a $\mathbb{Z}_2$ equivariant germ of codimension n. If $\alpha \in V$ is (f,U)-stable, then the bifurcation diagram for f_α is constituted by the following components:

(4.10.1) The line $x = 0$

(4.10.2) A finite number (possibly zero) of solution curves for $a_\alpha(x^2,\lambda) = 0$, crossing the line $x = 0$ at different stable branching points.

(4.10.3) A finite number (possibly zero) of isolated solution curves for $a_\alpha(x^2,\lambda) = 0$, i.e. curves that do not intersect the $x = 0$ line inside the domain of f_α.

The curves mentioned in (4.10.2) and (4.10.3) may also have a finite number of stable fold points. For each value of λ there is at most one stable branching point $(0,\lambda)$ or one pair of stable fold points $(\pm x,\lambda)$, $x \neq 0$. Thus the diagrams look like:

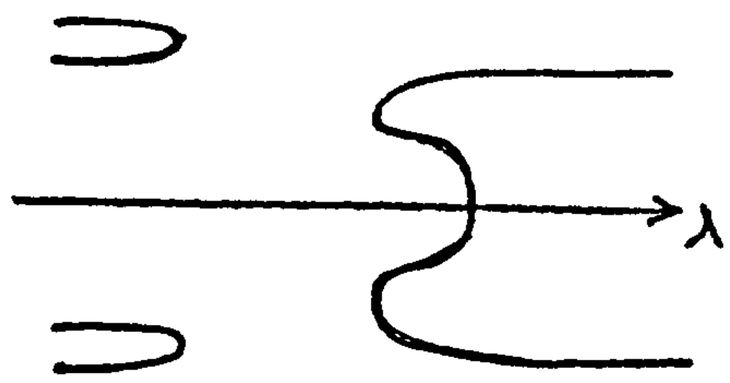

Proposition (4.10) is a direct consequence of the observations (4.9). The finite number of curves in (4.10.2) and (4.10.3) and of folds are a consequence of the representation of any finite-codimension germ as a polynomial. Finally, fold points and branching points cannot appear for the same value of λ, in order to avoid the double limit set.

(II) 5. ASYMPTOTIC STABILITY

Every reduction carries with it some loss of information. The one described in Sections 0 to 2 is no exception - all the dynamics of the non periodic orbits is ignored when the problem is restricted to the space $C^i_{2\pi/\theta_o}$ of periodic solutions. Nevertheless, if the reduced germ is stable, the classical Hopf bifurcation theorem may be used to give some insight into the behaviour of other orbits. In other words, the information we have lost is redundant. To see this we start, as usual, by introducing new terminology.

(5.1) Notation. Let $F:\mathbb{R}^n \to \mathbb{R}^n$ be a C^k map, $k \geq 4$, and denote by $\eta(t,x)$, the solution of

$$(5.1.1) \qquad \frac{d\eta}{dt} = F(\eta), \quad \eta(0,x) = x.$$

Suppose $x_o \in \mathbb{R}^n$ is such that $\eta(t,x_o)$ is periodic in t (with period possibly zero), and denote by $0(x_o)$ the image of $\eta(t,x_o)$.

(5.2) Definition. $\eta(t,x_o)$ (or $0(x_o)$) is *asymptotically stable* for F if and only if there is a neighbourhood U of $0(x_o)$ such that if $x \in U$ then

$$(5.2.1) \quad \lim_{t\to\infty} d(\eta(t,x),\ 0(x_o)) = 0$$

where d is the distance from the point $\eta(t,x)$ to the compact set $0(x_o)$. It is *asymptotically unstable* for F when (5.2.1) holds as $t \to -\infty$.

(5.3) Definition. The *basin of attraction* of an asymptotically stable orbit $0(x_o)$ is the set of points x for which (5.2.1) holds.

We can now state a C^k version of the Hopf theorem. The form we use is a variant from the versions in [13] and [24].

(5.4) Theorem: Let $F:U \to \mathbb{R}^n$ be a C^k map ($k \geq 4$) on $U \subset \mathbb{R}^{n+1}$ a neighbourhood of $(0,\lambda_o)$, satisfying the conditions in the definition of a generalized Hopf bifurcation germ (see Section 0). Suppose f satisfies the non-degeneracy condition:

(5.4.1) $\sigma'(\lambda_o) \neq 0$ where σ is as defined in (0.4).

Then the equation

(5.4.1.1) $\dot{v} = F(v,\lambda)$

has a family of periodic solutions, unique in some neighbourhood $I \times S$ of $(0,\lambda_o)$. In more precise terms, there exist open sets $S \subset \mathbb{R}^n$ and $I \subset \mathbb{R}$, with $0 \in S$ and $\lambda_o \in I$, and there exists $\varepsilon_o > 0$ and a C^{k+1} function

$$\lambda:(0,\varepsilon_o) \to I$$

such that $\lambda(0) = \lambda_o$, and for all $\varepsilon \in (0,\varepsilon_o)$ equations (5.4.1.1) have a nonzero periodic solution for $\lambda = \lambda(\varepsilon)$. There are no other periodic solutions of (5.4.1.1) in $I \times S$, except for the constant solution $x = 0$.

(5.4.2) If in addition we suppose that the bifurcation point $(0,\lambda_o)$ is asymptotically stable, and that the function $\lambda(\varepsilon)$ is an embedding,

then the points $(0,\lambda(\varepsilon))$ are not stable, and each periodic orbit is asymptotically stable.

(5.4.3) If n = 2 and (5.4.2) holds, then the basin of attraction of each periodic solution is S - {0}

Without loss of generality we may suppose $\lambda(\varepsilon) \geq \lambda_o$ for all $\varepsilon \in (0,\varepsilon_o)$. In this case the steady state $(0,\lambda)$ is asymptotically unstable for $\lambda > \lambda_0$, and asymptotically stable for $\lambda \leq \lambda_o$, with basin of attraction S.

(5.4.4) When n > 2, (5.4.2) holds, and all eigenvalues of $d_vF(0,\lambda_o)$ have strictly negative real parts, except for the pair in the hypothesis, the basin of attraction of each periodic solution is S - M_λ (see figure on next page), where M_λ is a n-2 dimensional submanifold of $\mathbb{R}^n$ (the stable manifold for F, [22]). The manifold M_λ is tangent at $(0,\lambda)$ to the eigenspace corresponding to the eigenvalues of $d_uF(0,\lambda)$ that are not in the curve $\sigma(\lambda) \pm i\theta(\lambda)$. Solutions of (5.4.1.1) starting on M_λ remain on M_λ for all t, (i.e. M_λ is invariant) and approach $(0,\lambda)$ as $t \to \infty$.

Remark. (5.4.3) and (5.4.4) do not usually appear in the statement of the Hopf theorem. The first is a direct consequence of the Poincaré-Bendixson theorem, the second can be seen using the results of Chafee [4] and the unicity of solutions. A more detailed discussion can be found in [3].

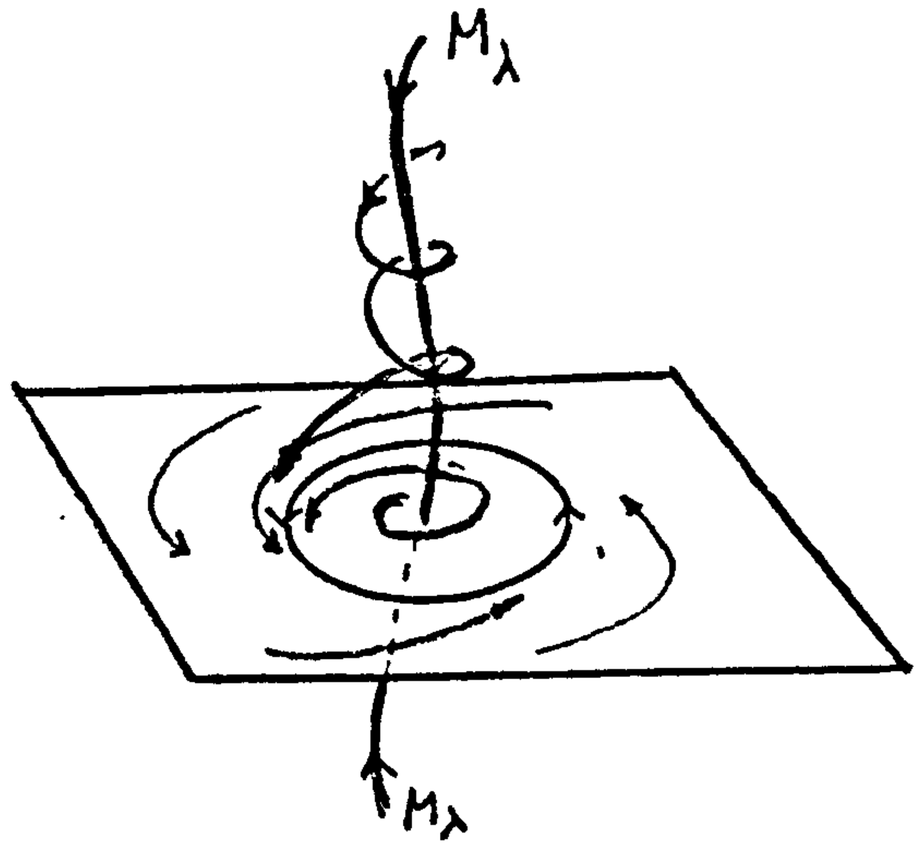

It can be shown [6] that hypothesis (5.4.1) is satisfied by all generalized Hopf bifurcation germs that are $\mathbb{Z}_2$ equivalent, after reduction to (III.1.1) (see Table II.3.12), since, for a reduced germ $r(F)(x,\lambda) = xa(x^2,\lambda)$ we have

$$\theta'(\lambda_o) = \frac{\partial a}{\partial \lambda}(0,\lambda_o) = a_\lambda .$$

If in addition we have

$$\frac{\partial a}{\partial u}(0,\lambda_o) \neq 0 \text{ for } u = x^2,$$

then the function $\lambda(\varepsilon)$ of Theorem (5.4) is invertible.

Assuming that $(0,\lambda_o)$ is asymptotically stable and if $n > 2$ that all other eigenvalues of $d_vF(0,\lambda_o)$ have negative real parts, and if $(0,\lambda_o)$ is a stable branching point (4.9.2) of r(F), then F satisfies conditions (5.4.3) or (5.4.4). In this case all the conclusions of (5.4) are true for F.

The assumptions above on the eigenvalues of $d_vF(0,\lambda_o)$ are quite mild - a necessary condition for the asymptotic stability of $(0,\lambda_o)$ is that all the eigenvalues of $d_vF(0,\lambda_o)$ have real parts that are ≤ 0. It is also clear that the neighbourhood to which (5.4) can be applied cannot contain any fold points or isolated periodic orbits. In order to extend the asymptotic stability assignments to any stable bifurcation diagram we use the Centre Manifold theorem [22], that guarantees the existence of a λ-parametrized family of asymptotically stable 2-dimensional manifolds B_λ. The centre manifolds B_λ are F-invariant and therefore contain all the periodic solutions of $\dot{v} = F(v,\lambda)$ that intersect the basin of attraction of B_λ. For the remainder of this chapter we shall suppose the system reduced to the Centre Manifold, and therefore $F \in H_2$. For proofs and discussion of the Centre Manifold Theorem in a Hopf bifurcation context see [13] [24].

The reduction to two dimensions is not sufficient in itself to extend the stability assignments to bifurcation diagrams containing isolated solution branches and folds, because we cannot rule out the existence, away from $(0,\lambda_o)$, of periodic solutions of (5.4.1.1) having a period bounded away from $2\pi/\theta_o$. Such periodic orbits would not appear as zeros of the reduced germ r(F). In Fig. II.5.5 we indicate the way in which the presence of an undetected solution branch (dotted line) may affect the stability assignments in a bifurcation diagram. The direction of the flow is indicated by the vertical arrows.

Fig II.5.5

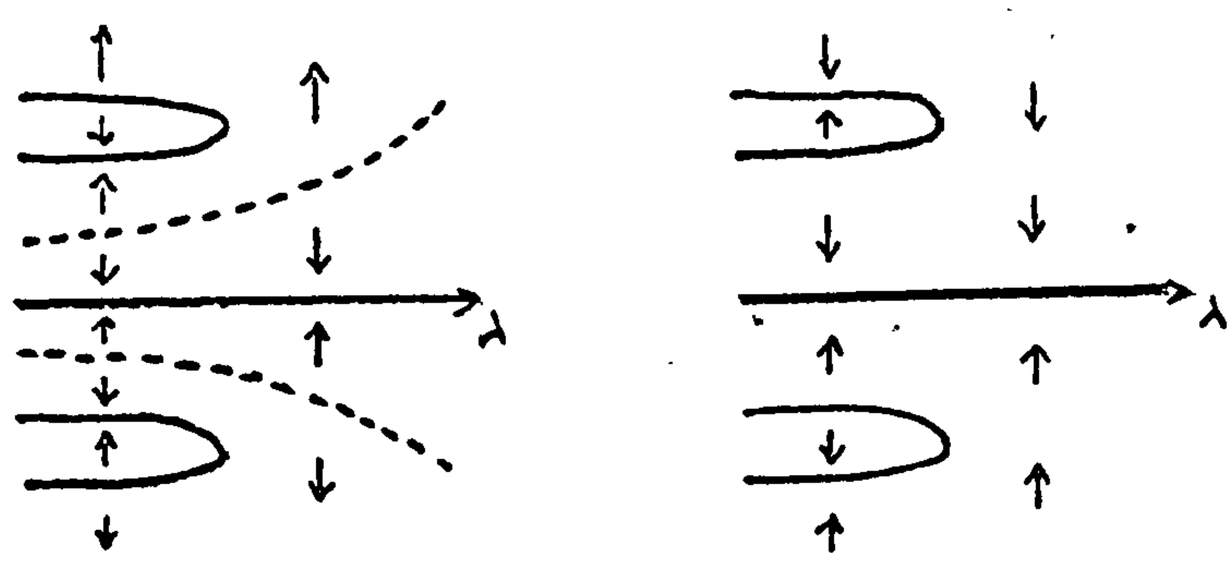

On stable diagrams occurring in the unfolding of a finite codimension $\mathbb{Z}_2$-equivariant germ, isolated solution branches and folds are created when unfolding parameters cross the critical sets B_1 and $H_0 \cup H_1$ respectively. For folds a continuity argument shows that we can indeed extend the conclusions about the asymptotic stability of solutions by deforming the diagram into one without folds, as in Fig. II.5.6a.

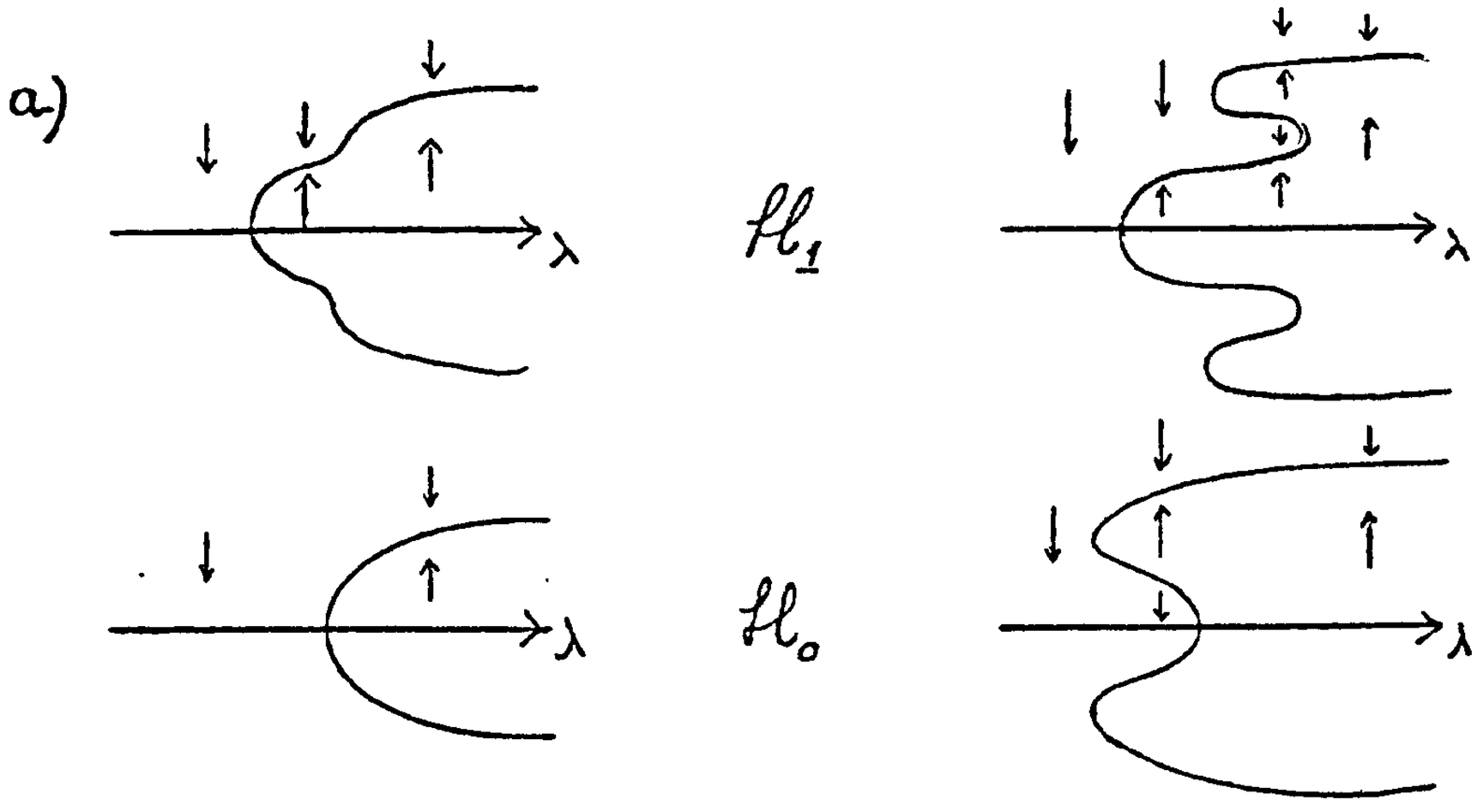

Fig. II.5.6 Asymptotic stability assignments across the critical set.

Crossing B_1 has either the effect of splitting an existing solution branch into two, as is illustrated in Fig. II.5.6b, or that of creating an altogether new solution branch (Fig. II.5.6c). The two types of behaviour correspond to points α in the unfolding where the surface $\{(u,\lambda, A(u,\lambda,\alpha)), u > 0\} \subset \mathbb{R}^3$ has positive (Fig. II.5.6c) or negative (Fig. II.5.6b) Gaussian curvature. This divides B_1 into two clearly defined sectors, B_1^+ and B_1^- where the $\pm$ sign corresponds to that of the Gaussian curvature.

When a diagram is moved across B_1 asymptotic stability of orbits can be decided with continuity arguments as illustrated in Fig. II.5.6b, whereas for solution branches appearing at a B_1^+ crossing it is not possible to decide the direction of flow everywhere (Fig. II.5.6c). However, if B_1^+ has no self intersections it is possible to decide the stability of all solution branches, because any region (i.e. component of $\mathbb{R}^n - \Sigma$) can be reached without passing through B_1^+. This is found to be the case (by inspection of the geometry of the critical sets) for all Z_2 equivariant germs of codimension smaller than 4, as will be seen in the next chapter.

CHAPTER III : PICTURES OF DEGENERATE HOPF BIFURCATIONS.

0. INTRODUCTION

In this chapter we describe the universal unfoldings of low (≤ 3) codimension $\mathbb{Z}_2$-equivariant bifurcation problems:

$$xa(x^2,\lambda) = 0 \tag{0.1}$$

i.e. reduced *generalized* Hopf bifurcation germs.

In each case we state conditions that a germ $\tilde{a}$ must satisfy to be $\mathbf{Z}$-equivalent to a. These, called *defining conditions*, are given in terms of the derivatives of $\tilde{a}$ at the bifurcation point, which we take to be $\lambda_c = 0$. We also draw the set $\{(x,\lambda);\ xa(x^2,\lambda) = 0\}$, called a *bifurcation diagram* for a. Since all bifurcation diagrams are symmetric with respect to reflection around the $x = 0$ axis, we only sketch the part falling into the $x \geq 0$ half-plane. Bifurcation diagrams are always represented with λ on the horizontal axis, x on the vertical. In all cases we *omit* the x (vertical) axis. Since $x = 0$ is always a solution of (0.1) the horizontal axis is always drawn. In this way the bifurcation diagrams can be interpreted as amplitude diagrams for the periodic solutions of a *generalized* Hopf bifurcation germ.

The cases where there is only a finite number of $\mathbb{Z}_2$-orbits in a neighbourhood of zero on the unfolding of a, are grouped in Section 1. Germs having this property are called *simple* or *0-modal*. The bifurcation diagrams for the simple germs of codimension ≤ 2 were first described in [6].

In Section 2 a 1-parameter family of topologically equivalent codimension 3 germs is described, as well as the codimension 3 germs that contain this family in their unfolding. These germs are called *1-modal* or *unimodal*. Part of the description of the 1-parameter family (2.1) appears in [6] where it is also shown that the germs described in this chapter form a complete list of $\mathbb{Z}_2$-equivariant germs of codimension ≤ 3.

(0.1) Notation

The remainder of this chapter analyses the geometry of the $\mathbb{Z}_2$-equivariant germs listed in Tables III.3.1 and III.3.2. In each case we study a function $xa(x^2,\lambda)$, with universal unfolding $xA(x^2,\lambda,\alpha,\beta,\gamma)$. In order to avoid repetition we give here a list of symbols:

$u = x^2$

$\phi,\varepsilon,\delta = \pm 1$

α,β,γ will always be unfolding parameters.

Asymptotically unstable branches are always represented as dotted lines on the diagrams.

We also use the notation:

$$a_u = \frac{\partial a}{\partial u}(0,0) \qquad a_u(u,\lambda) = \frac{\partial a}{\partial u}(u,\lambda)$$

$$a_{\lambda u} = \frac{\partial^2 a}{\partial \lambda \partial u}(0,0) \ .$$

and analogous definitions for the other partial derivatives with respect to λ and u.

1. SIMPLE GERMS

(1.1) Organizing centre:

$$a(u,\lambda) = \varepsilon u + \delta\lambda$$

$\mathbb{Z}_2$-codimension = 0 (non-degenerate case)

Defining conditions: $a_u \neq 0$, $a_\lambda \neq 0$

Bifurcation diagrams are shown in Fig. 1.1.

(1.2) Organizing centre:

$$a(u,\lambda) = \varepsilon u + \delta\lambda^2$$

$\mathbb{Z}_2$-codimension = 1

Defining conditions: $a_\lambda = 0$

$a_u \neq 0$, $a_{\lambda\lambda} \neq 0$

Fig III.1.1 — Classical Hopf bifurcation (1.1)

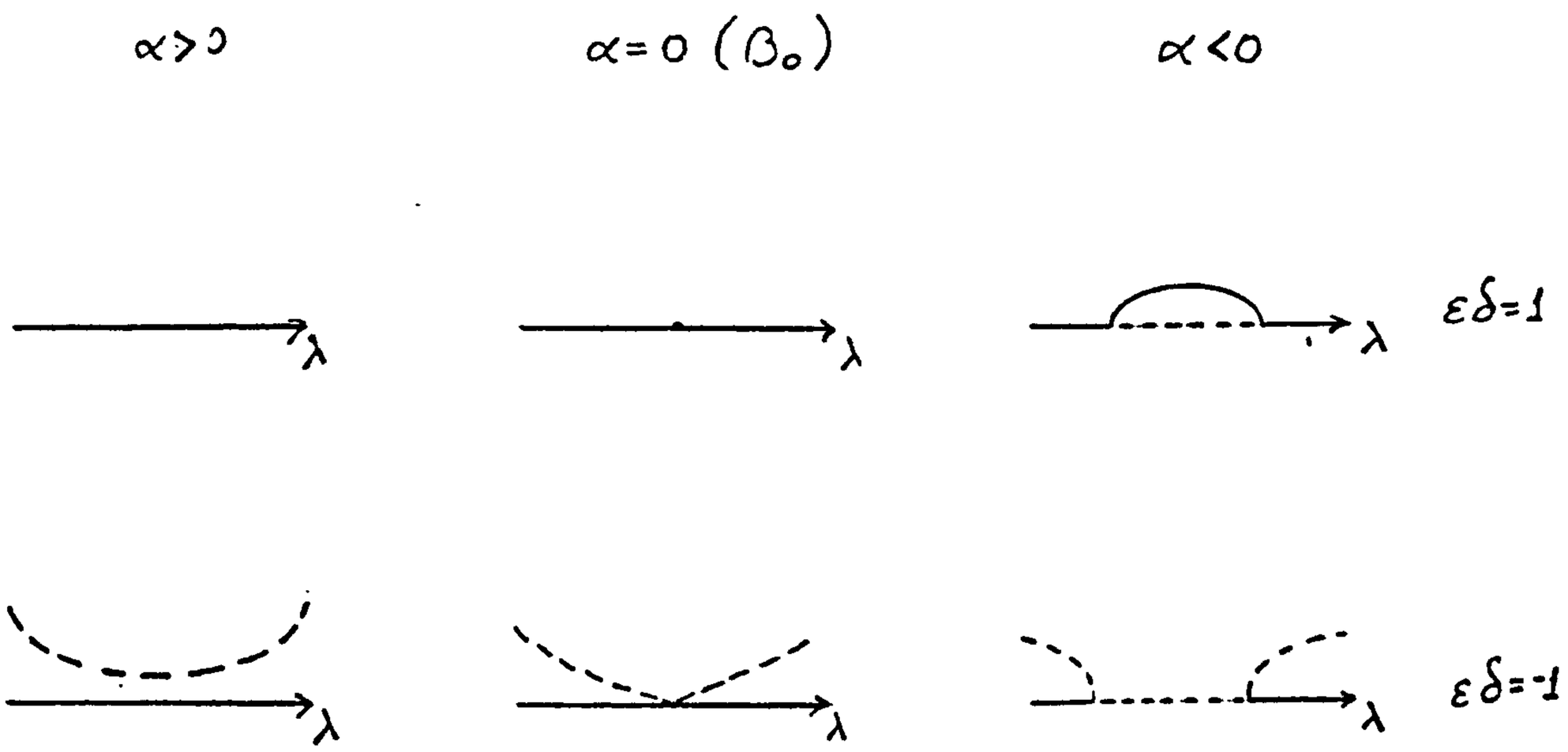

Fig III.1.2 — Bifurcation diagrams for the unfolding of (1.2)

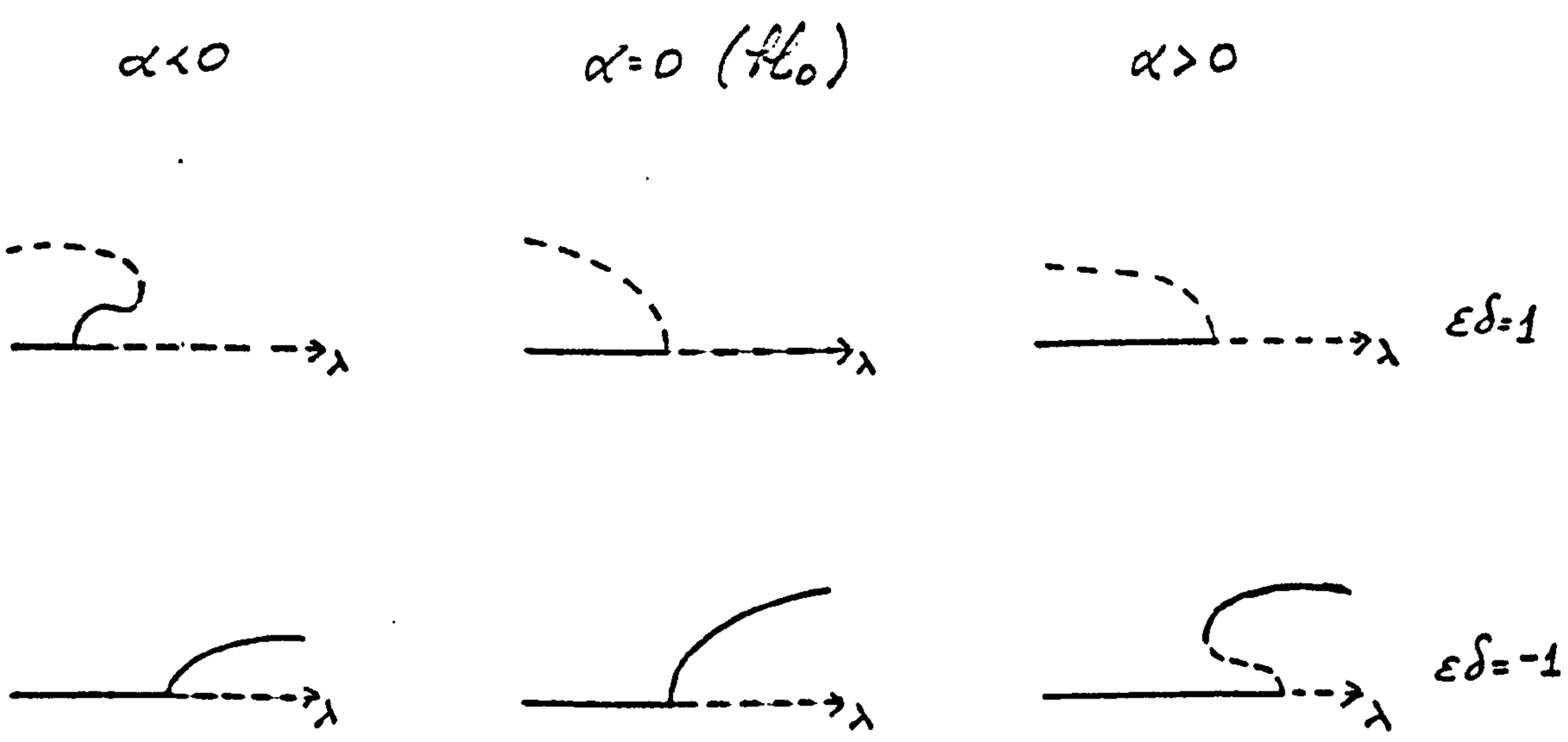

Fig III.1.3

Universal unfolding:

$$A(u,\lambda,\alpha) = \varepsilon u + \delta\lambda^2 + \alpha$$

Critical sets:

$$B_0 = \{\alpha = 0\}$$

$$B_1 = H_0 = H_1 = DL_0 = DL_1 = \Phi$$

Bifurcation diagrams are shown in Fig. III. 1.2.

(1.3) Organizing centre:

$$a(u,\lambda) = \varepsilon u^2 + \delta\lambda$$

Z_2-codimension = 1

Defining conditions: $a_u = 0$

$a_\lambda \neq 0$, $a_{uu} \neq 0$

Universal unfolding:

$$A(u,\lambda,\alpha) = \varepsilon(u^2 + \alpha u) + \delta\lambda$$

Critical sets:

$$H_0 = \{\alpha = 0\}$$

$$B_0 = B_1 = H_1 = DL_0 = DL_1 = \Phi$$

Bifurcation diagrams are shown in Fig. III.1.3

(1.4) Organizing centre:

$$a(u,\lambda) = \varepsilon u + \delta\lambda^3$$

$\mathbb{Z}_2$-codimension = 2

Defining conditions: $a_\lambda = 0$, $a_{\lambda\lambda} = 0$

$a_u \neq 0$, $a_{\lambda\lambda\lambda} \neq 0$

Universal unfolding:

$$A(u,\lambda,\alpha,\beta) = \varepsilon u + \delta(\lambda^3 + \beta\lambda + \alpha)$$

Critical sets:

$$B_0 = \{(\alpha,\beta): (\tfrac{\alpha}{2})^2 = (\tfrac{\beta}{3})^3\}$$

$$B_1 = H_0 = H_1 = DL_0 = DL_1 = \Phi$$

Critical sets and stable bifurcation diagrams are shown in Fig. III.1.4.

(1.5) Organizing centre:

$$a(u,\lambda) = \varepsilon u^3 + \delta\lambda$$

$\mathbb{Z}_2$-codimension = 2

Defining conditions: $a_u = 0$, $a_{uu} = 0$

$a_{uuu} \neq 0$, $a_\lambda \neq 0$

Universal unfolding:

$$A(u,\lambda,\alpha,\beta) = \varepsilon u^3 + \beta u^2 + \alpha u + \delta\lambda$$

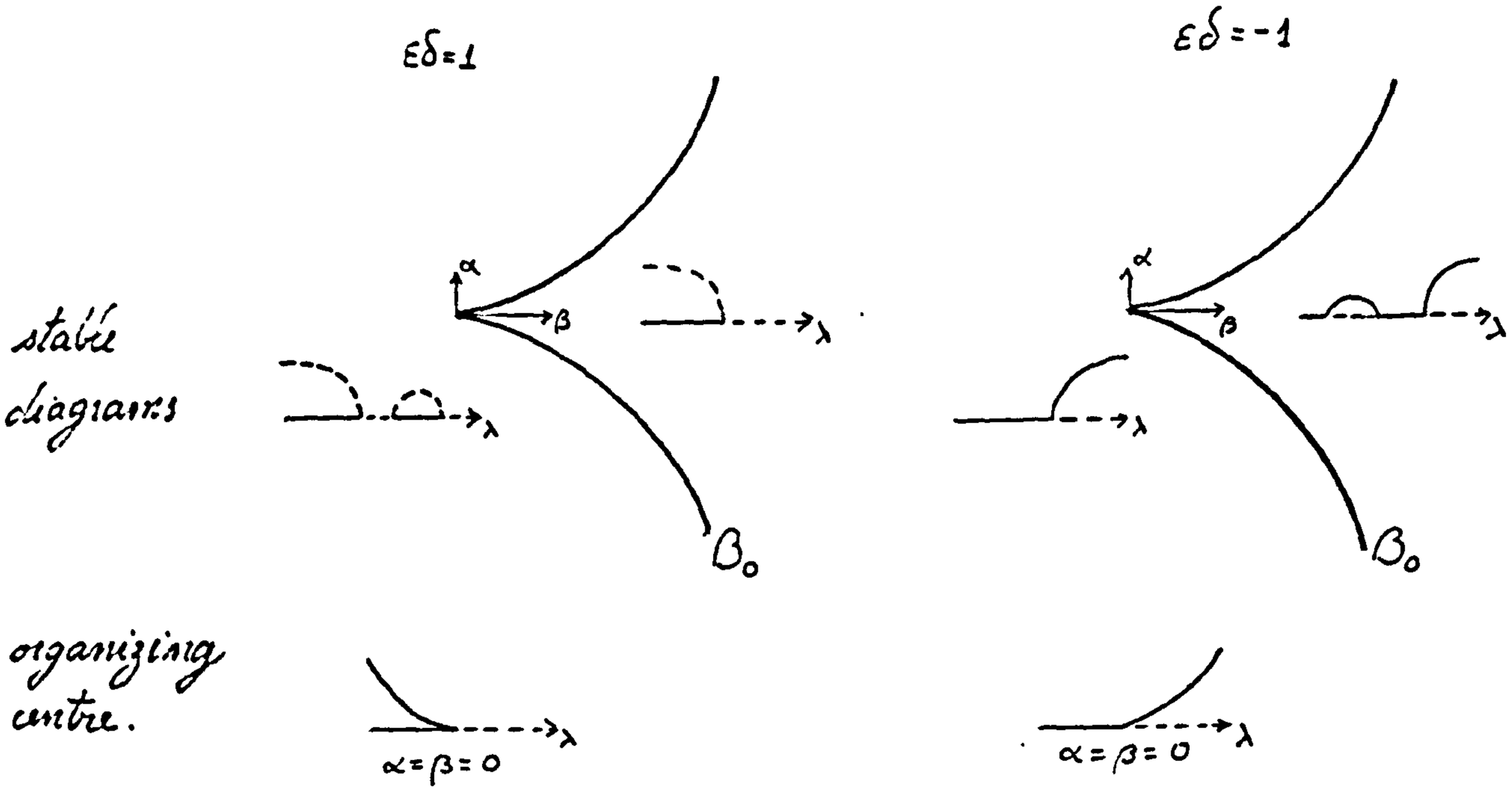

Fig. III.1.4

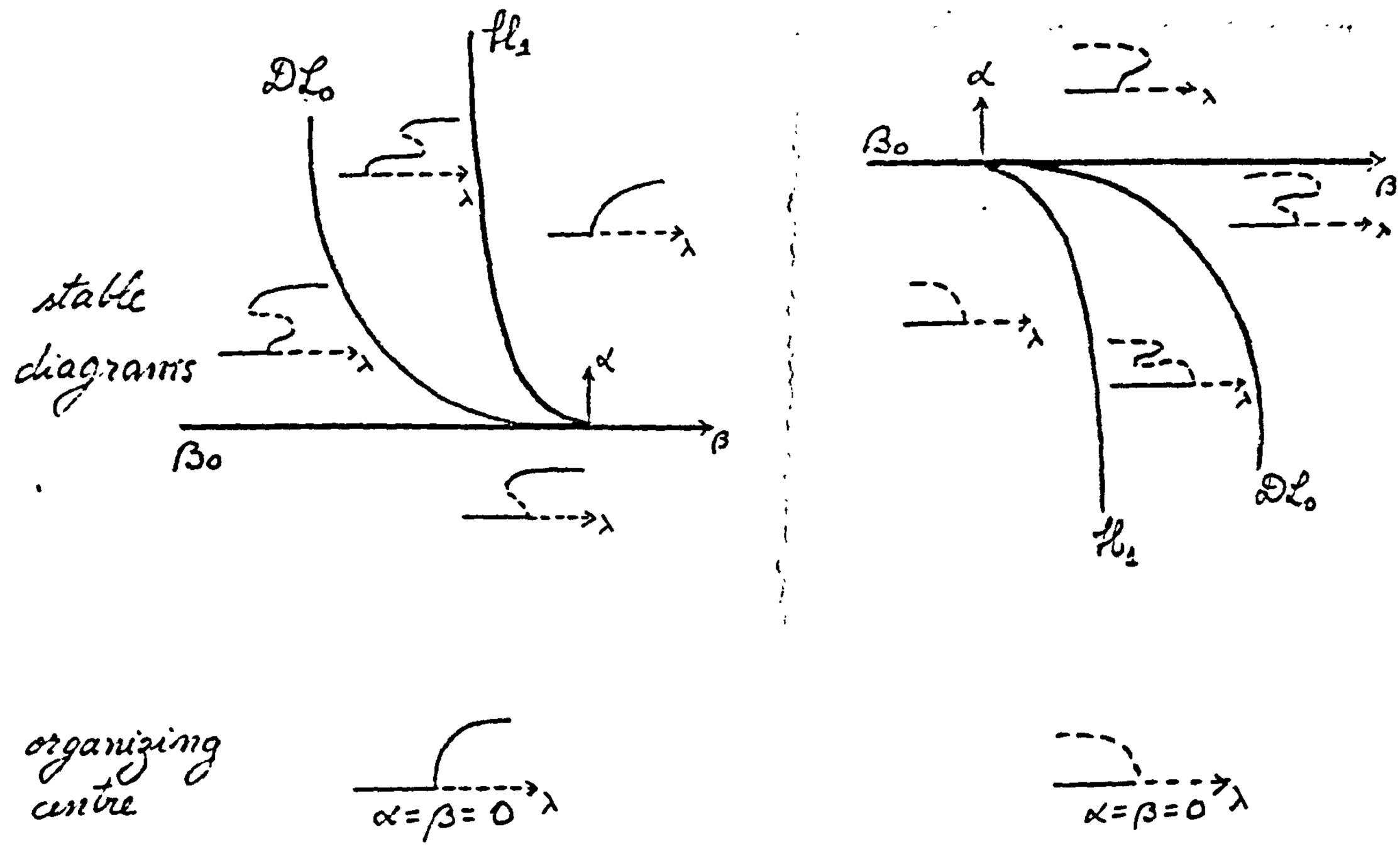

Fig III.1.5

Critical sets:

$$B_0 = \phi$$

$$B_1 = \phi$$

$$H_0 = \{(\alpha,\beta):\alpha = 0\}$$

$$H_1 = \{(\alpha,\beta):\alpha = \frac{\varepsilon\beta^2}{3}\ ,\ \varepsilon\beta < 0\}$$

$$DL_0 = \{(\alpha,\beta):\alpha = \frac{\varepsilon\beta^2}{4}\ ,\ \varepsilon\beta < 0\}$$

$$DL_1 = \phi$$

Stable bifurcation diagrams are shown in Fig. III.1.5, as well as the critical sets.

(1.6) Organizing centre:

$$a(u,\lambda) = \varepsilon u + \delta\lambda^4$$

$\mathbb{Z}_2$-codimension = 3

Defining conditions: $a_\lambda = a_{\lambda\lambda} = a_{\lambda\lambda\lambda} = 0$

$a_u \neq 0, \quad a_{\lambda\lambda\lambda\lambda} \neq 0$

Universal unfolding:

$$A(u,\lambda,\alpha,\beta,\gamma) = \varepsilon u + \delta[\lambda^4 + \gamma\lambda^2 + \beta\lambda + \alpha]$$

Critical sets:

$B_0 = \{(\alpha,\beta,\gamma);\alpha = \lambda^2(3\lambda^2+\gamma), \beta = -2\lambda(2\lambda^2+\gamma)$ for some $\lambda \in \mathbb{R}\}$

$B_1 = H_0 = H_1 = DL_0 = DL_1 = \phi$

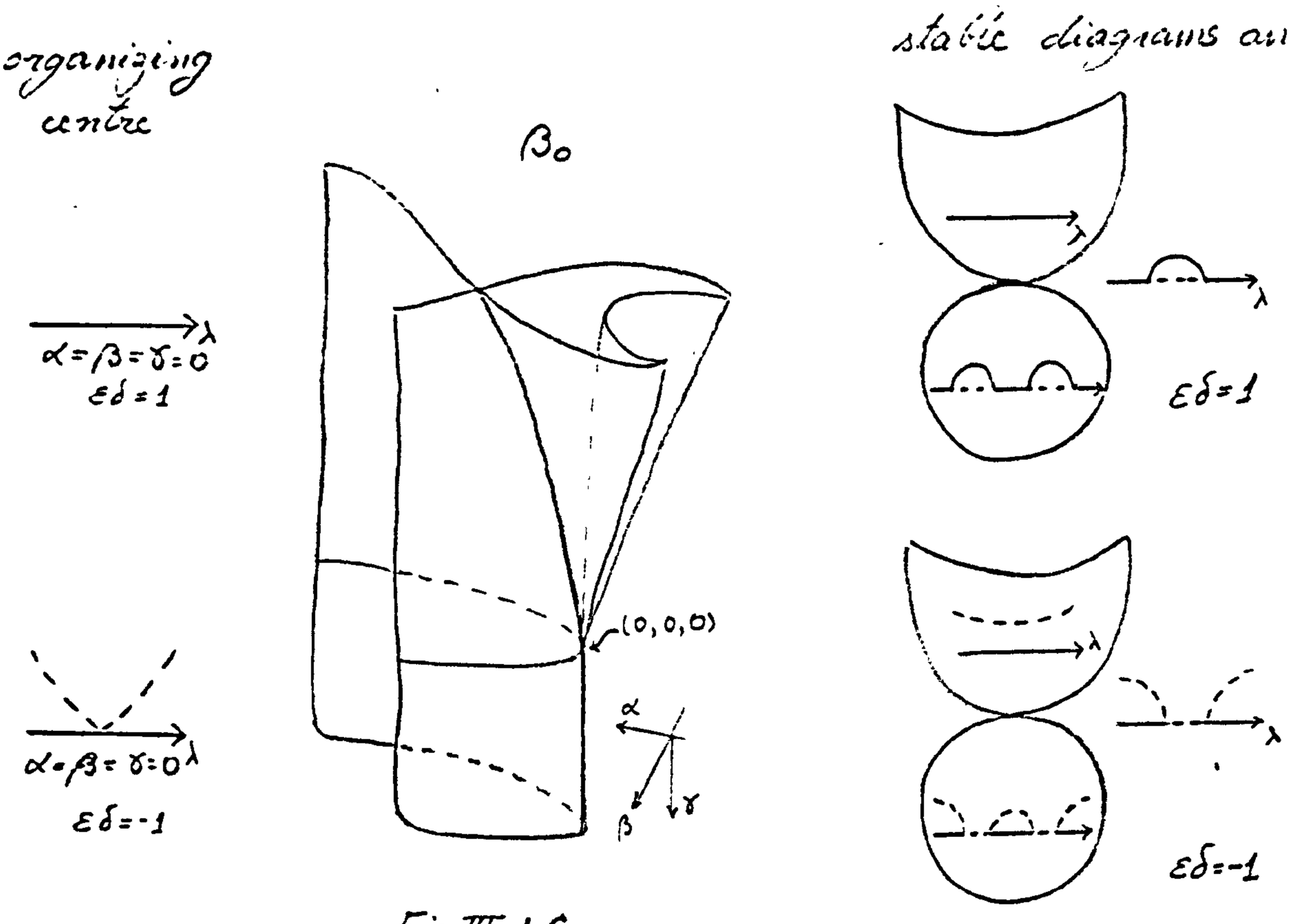

Fig III.1.6

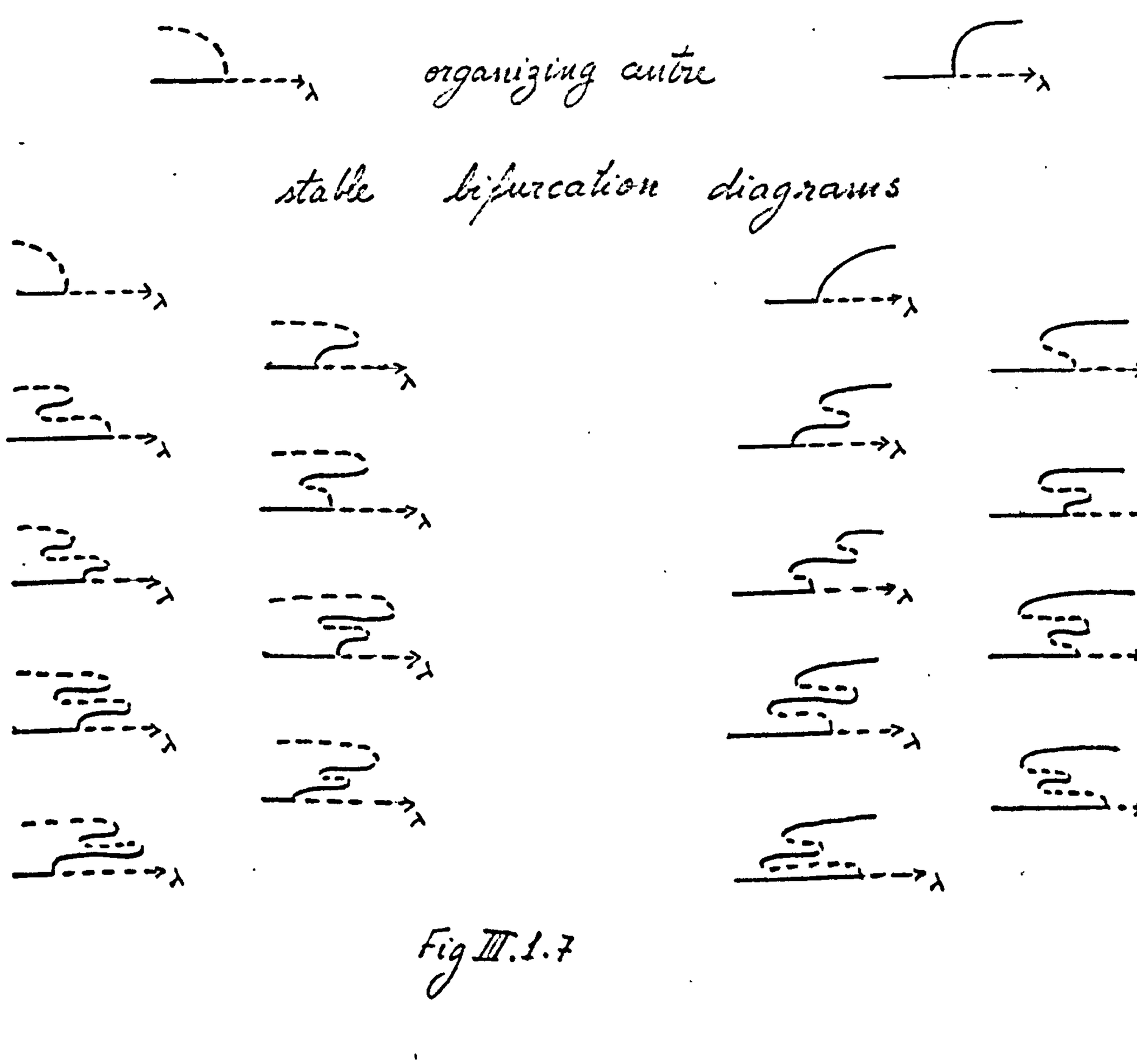

Fig III.1.7

The bifurcation variety B_0, and stable bifurcation diagrams are shown in Fig. III.1.6. This is the first case not described in [6].

(1.7) Organizing centre:

$$a(u,\lambda) = \varepsilon u^4 + \delta\lambda$$

$\mathbb{Z}_2$-codimension = 3

Defining conditions: $a_u = 0$, $a_{uu} = 0$, $a_{uuu} = 0$

$a_\lambda \neq 0$, $a_{uuuu} \neq 0$

Universal unfolding:

$$A(u,\lambda,\alpha,\beta,\gamma) = \varepsilon(u^4 + \gamma u^3 + \beta u^2 + \alpha u) + \delta\lambda = 0$$

Critical sets:

$B_0 = \phi$

$B_1 = \phi$

$H_0 = \{(\alpha,\beta,\gamma): \alpha = 0\}$

$H_1 = \{(\alpha,\beta,\gamma): \alpha = u^2(8u+3\gamma);\ \beta=-3u(2u+\gamma);u > 0\}$

$DL_0 = \{(\alpha,\beta,\gamma): \beta = -u(3u+2\gamma);\ \alpha= u^2(2u+\gamma);u > 0\}$

$DL_1 \neq \phi$.

Stable bifurcation diagrams are shown in Fig. III.1.7.

2. UNIMODAL GERMS

In this section we study a one-parameter family of $\mathbb{Z}_2$-equivariant germs $x\, a_b(x^2,\lambda)$ of special importance for the nerve impulse equations.

(2.1) Organizing centre:

$$a_b(u,\lambda) = \varepsilon u^2 + 2b\lambda u + \delta\lambda^2$$

with $b \neq 0$ and $b^2\delta \neq 1$

$\mathbb{Z}_2$-codimension = 3.

Defining conditions: $a_u = 0 = a_\lambda$

$a_{uu} \neq 0,\ a_{\lambda\lambda} \neq 0,\ a_{u\lambda} \neq 0$

$b = a_u\lambda.(|a_{uu}.a_{\lambda\lambda}|^{-\frac{1}{2}})$

$\varepsilon = \text{sign}\ (a_{uu})$

$\delta = \text{sign}\ (a_{\lambda\lambda})$

Universal unfolding:

$$\bar{A}_b(u,\lambda,\alpha,\beta,\gamma) = \varepsilon(u^2+2\beta u)+2(b+\gamma)\lambda u+\delta(\lambda^2+\alpha).$$

Since $\bar{A}_b(u,\lambda,\alpha,\beta,\gamma) = \bar{A}_{b+\gamma}(u,\lambda,\alpha,\beta,0)$, we can rewrite the unfolding as:

$$(2.1.1)\qquad A(u,\lambda,\alpha,\beta,b) = \bar{A}_b(u,\lambda,\alpha,\beta,0) = \varepsilon(u^2+2\beta u)+2b\lambda u+\delta(\lambda^2+\alpha)$$

and have b playing the double rôle of modal parameter and unfolding parameter.

Since

$$(2.1.2) \qquad A_{\varepsilon\delta}(u,\lambda,\alpha,\beta,b) = -A_{(-\varepsilon)(-\delta)}(u,\lambda,\alpha,\beta,-b),$$

the numbers ε and $B = \varepsilon b$ form a complete set of invariants for the family of germs (2.1) under $\mathbb{Z}_2$-equivalence.

If $\varepsilon\delta = -1$, we can divide the family a_b into two classes, corresponding to $B > 0$ and $B < 0$. For values of B within one of these classes any two bifurcation problems a_b are $\mathbb{Z}_2$-*topologically equivalent*, i.e. $\mathbb{Z}_2$-equivalent (II.3.2) without the assumption of differentiability in the change of coordinates $T(x^2,\lambda)$, $\Lambda(\lambda)$ and $X(x^2,\lambda)$ of (II. 3.2.1). As the family a_b as a whole has $\mathbb{Z}_2$ codimension 2, each germ a_b with $\varepsilon\delta = -1$, $b \neq 0$ is said to have *topological* $\mathbb{Z}_2$-*codimension* 2. This is case (2.2).

For $\varepsilon\delta = 1$ the family a_b splits into four topological classes, corresponding to the connected components of B-space $= \mathbb{R} - \{0,1,-1\}$. These germs are described in (2.3), followed by the transition cases $B = 0$ (2.4) where the topological $\mathbb{Z}_2$-codimension equals the (differentiable) $\mathbb{Z}_2$-codimension.

(2.2) Organizing centre:

$$a_b(u,\lambda) = \varepsilon(u^2 - \lambda^2) + 2b\lambda u \qquad b \neq 0$$

Z_2-codimension = 3, topological codimension = 2

Defining conditions: $a_u = a_\lambda = 0$; $a_{uu}.a_{u\lambda}.a_{\lambda\lambda} \neq 0$

$a_{uu}.a_{\lambda\lambda} < 0$.

Universal unfolding:

$$A(u,\lambda,\alpha,\beta,b) = \varepsilon(u^2 + 2\beta u - \alpha - \lambda^2) + 2b\lambda u$$

Critical sets:

$$B_0 = \{(\alpha,\beta,b): \alpha = 0\}$$

$$B_1 = \{(\alpha,\beta,b): \alpha = \frac{-\beta^2}{b^2+1} \text{ and } \beta < 0\}$$

$$H_0 = \{(\alpha,\beta,b): \alpha = \frac{-\beta^2}{b^2}\}$$

$$H_1 = DL_0 = DL_1 = \phi$$

Critical sets and stable bifurcation diagrams for the case $\varepsilon = 1$ are shown in Fig. III.2.2. On top we draw a cylinder $\alpha^2 + \beta^2 = r^2$, cut open along the line $\alpha = 0$, $\beta = r^2$. The intersection of the critical sets with this cylinder is indicated, as well as the stable bifurcation diagrams corresponding to each region of α-β-b-space. Notice the change of behaviour as we cross the hysteresis variety at $b = 0$, and the bifurcation diagrams at the origin $\alpha = \beta = 0$.

Stable diagrams and critical sets in a cylinder. $\varepsilon = 1$, $\delta = -1$

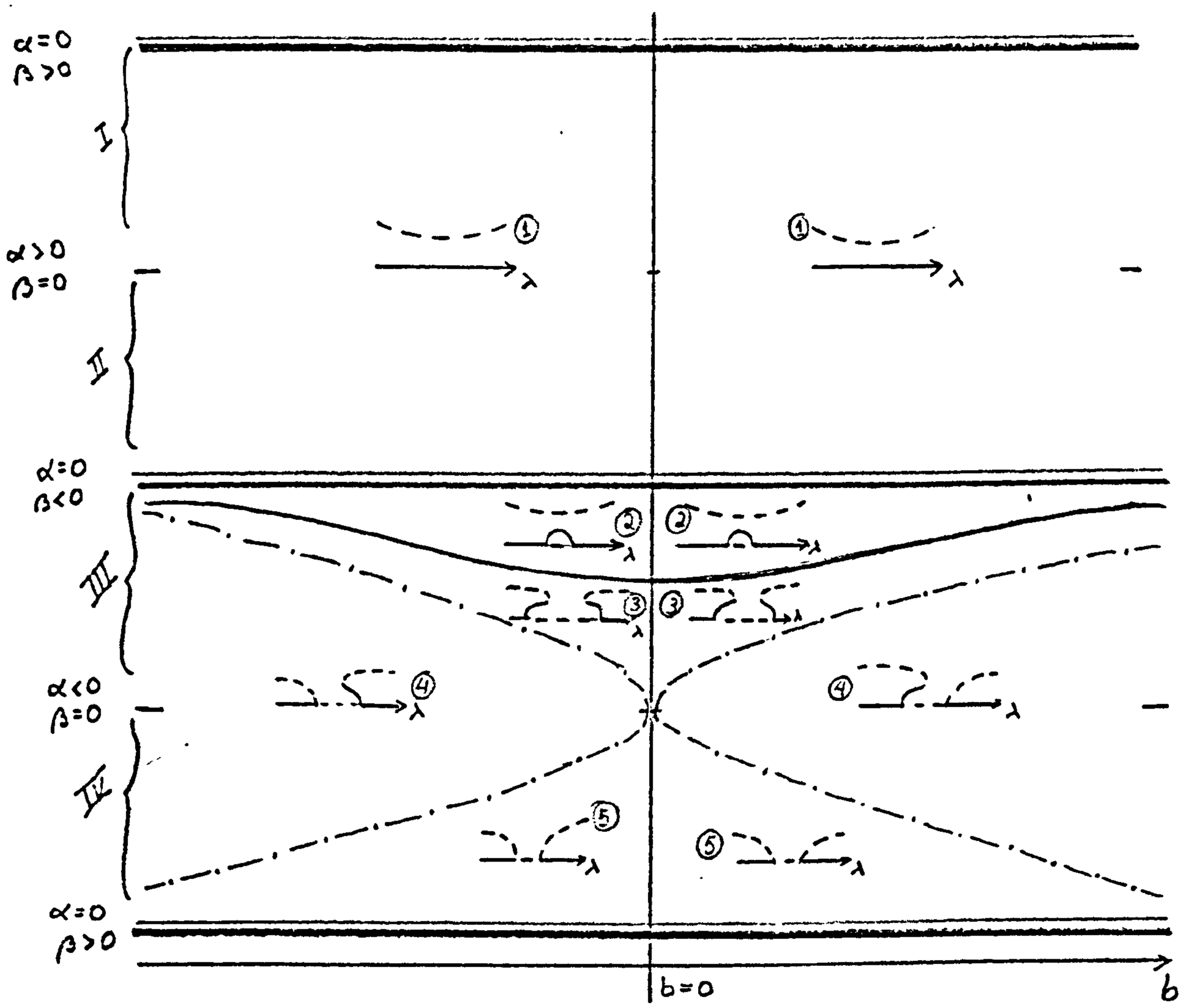

critical sets for b = constant

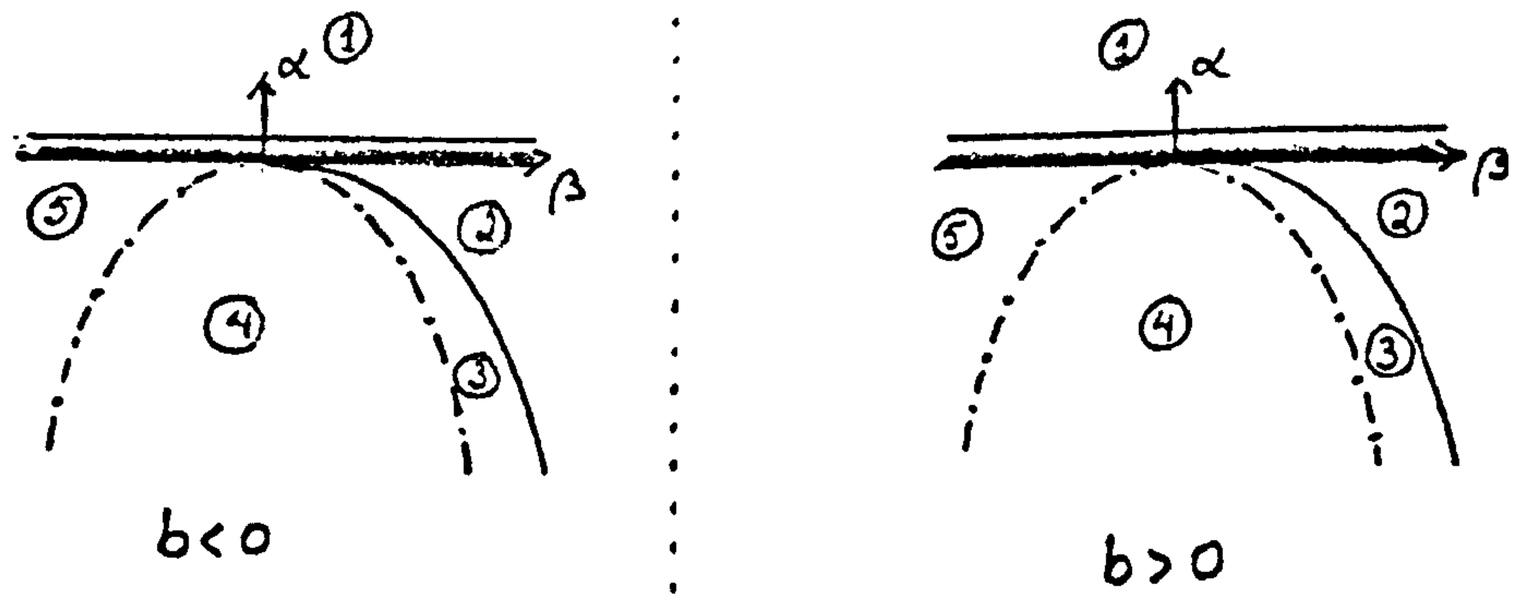

organizing centre

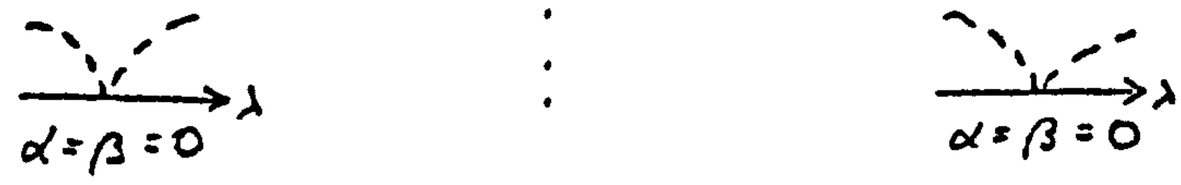

Conventions:

C_1 C_0 H_0

Fig III. 2.2

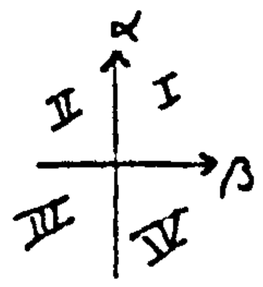

On the bottom we show the critical sets in α-β-plane, for $b \neq 0$ fixed. The case $\varepsilon = -1$ can be obtained substituting -b for b throughout.

(2.3) Organizing centre:

$$a_b(u,\lambda) = \varepsilon(u^2 + \lambda^2) + 2b\lambda u, \quad b \neq 0, \pm 1$$

$\mathbb{Z}_2$-codimension = 3; topological codimension = 2

Defining conditions: $a_u = a_\lambda = 0$, $a_{u\lambda} \neq 0$, $a_{uu}.a_{\lambda\lambda} > 0$
$b^2 = a_{u\lambda}^2/(a_{uu}.a_{\lambda\lambda}) \neq 1$

Universal unfolding:

$$A(u,\lambda,\alpha,\beta,b) = \varepsilon(u^2 + 2\beta u + \alpha + \lambda^2) + 2b\lambda u.$$

Critical sets:

$$B_0 = \{(\alpha,\beta,b): \alpha = 0\}$$
$$B_1 = \{(\alpha,\beta,b): \alpha = \frac{\beta^2}{1-b^2}, \frac{\beta}{1-b^2} < 0\}$$
$$H_0 = \{(\alpha,\beta,b): \alpha = \frac{-\beta^2}{b^2}\}$$
$$H_1 = DL_0 = DL_1 = \Phi$$

Critical sets and stable bifurcation diagrams for the case $\varepsilon = 1$; $b \neq 0, \pm 1$, are shown in Fig. III.2.1a. The critical sets are shown in the $\alpha \times \beta$-plane for fixed values of the modal parameter b (bottom), and also intersected with

Stable diagrams and critical sets in a cylinder

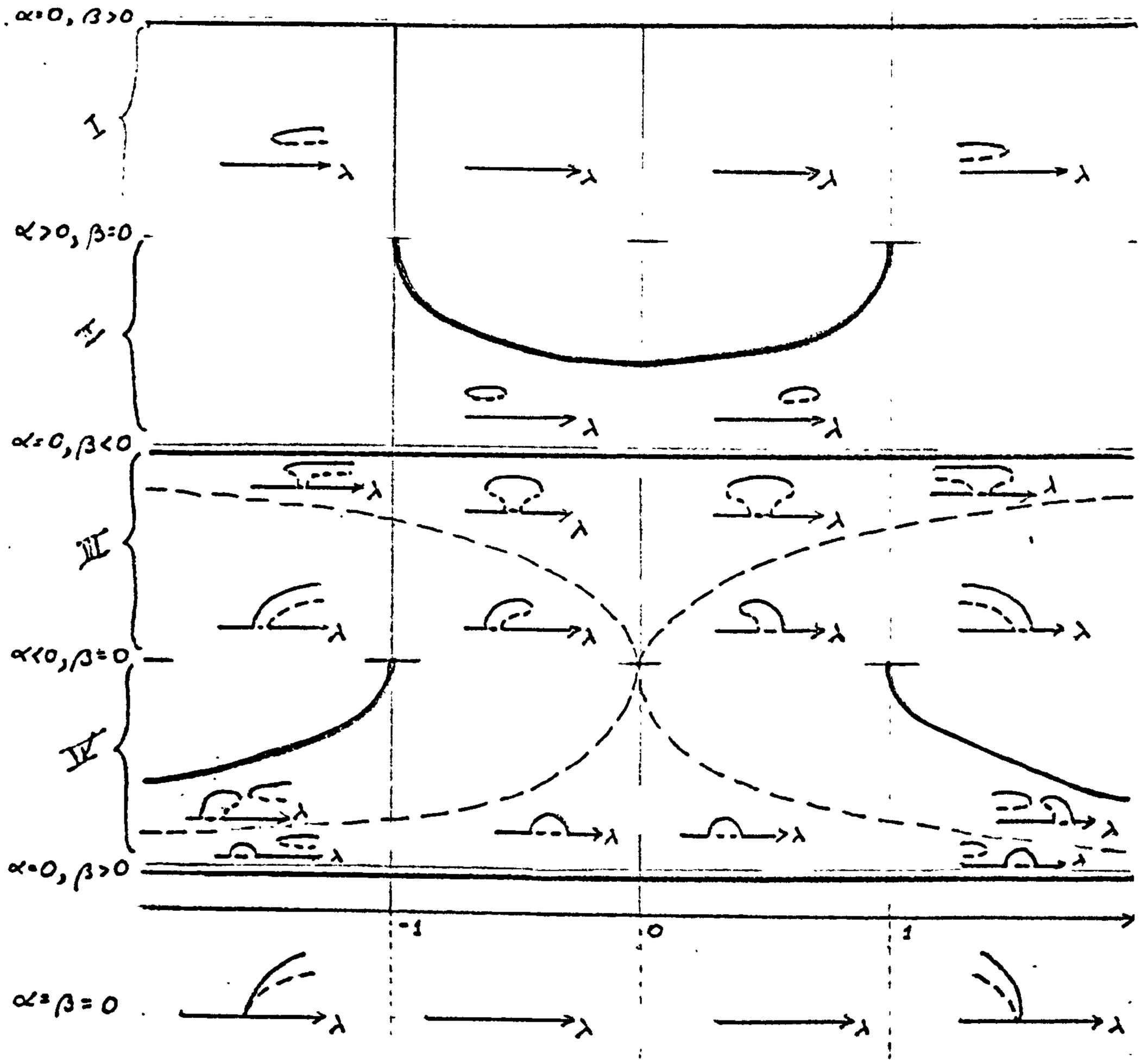

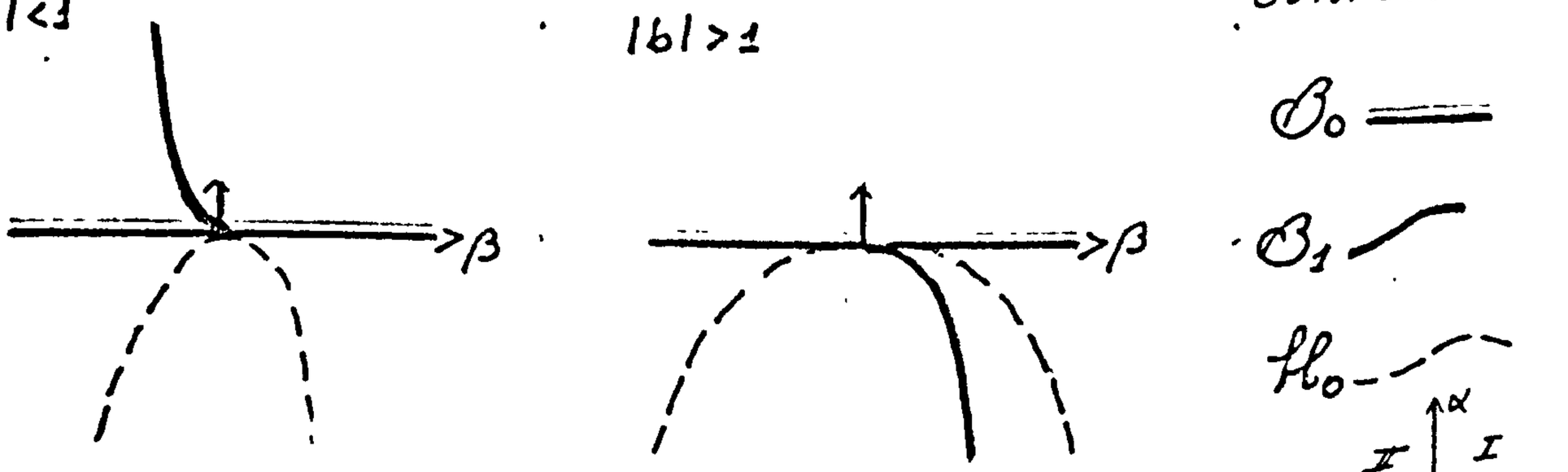

Fig III.2.3, $\varepsilon = \delta = 1$.

the cylinder $\alpha^2 + \beta^2 = 1$, drawn on top, as if cut open along the line $\alpha = 0$, $\beta = 1$. Substituting -b for b yields the diagrams for $\varepsilon = -1$, $b \notin \{0,\pm 1\}$.

(2.4) Organizing centre:

$$a(u,\lambda) = \varepsilon u^2 + \delta\lambda^2$$

$\mathbf{Z}_2$-codimension = 3 = $\mathbf{Z}_2$ topological codimension

Defining conditions: $a_u = a_\lambda = a_{u\lambda} = 0$

$$a_{uu}.a_{\lambda\lambda} \neq 0$$

Universal unfolding:

$$A(u,\lambda,\alpha,\beta,b) = \varepsilon(u^2+2\beta u) + \delta(\lambda^2+\alpha)+2b\lambda u.$$

This is the b = 0 case of (2.1). It differs from (2.2) and (2.3) in the fact that the self-intersection of the hysteresis variety H_o at $\alpha < 0$, $\beta = 0$, $b = 0$ is unavoidable, i.e. it intersects every neighbourhood of the origin $\alpha = \beta = b = 0$ of the unfolding. Recall that, after rewriting the unfolding of the family a_b in (2.1.1), the origin of the new unfolding A becomes (0,0,b). Therefore, for $b \neq 0$, the line $b = \beta = 0$ is bounded away from the origin, whereas for b = 0 it is not. This is the reason why (2.4) is not topologically $\mathbb{Z}_2$-equivalent to any of the germs considered before, although the expression for its unfolding

$\varepsilon.\delta = -1$

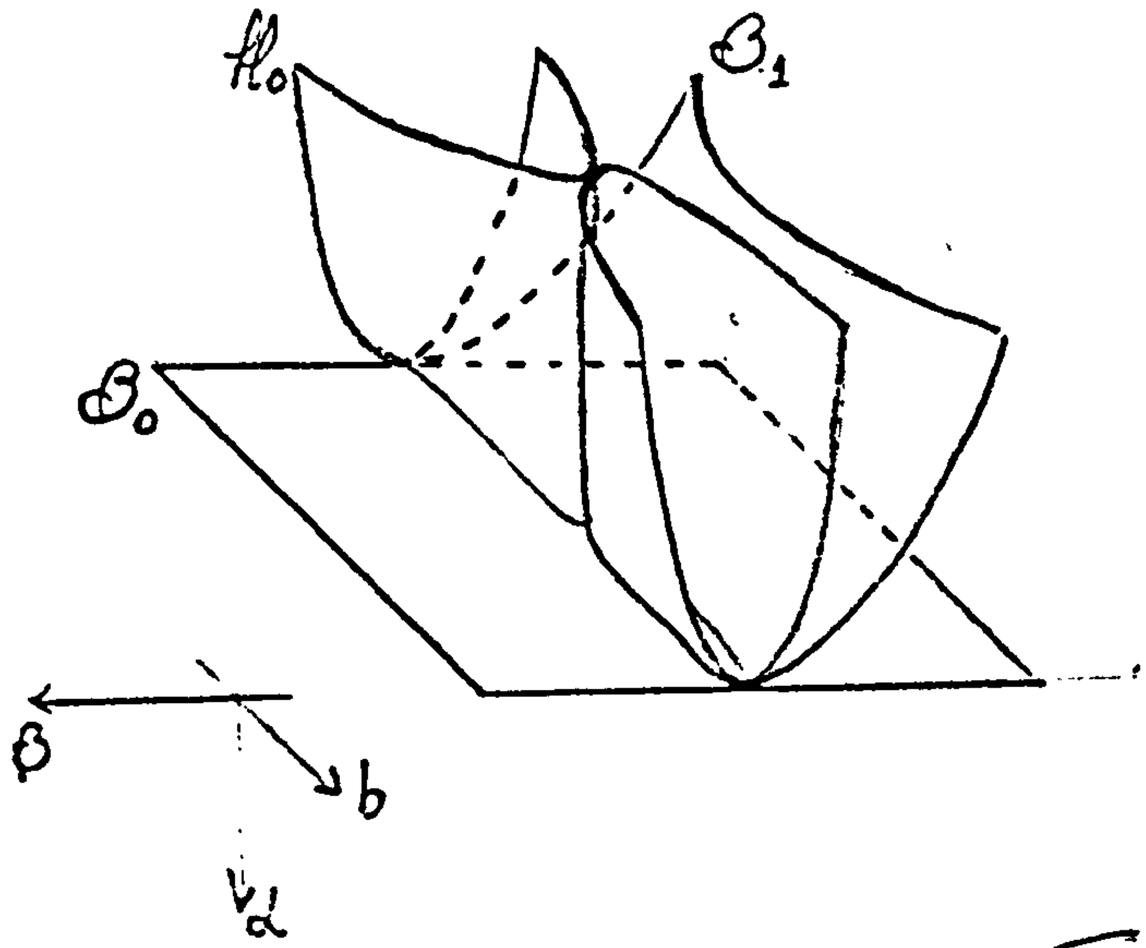

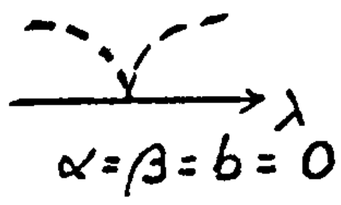

$\alpha = \beta = b = 0$

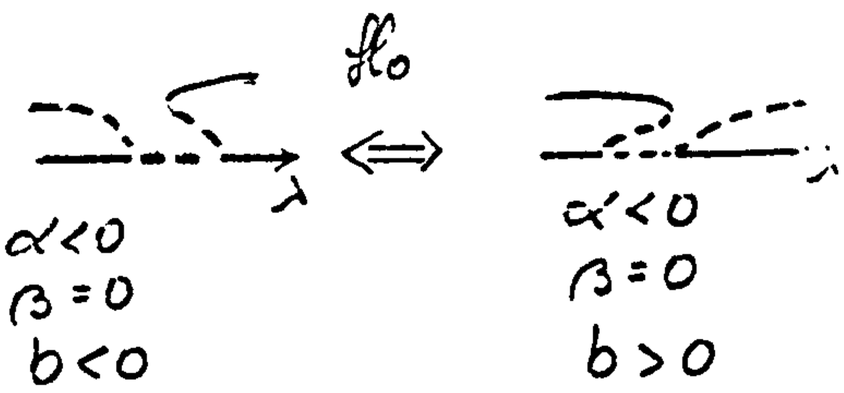

$\varepsilon.\delta = 1$

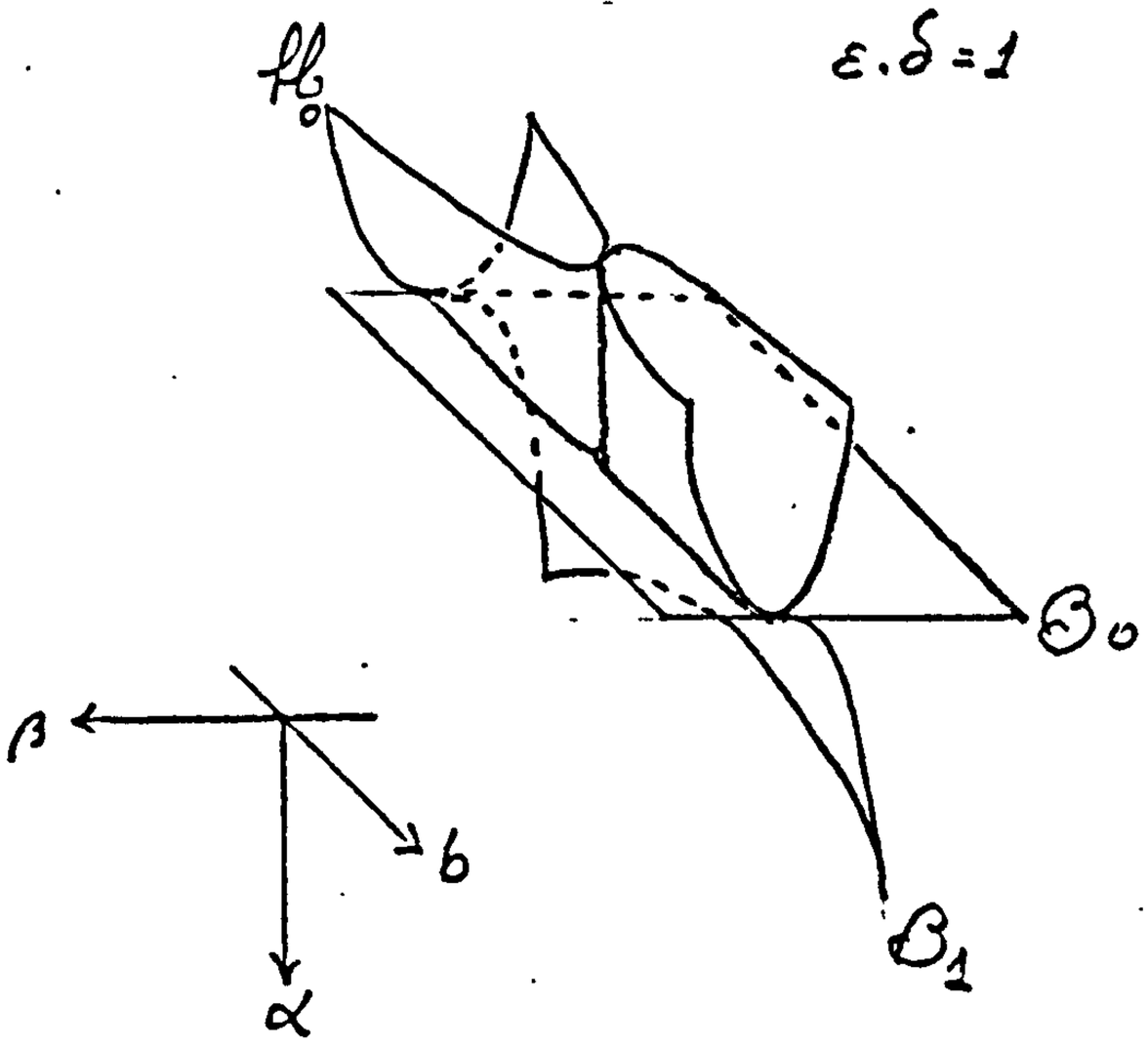

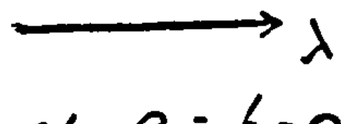

$\alpha = \beta = b = 0$.

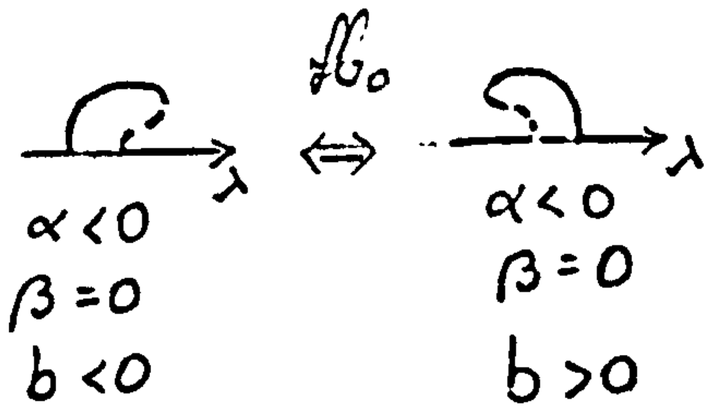

Fig III. 2.4

is the same. In other words, in order to unfold the germ (2.4) we perturb b away from 0, thus obtaining the family a_b, that we then proceed to unfold. Bifurcation diagrams obtained in this fashion are those for b near 0 ($|b| < 1$) shown in Figs. III.2.2 and III.2.3. Critical sets are drawn in three dimensions in Fig. III.24, the case $\varepsilon\delta = -1$ on top, with $\varepsilon\delta = 1$ below. We stress the particular behaviour of this germ, by describing the zero set on both sides of the self intersection of H_o - *no other member of the family* a_b *has this "double hysteresis".*

(2.5) The discussion of case (2.4) (b = 0) illustrates a common feature of parametrized families of germs: topologically equivalent regions, separated by lower dimensional strata (in this case points) with higher codimension, where non-trivial changes take place.

The "separating set" for the germ 2.3 includes two extra points, b = ±1. At these points, however, the codimension jump is higher: the germ

$$a(u,\lambda) = \varepsilon u^2 + 2\phi\lambda u + \delta\lambda^2 \qquad (2.5)$$

has infinite codimension, which means that there is an infinite set of non Z_2-equivalent germs, sharing (2.5) as their Taylor expansion of order 2. Nevertheless, the addition of suitable higher terms leads to the *same* codimension, namely 3, as for the non-degenerate values of b. So the codimension-3 stratum has a more complicated

structure than might be supposed. The remainder of this chapter is a description of the codimension 3 germs that belong to this class.

(2.6) Organizing centre:

$$a(u,\lambda) = \phi u^3+\varepsilon(u^2+\lambda^2)+2\delta\lambda u$$

$\mathbb{Z}_2$-codimension = 3 = topological codimension

Definign conditions: $a_u = a_\lambda = 0$

$$a_{uu}.a_{\lambda\lambda} > 0$$

$$a_{uu}.a_{\lambda\lambda} = a_{u\lambda}$$

and

$$D^2a(v,v) = 0,\ v \neq 0 \Rightarrow D^3a(v,v,v) \neq 0.$$

Universal unfolding:

$$A(u,\lambda,\alpha,\beta,\gamma) = \phi u^3+\varepsilon(u^2+\beta u+\alpha+\lambda^2)+2\delta(\gamma+1)\lambda u$$

Critical sets:

$$B_0 = \{(\alpha,\beta,\gamma):\ \alpha = 0\}$$

$$B_1 = \{(\alpha,\beta,\gamma):\alpha=u^2(2\varepsilon\phi u-s),\beta = u(2s-3\varepsilon\phi u),$$

$$u > 0,\ s = \gamma^2 + 2\gamma\}.$$

$$H_0 = \{(\alpha,\beta,\gamma):\alpha = \frac{-\beta^2}{4(\gamma+1)^2}\}.$$

$H_1 = DL_0 = DL_1 = \phi$ for $\varepsilon\phi = 1$, and these three sets are non-empty but bounded away from the origin $\alpha = \beta = \gamma = 0$ for $\varepsilon\phi = -1$.

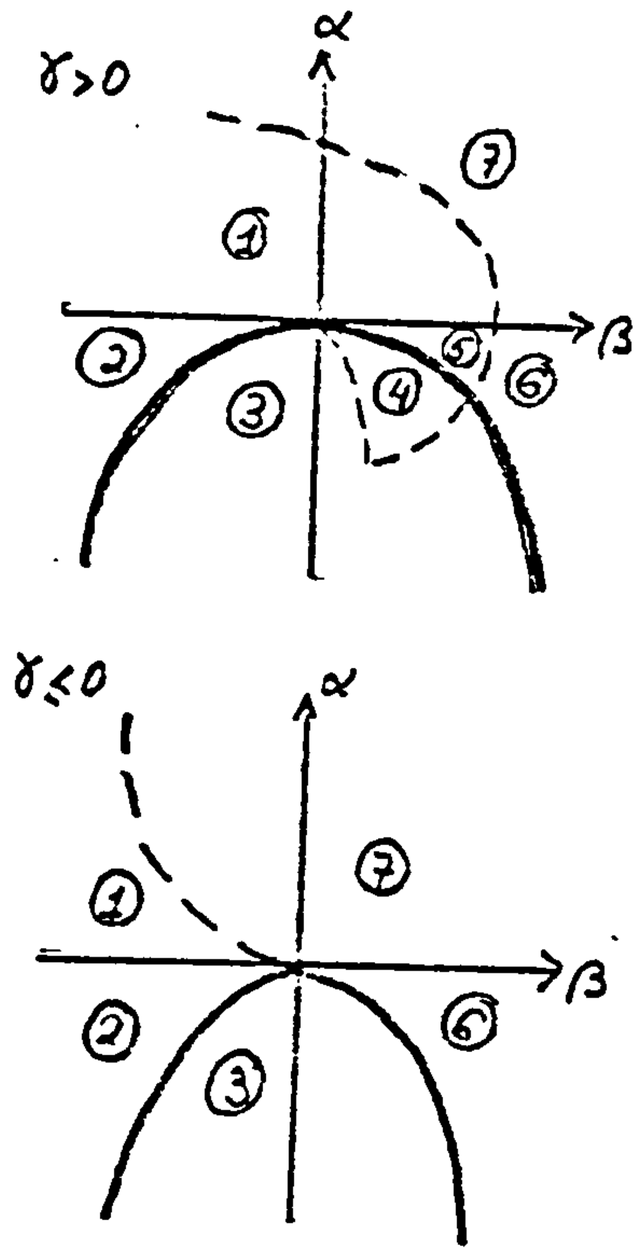

$\varepsilon\rho=1$

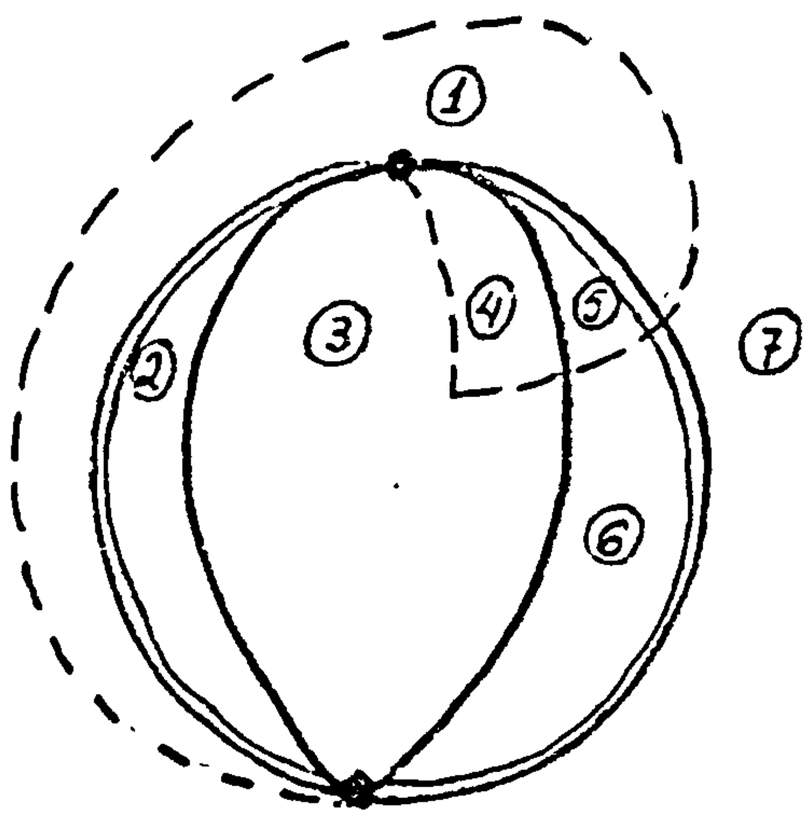

$\delta=1$

Bifurcation Diagrams

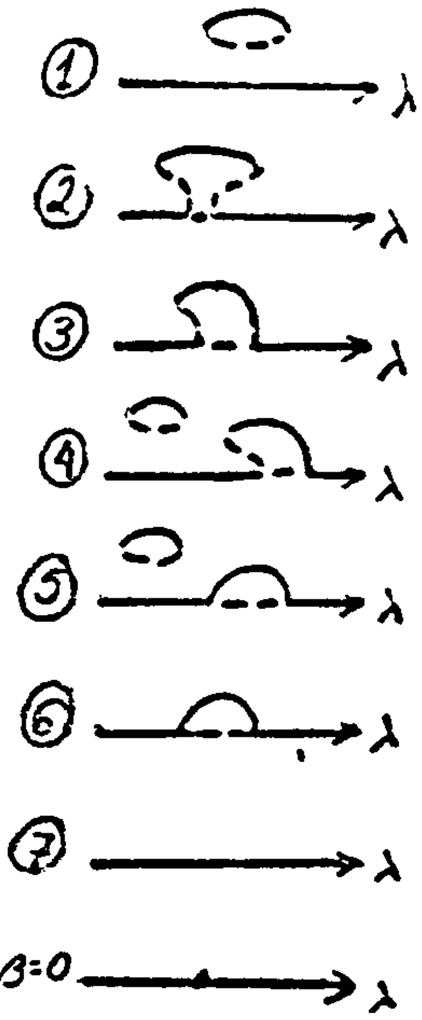

$\varepsilon\rho=-1$

$\delta=1$

Bifurcation Diagrams

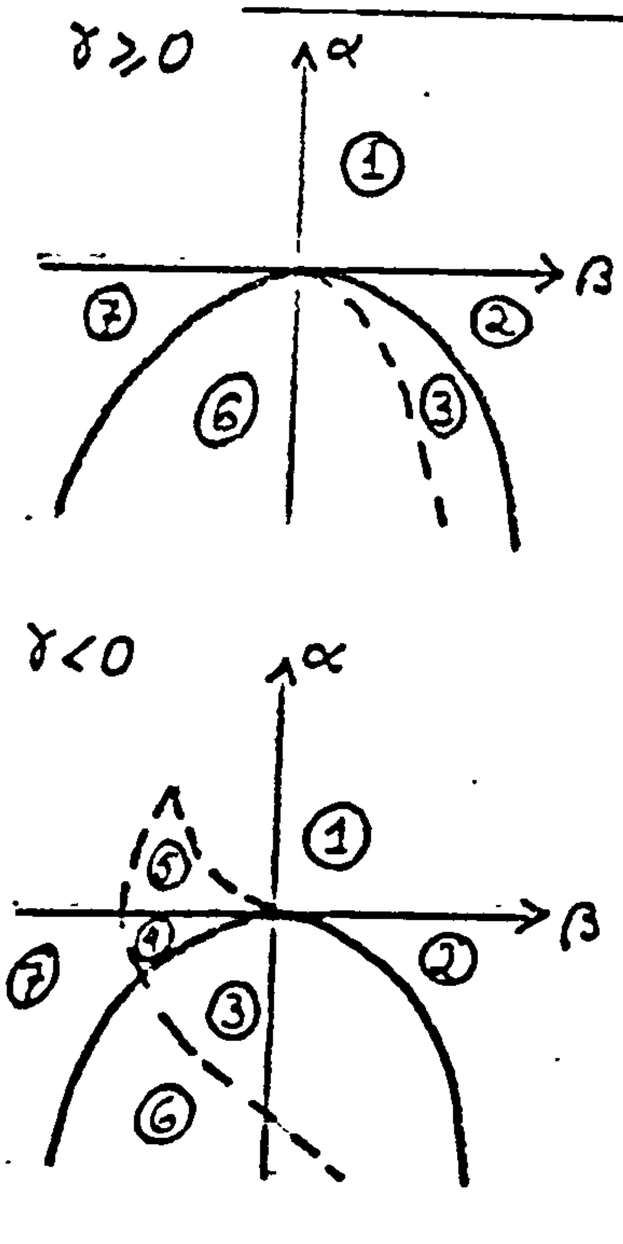

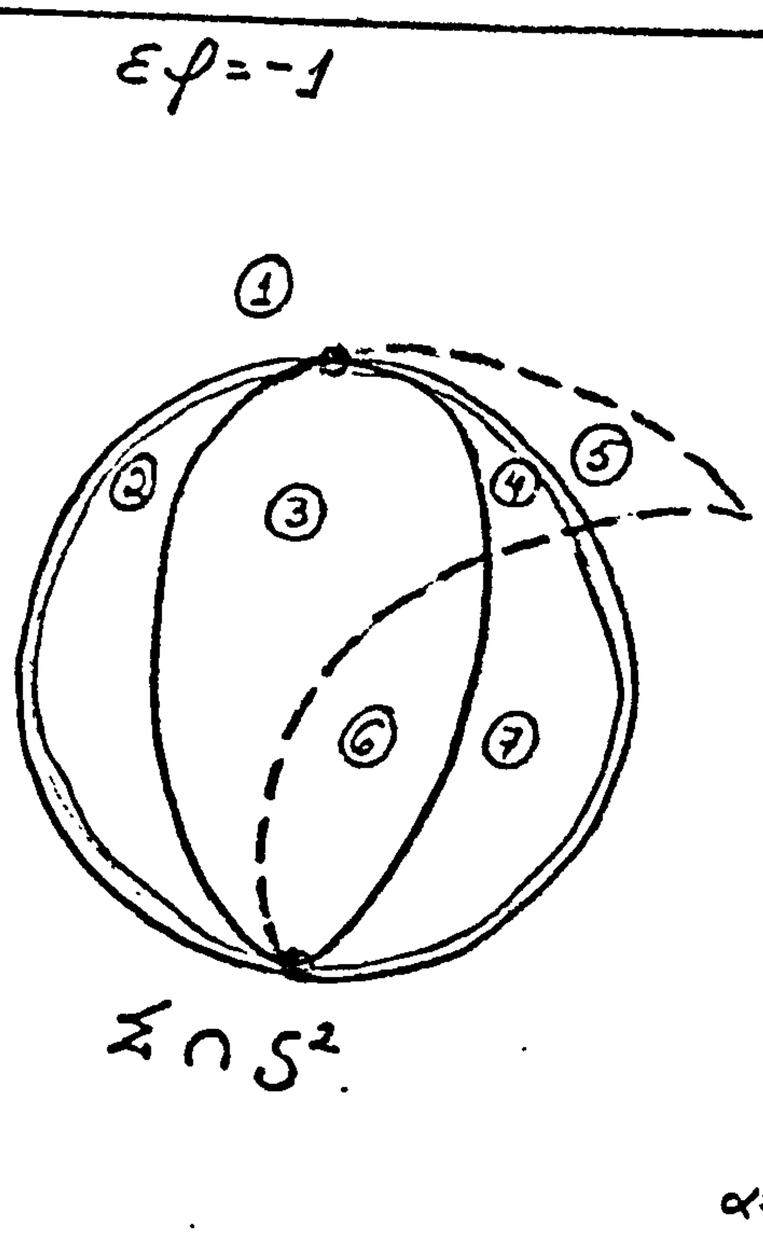

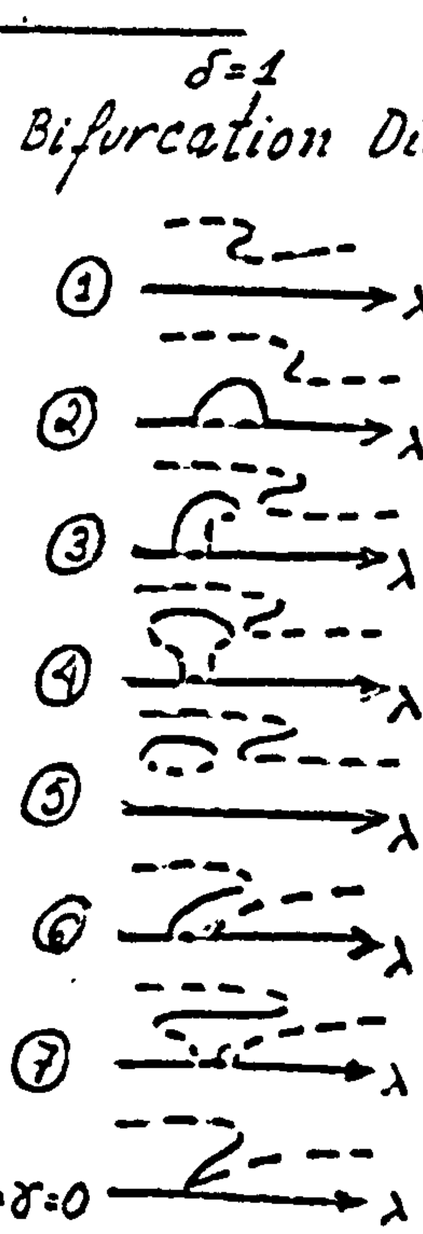

$---\ B_1$

$\overline{\qquad}\ B_0$

$\sim\ fl_0$

Fig III. 2.6

This is the codimension 3 case of (2.3), with $B = \pm 1$. Indeed, for $\gamma \neq 0$, the germs $A(u,\lambda,0,0,\gamma)$ are $\mathbb{Z}_2$ equivalent to (2.3) where the modal parameter is:

$$B = \varepsilon\delta(\gamma + 1).$$

The unstable bifurcation diagrams for $A(u,\lambda,0,0,\gamma)$ are shown in Fig. III.2.6a for $\varepsilon\phi = +1 = \varepsilon\delta$, where they are compared to the corresponding diagrams for (2.3). For $\gamma < 0$, the diagrams are identical to those of (2.3), $0 < B < 1$, but for $\gamma > 0$ the $B > 1$ diagrams appear "capped off" - the $\mathbb{Z}_2$ equivalence is valid in a small neighbourhood of the bifurcation point. This is a recurring feature of one parameter families of germs, and will be discussed again in Section IV.2. Capped off diagrams for (2.3), $B > 1$ will appear again in cases (2.7), $\varepsilon\delta = -1$ and (2.8), $\varepsilon\phi = 1$, below.

The bifurcation diagrams for $A(u,\lambda,0,0,\gamma)$ when $\varepsilon\phi = -1 = \varepsilon\delta$ are compared to those of (2.3) in Fig. III.2.6b. All the diagrams exhibit global differences to their $\mathbb{Z}_2$-equivalent counterparts. This time the difference is a prolongation of solution branches in the $\lambda \to \pm\infty$ directions, analogous to case (2.8), $\varepsilon\phi = -1$ below.

The stable bifurcation diagrams retain the same relationship to the unfolding of (2.3) as that discussed above for the organizing centre $\alpha = \beta = 0$. Diagrams from the unfolding of the $0 < B < 1$ case dominate the picture when $\varepsilon\phi = +1 = \varepsilon\delta$, with those for $B > 1$ appearing capped off. Similarly for $\varepsilon\phi = -1 = \varepsilon\delta$, stable diagrams can be obtained from those of (2.3) by suitable prolongation in the $\lambda = \pm \infty$ directions (Fig. III.2.6d). For each choice of $\varepsilon\phi$, the diagrams for case $-\varepsilon\delta$ are obtained from case $\varepsilon\delta$ by substituting $-\lambda$ for λ throughout.

In both Figs. III.2.6c and III.2.6d we show the critical set $\Sigma = B_0 \cup B_1 \cup H_0$ intersected with the planes γ = small constant. We also draw the intersection of Σ with a sphere of centre (0,0,0) and small radius. In this, as in all other cases we only draw those components of $\mathbb{R}^n - \Sigma$ that contain the origin in their closure. Bifurcation diagrams in any other regions may be different, depending on the choice of representative for the $\mathbb{Z}_2$ equivalence class.

We now proceed to describe the codimension 3 germs abutted by (2.1) as $B \to \pm \infty$. These germs form a transition case from (2.2) to (2.3).

(2.7) Organizing centre:

$$a(u,\lambda) = \varepsilon u^2 + 2\delta\lambda u + \phi\lambda^3$$

$\mathbf{Z}_2$-codimension = 3

Defining conditions: $a_u = a_\lambda = a_{\lambda\lambda} = 0$

$$a_{uu} \neq 0,\ a_{u\lambda} \neq 0,\ a_{\lambda\lambda\lambda} \neq 0$$

Universal unfolding:

$$A(u,\lambda,\alpha,\beta,\gamma) = \varepsilon u^2 + 2\delta\lambda u + \phi(\lambda^3+\gamma\lambda^2+ \beta\lambda+ \alpha)$$

Critical sets:

$$B_0 = \{(\alpha,\beta,\gamma):\ \alpha= \lambda^2(\gamma+2\lambda);\beta=-\lambda(2\gamma+3\lambda),\ \lambda \in \mathbb{R}\}$$

$$B_1 = \{(\alpha,\beta,\gamma):\ \alpha=\lambda^2(2\lambda+\gamma-\varepsilon\phi);\beta=-\lambda(3\lambda+2(\gamma-\varepsilon\phi));\varepsilon\delta\lambda < 0\}$$

$$H_0 = \{(\alpha,\beta,\gamma):\ \alpha = 0\}$$

$$H_1 = DL_0 = DL_1 = \phi$$

Critical sets and stable bifurcation diagrams for the case when $\varepsilon\phi = 1$ are shown in Fig. III.2.7. When $\varepsilon\phi = -1$ the bifurcation diagrams can be obtained substituting $-\lambda$ for λ, in the case $-\varepsilon\phi$, $-\varepsilon\delta$.

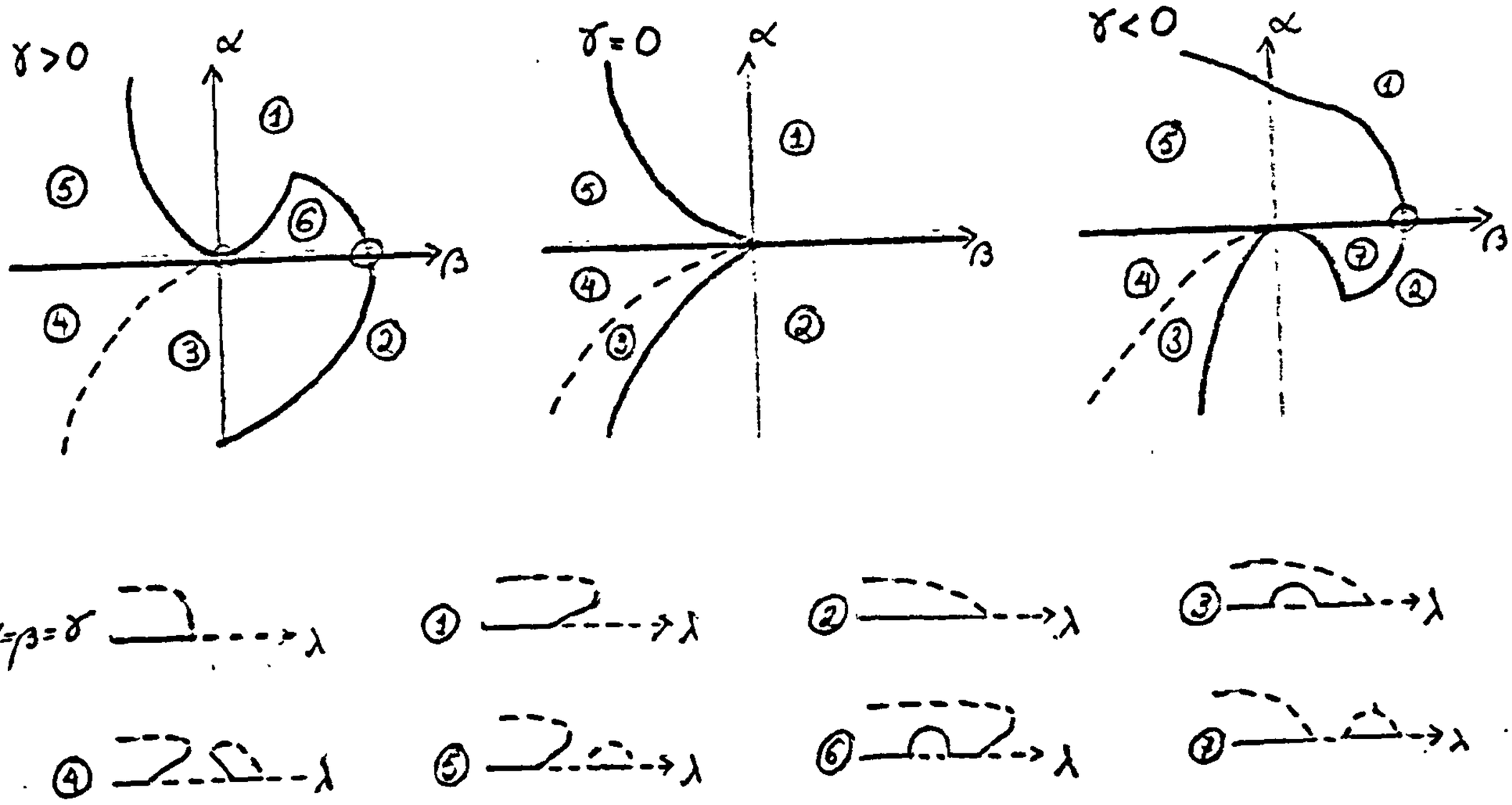

$\varepsilon\rho = 1$, $\varepsilon\delta = 1$

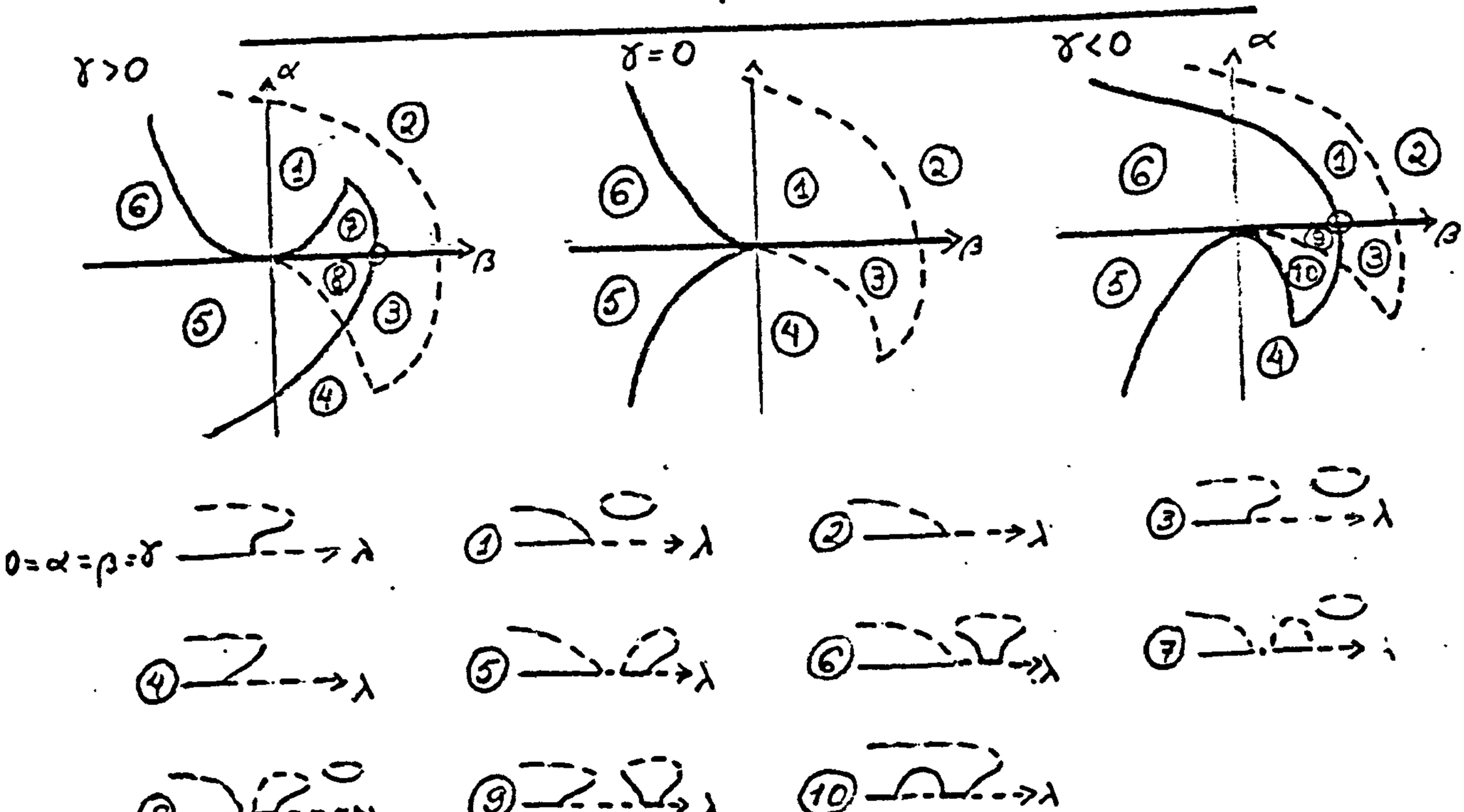

$\varepsilon\rho = 1$, $\varepsilon\delta = -1$

Conventions:

Π_0 $\quad B_0$ $\quad B_1$

$0 : B_0 \cap \Pi_0$

Fig. III. 2.7

These are the first instances of unimodal germs that are not members of the one-parameter family (2.1) - they fail to satisfy the condition $a_{\lambda\lambda} \neq 0$. The germs $A(u,\lambda,\alpha,\beta,\gamma)$ on the universal unfolding of (2.7), however, are $\mathbb{Z}_2$-equivalent to a_b when (α,β,γ) is in $H_o \cap B_o$ and $A_{\lambda\lambda} \neq 0$, or, equivalently, when (α,β,γ) satisfies:

$$\begin{aligned} &\alpha = 0 \\ &\beta = \frac{\gamma^2}{4} \\ &\gamma \neq 0 \end{aligned} \qquad (2.7.1)$$

$$\varepsilon b = \varepsilon\delta/\sqrt{|\gamma/2|}.$$

i.e. the germs $A(u,\lambda,0,\frac{\gamma^2}{4},\gamma)$ are equivalent to (2.2) when ε sign $(\gamma) > 0$ and to (2.3) otherwise.

As γ approaches 0 (and therefore $\beta \to 0$), the modal parameter b tends to $\pm\infty$. In this way (2.7) can be seen as forming a transition between (2.2) and (2.3).

(2.8) Organizing centre:

$$a(u,\lambda) = \varepsilon u^3 + \delta\lambda u + \phi\lambda^2$$

$\mathbb{Z}_2$-codimension = 3

Defining conditions: $a_u = a_{uu} = a_\lambda = 0$

$a_{uuu} \neq 0,\ a_{\lambda\lambda} \neq 0,\ a_{u\lambda} \neq 0$

Universal unfolding:

$$A(u,\lambda,\alpha,\beta,\gamma) = \varepsilon(u^3+\gamma u^2+\beta u+\alpha) + \delta\lambda u + \phi\lambda^2$$

Critical sets:

$$B_0 = \{(\alpha,\beta,\gamma): \alpha = 0\}$$

$$B_1 = \{(\alpha,\beta,\gamma): \alpha = u^2(2u+s); \beta = -u(3u+2s); s = \gamma - \frac{\varepsilon\phi}{4}; u > 0\}$$

$$H_0 = \{(\alpha,\beta,\gamma): \alpha = -\varepsilon\phi\beta^2\}$$

$$H_1 = \{(\alpha,\beta,\gamma): \alpha = \frac{\gamma^3}{27} - \varepsilon\phi(\frac{\gamma^2}{3} - \beta)^2, \gamma < 0\}$$

$$DL_0 = \{(\alpha,\beta,\gamma): \alpha = -\varepsilon\phi(\frac{\gamma^2}{4} - \beta)^2, \gamma < 0\}$$

$$DL_1 = \Phi$$

The germs $A(u,\lambda,\alpha,\beta,\gamma)$ satisfy

$$A(0,\lambda,\alpha,\beta,\gamma) = A_u(0,\lambda,\alpha,\beta,\gamma) = A_\lambda(0,\lambda,\alpha,\beta,\gamma) = 0$$

if and only if $\alpha = \beta = 0$ and $\lambda = 0$, and if $\gamma \neq 0$ we have

$$A_{uu}(0,0,0,0,\gamma).A_{\lambda\lambda}(0,0,0,0,\gamma) = 4\varepsilon\phi\gamma \neq 0$$

Therefore, the germs $A(u,\lambda,0,0,\gamma)$ are $\mathbb{Z}_2$-equivalent at $u = 0$, $\lambda = 0$ to one of the germs (2.1), according to the following table:

(2.8) (2.1)

$\varepsilon\phi = 1$ $\begin{cases} \gamma > 0 & (2.3) \quad \varepsilon B = \dfrac{\varepsilon\delta}{2\sqrt{|\gamma|}} \\ \gamma < 0 & (2.2) \quad \varepsilon B = \dfrac{-\varepsilon\delta}{2\sqrt{|\gamma|}} \end{cases}$

$\varepsilon\phi = -1$ $\begin{cases} \gamma > 0 & (2.2) \quad \varepsilon B = \dfrac{\varepsilon\delta}{2\sqrt{|\gamma|}} \\ \gamma < 0 & (2.3) \quad \varepsilon B = \dfrac{-\varepsilon\delta}{2\sqrt{|\gamma|}} \end{cases}$

Critical sets and stable bifurcation diagrams for cases $\varepsilon\delta = +1$ are shown in Figs. III.2.8 (for $\varepsilon\phi = -1$), III.2.9 and III.2.10 (for $\varepsilon\phi = +1$). Where $\varepsilon\delta = -1$ the bifurcation diagrams can be obtained substituting $-\lambda$ for λ in the case with the same values of ε and ϕ.

Figure III.2.8a shows the unstable diagrams for $\varepsilon\phi = -1$, $\alpha = \beta = 0$, and those of the organizing centres of (2.2) and (2.3).

In Fig. III.2.8b and c) we show the intersection of the critical sets with the planes γ= constant, $|\gamma|$ small (actually $|\gamma| < \frac{1}{12}$). If $\gamma > 0$ (Fig. III.2.8b), only the critical sets B_0, H_0, and B_1 are present, and the bifurcation diagrams are identical to those appearing in the unfolding of (2.2). For $\gamma < 0$ (Fig. III.2.8c) the varieties H_1 and DL_0 approach H_0 as γ tends to zero, and the critical sets divide $\mathbb{R}^3$ into 15 different components containing the origin in their closure. Five of these regions are connected to those

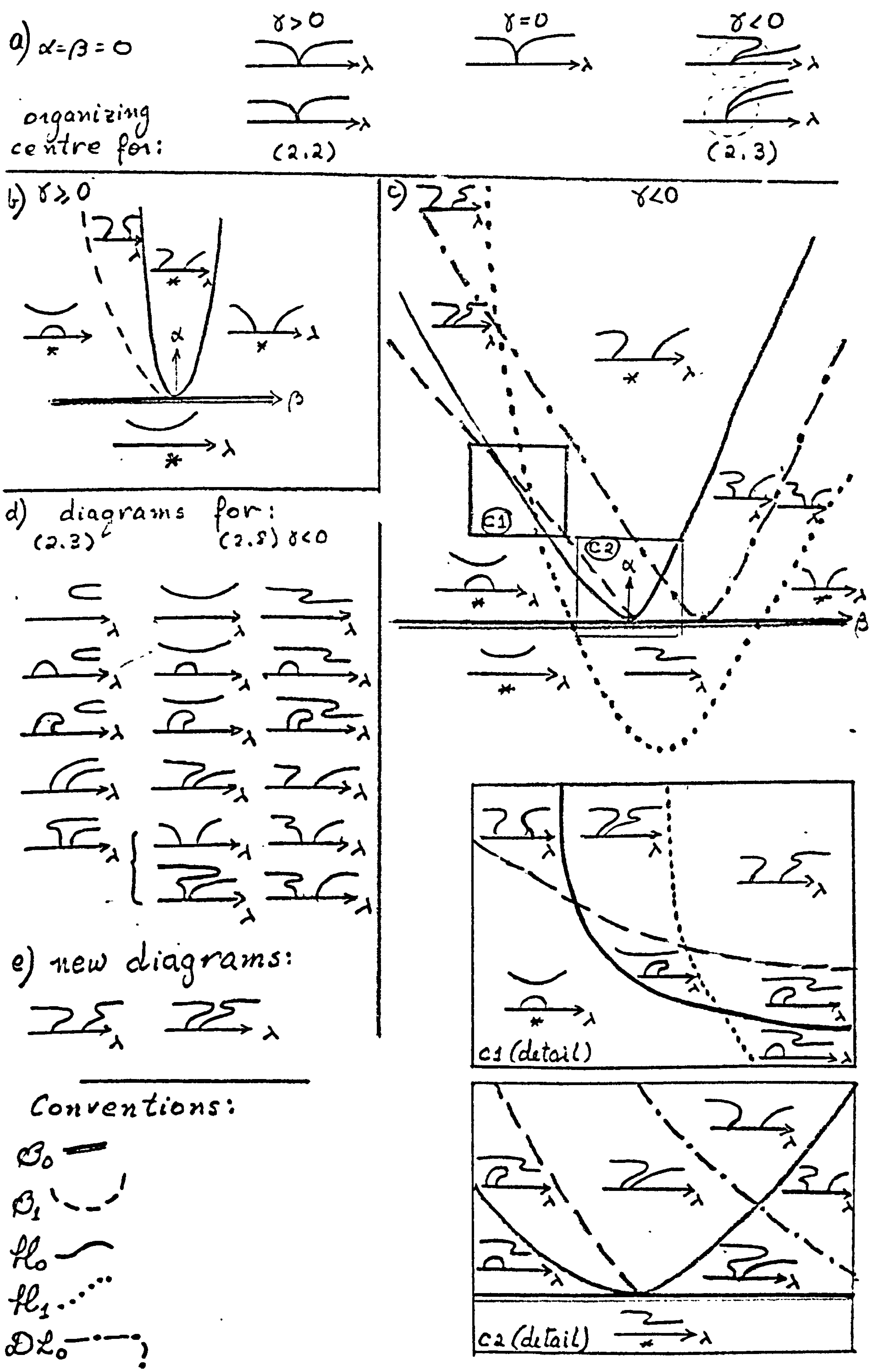

Fig III.2.8 - (germ 2.8, $\varepsilon\varphi=-1$)

in the $\gamma > 0$ half-space, and the bifurcation diagrams in twelve of the new regions can be obtained from the unfolding of (2.3) (see, Fig. III.2.8d), including 4 repetitions, marked *. The two altogether new diagrams are shown in Fig. III.2.8e.

Stable diagrams for the case $\varepsilon\phi = +1 = \varepsilon\delta$ are shown in Fig. III.2.9, as well as the unstable ones at $\alpha = \beta = 0$ (III.2.9a). Diagrams present in the unfolding of the family (2.1) are reproduced for comparison. The critical sets divide a small neighbourhood of the origin in $\mathbb{R}^3$ into 16 components, represented in Fig. III.2.10. The numbering of diagrams in Fig. III. 2.9 indicates the corresponding region in III.2.10.

organizing centre

a)

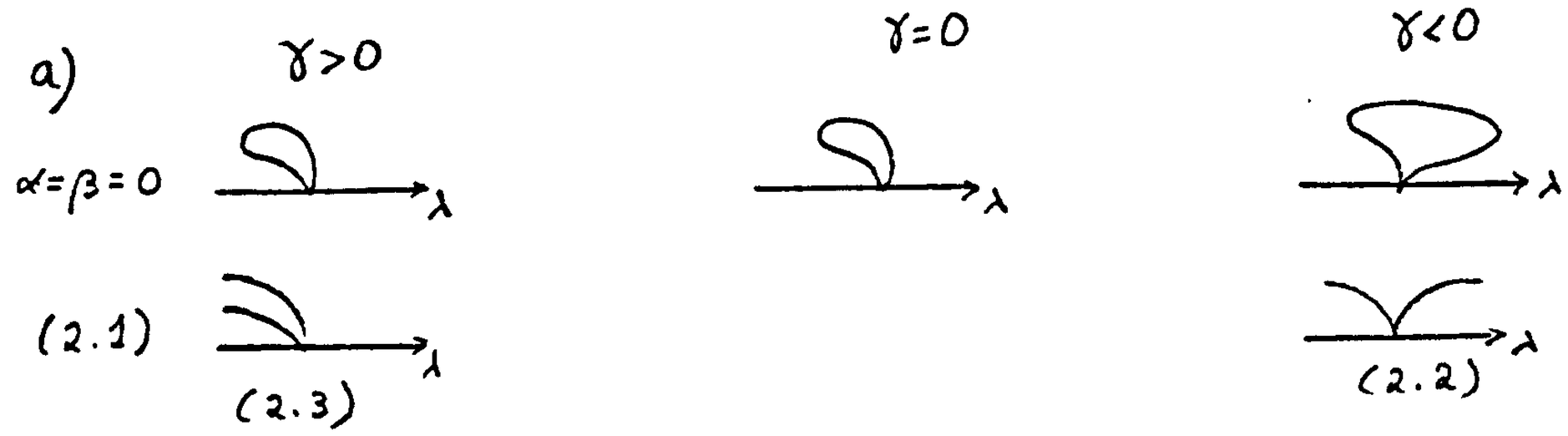

---

b) (2.2) (2.8), γ<0 — stable diagrams

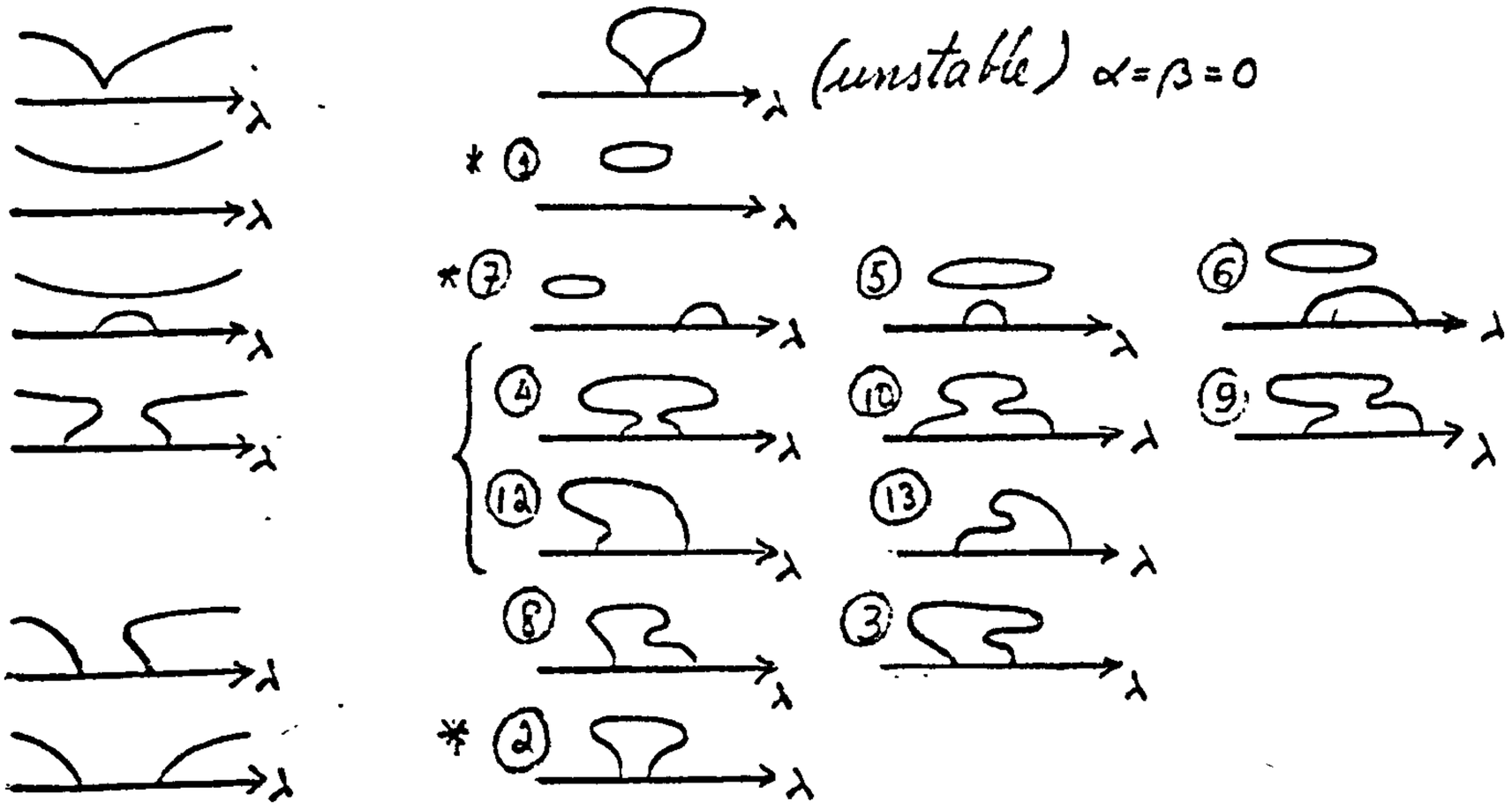

---

c) (2.3) (2.8), γ≥0

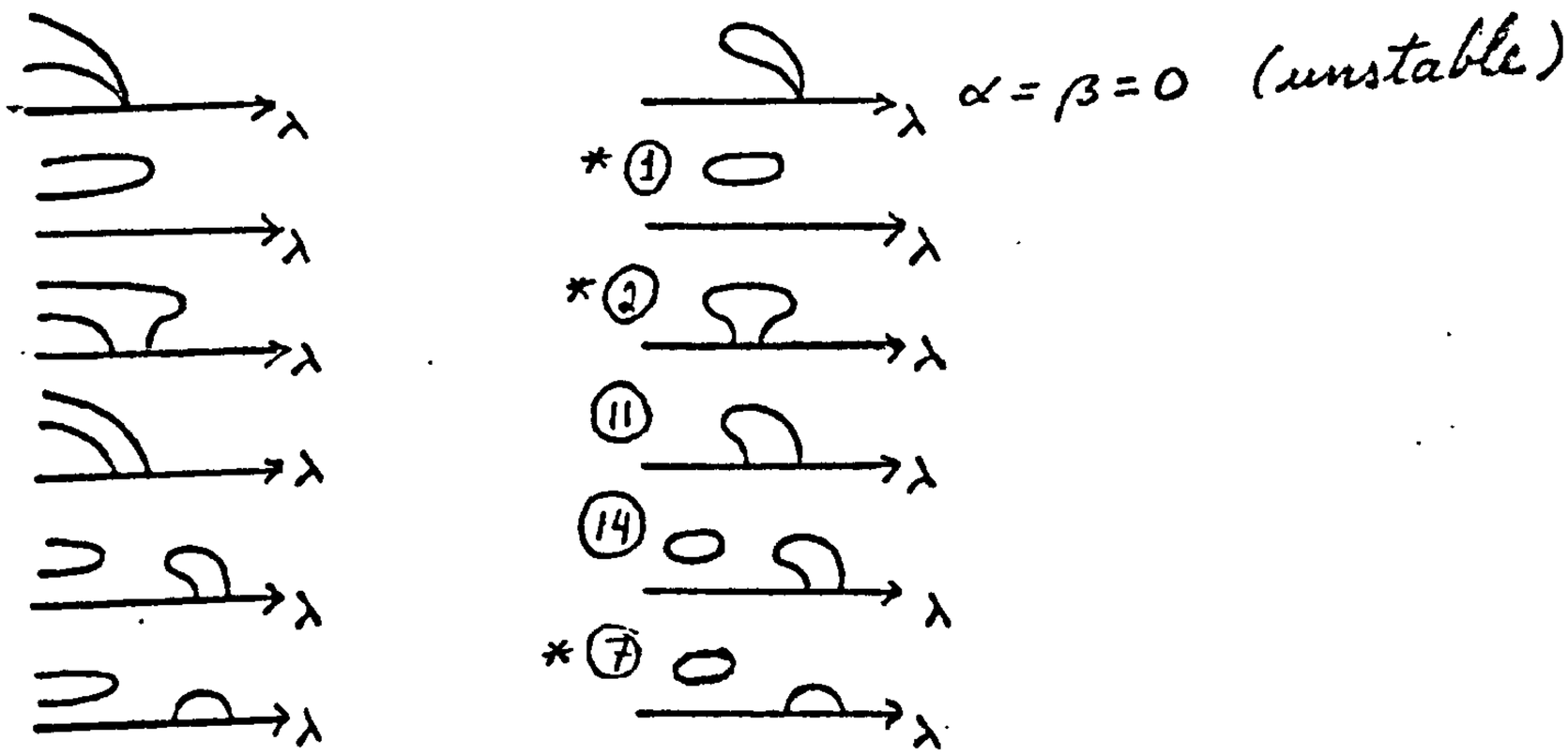

---

d) New diagrams:

Fig III.2.9 Diagrams for (2.8), εβ=1. Numbers in circles refer to areas in Fig III.2.10.

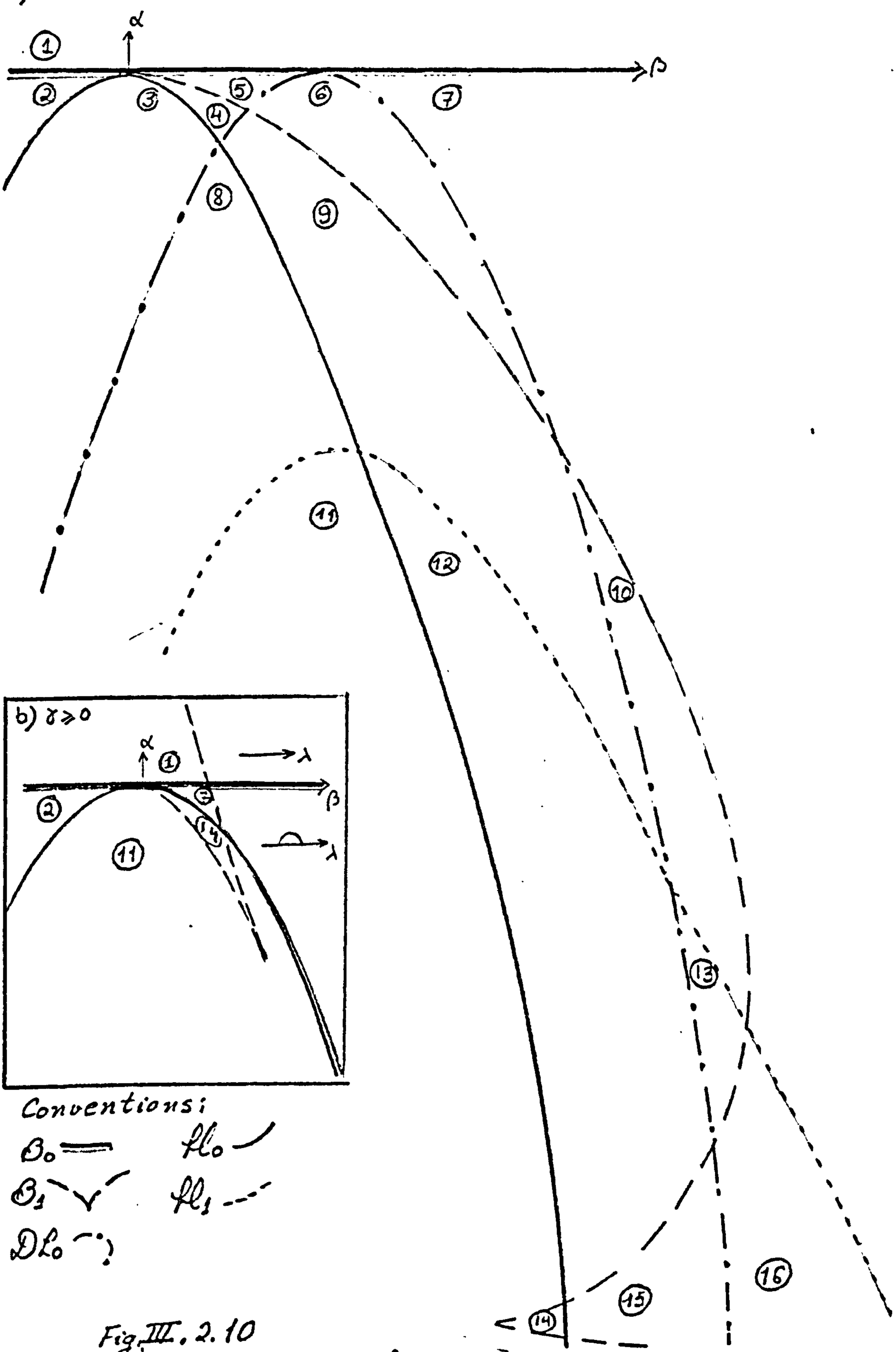

Fig. III. 2.10
Critical sets for germ (2.8), $\varepsilon\rho = +1$

CHAPTER IV : NERVE IMPULSE EQUATIONS

0. INTRODUCTION

The classical experiments by Hodgkin, Huxley and Katz [16], [17], [18], [19] consisted of applying an electrical shock of known intensity (I) to a neurone and measuring the resulting change in the difference of electric potential (V) across the cell membrane. The generally accepted explanation of what takes place involves changes in membrane permeability to Na^+, K^+ and other ions. The model is described by the following system of differential equations, known in the literature as clamped Hodgkin and Huxley equations [17]:

$$H1 \qquad \begin{cases} \frac{dV}{dt} = - G(V,M,N,H) - I \\ \frac{dM}{dt} = \Phi(T)[(1-M)\alpha_m(V) - M\beta_m(V)] \\ \frac{dN}{dt} = \Phi(T)[(1-N)\alpha_n(V) - N\beta_n(V)] \\ \frac{dH}{dt} = \Phi(T)[(1-H)\alpha_h(V) - H\beta_h(V)] \end{cases}$$

or, writing $U = (V,M,N,H)$, $\frac{dU}{dt} = \Gamma(U,I,T)$, where M, N and H are ionic conductances across the membrane, T is the temperature,

$\Phi(T) = 3^{\frac{T-6.3}{10}}$, and the function G is given by:

$$G(V,M,N,H) = \bar{g}_{Na}M^3H(V-V_{Na}) + \bar{g}_KN^4(V-V_k)+\bar{g}_L(V-V_L).$$

The constants:

$$\bar{g}_{Na} = 120. \qquad \bar{g}_K = 36. \qquad \bar{g}_L = 0.3$$

$$V_{Na} = -115. \qquad V_K = 12. \qquad V_L = 10.599.$$

were obtained by Hodgkin, Huxley and Katz from experimental data, and have the dimensions of conductance/cm^2 for the $\bar{g}$s, and volts for the Vs.

The functions α_j and β_j, j = M,N,H, are given by:

$$\alpha_M(V) = \Psi(\frac{V+25}{10}) \qquad \beta_M(V) = 4\ e^{(V/18)}$$

$$\alpha_N(V) = \Psi(\frac{V+10}{10}) \qquad \beta_N(V) = 0.125\ e^{(V/80)}$$

$$\alpha_H(V) = 0.07\ e^{(V/20)} \qquad \beta_H(V) = \left(1 + e^{(V+30)/10}\right)^{-1}$$

where $\Psi(0) = 1$, and $\Psi(x) = \frac{x}{e^x-1}$ for $x \neq 0$.

Notice that $\alpha_j(V) + \beta_j(V) \neq 0$ for all x and j.

For any choice of the parameters I and T, equations H1 have a steady-state solution (V_*,M_*,N_*,H_*,I,T), satisfying:

$$J_* = \frac{\alpha_J(V_*)}{\alpha_J(V_*) + \beta_J(V_*)} = j_\infty(V_*), \quad J = M,N,H$$

as well as $f(V_*) = G(V_*, m_\infty(V_*), n_\infty(V_*), h_\infty(V_*)) = -I$.

Since within physiologically meaningful range f is monotonically increasing (Fig. IV.0.1), it is invertible, and therefore we can change coordinates:

$$\lambda = f^{-1}(-I) \qquad v = V-\lambda \qquad u = (v,m,n,h)$$

$$m = M-m_\infty(\lambda) \qquad n = N-n_\infty(\lambda) \qquad h = H-h_\infty(\lambda).$$

In the new coordinates the equations become

$$\frac{du}{dt} = \gamma(u,\lambda,T) \text{ with } \gamma(0,\lambda,T) \equiv 0 \text{ or:}$$

$$\text{HH} \begin{cases} \frac{dv}{dt} = C(v,m,n,h,\lambda) \\ \\ \frac{dj}{dt} = \Phi(T)\ [(1-j-j_\infty(\lambda))\ \alpha_J(v+\lambda) - (j-j_\infty(\lambda))\ \alpha_J(v+\lambda)] \end{cases}$$

where $j = m,n,h$ and

$$C(u,\lambda) = \bar{g}_{Na}[m_\infty^3(\lambda)h_\infty(\lambda)(\lambda-V_{Na}) -$$

$$- (m+m_\infty(\lambda))^3(h+h_\infty(\lambda))(\lambda+v-V_{Na})] +$$

$$+ \bar{g}_K[n_\infty^4(\lambda)(\lambda-V_K) - (n+n_\infty(\lambda))^4(\lambda+v-V_K)] - \bar{g}_L v.$$

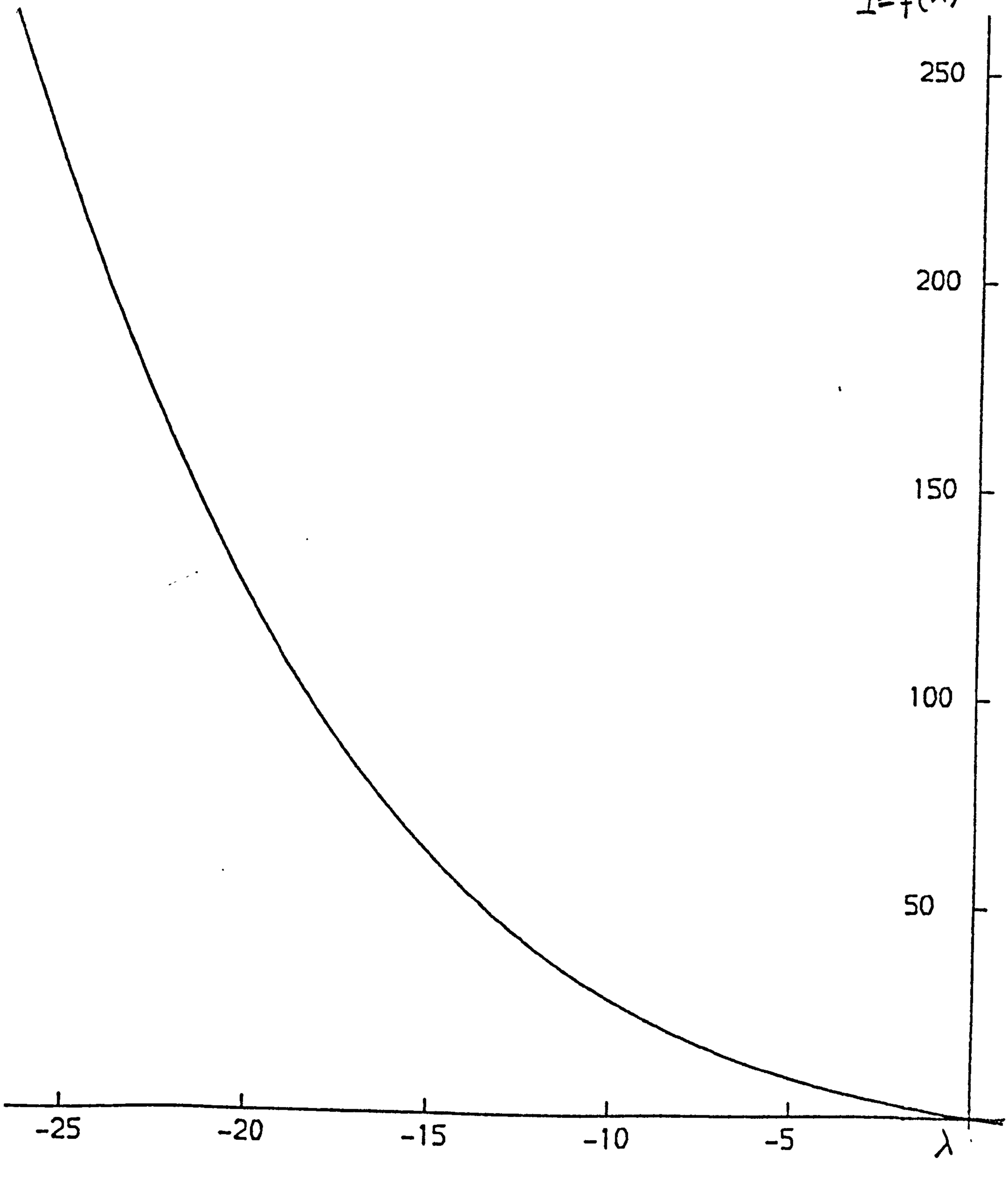

Fig. IV.0.1 graph of $\bar{f}(\lambda) = \bar{G}(\lambda, m_\infty(\lambda), n_\infty(\lambda), h_\infty(\lambda))$

This change of variables reduces the problem to the form used in previous chapters for the classification of degenerate Hopf bifurcation germs. It also has the advantage of eliminating one error factor in numerical computations, because it is no longer necessary to evaluate f^{-1}, but since λ decreases when I grows, all our pictures are mirror images of those obtained by other authors. From now on we shall refer to HH as the Hodgkin and Huxley equations, or the nerve impulse equations.

IV. 1 PRELIMINARY RESULTS.

The eigenvalues of $\frac{d\gamma}{du}(0,\lambda,T)$ were computed numerically for several values of λ and T within physiologically significant range, using analytical expressions for the partial derivatives of γ and NAG subroutines for the linear algebra.

We found that for each value of λ and T there are two real eigenvalues and a complex conjugate pair,

(1.1) $\qquad \sigma(\lambda,T) + i\theta(\lambda,T).$

For temperatures greater than $29^{o}C$ the complex eigenvalues have strictly negative real parts (see Fig. IV.1.1), while below $28.5^{o}C$ the picture changes and the complex pair

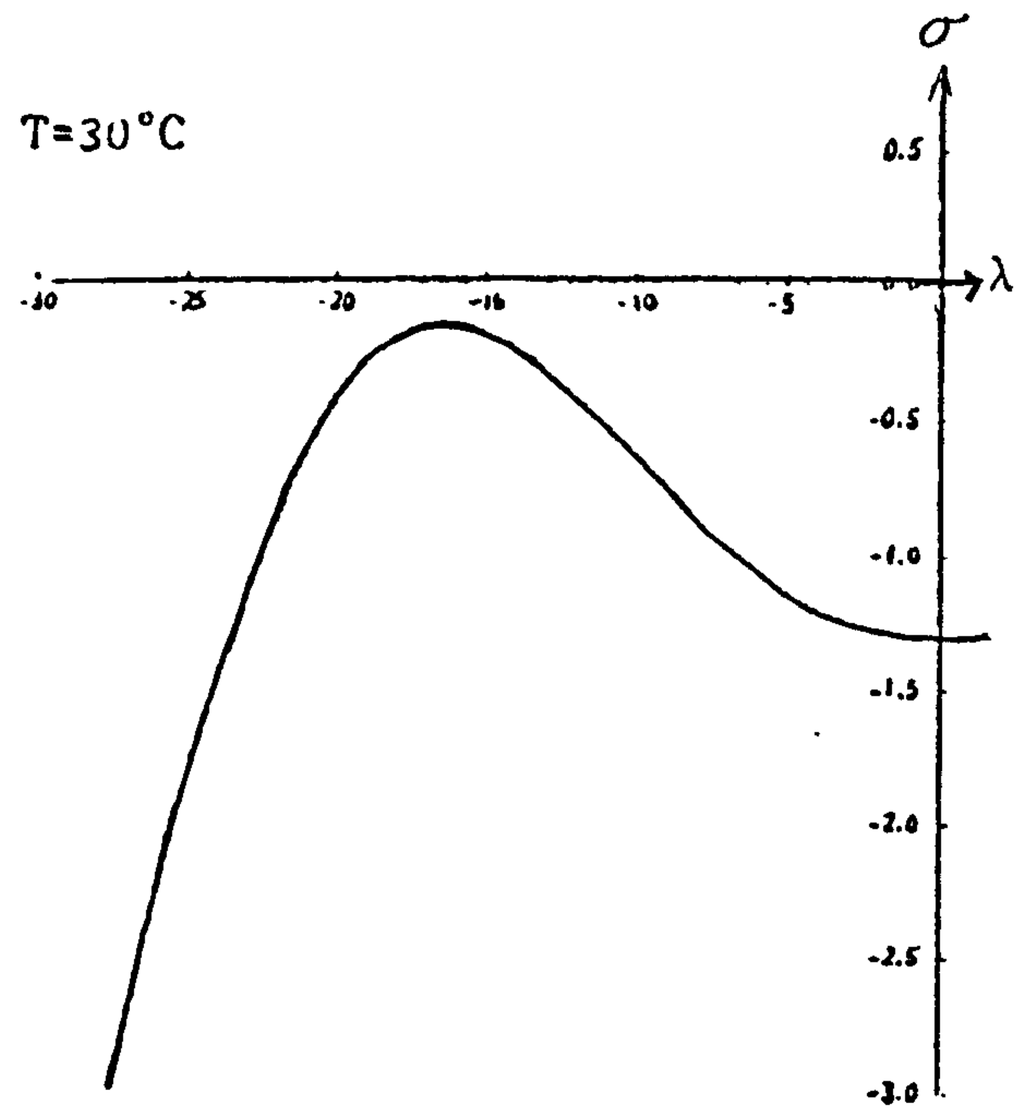

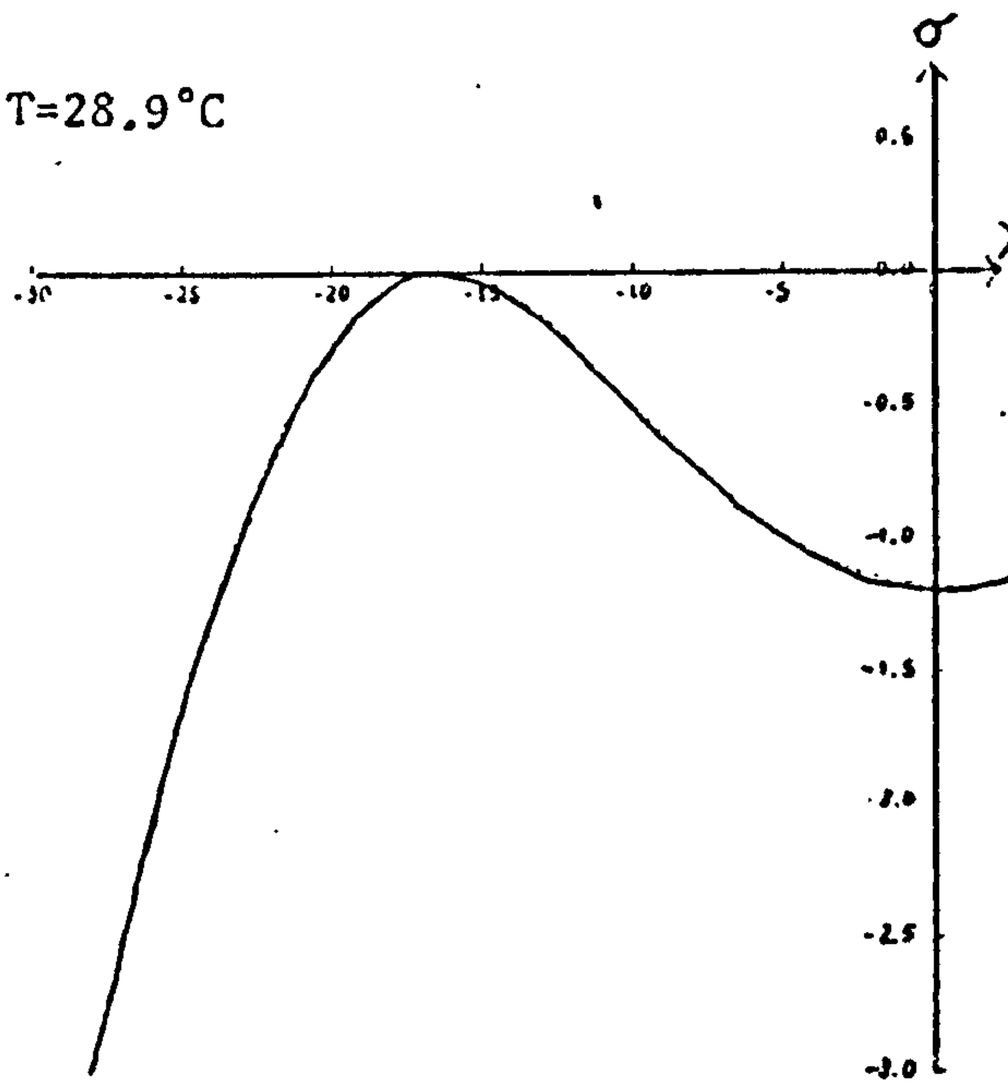

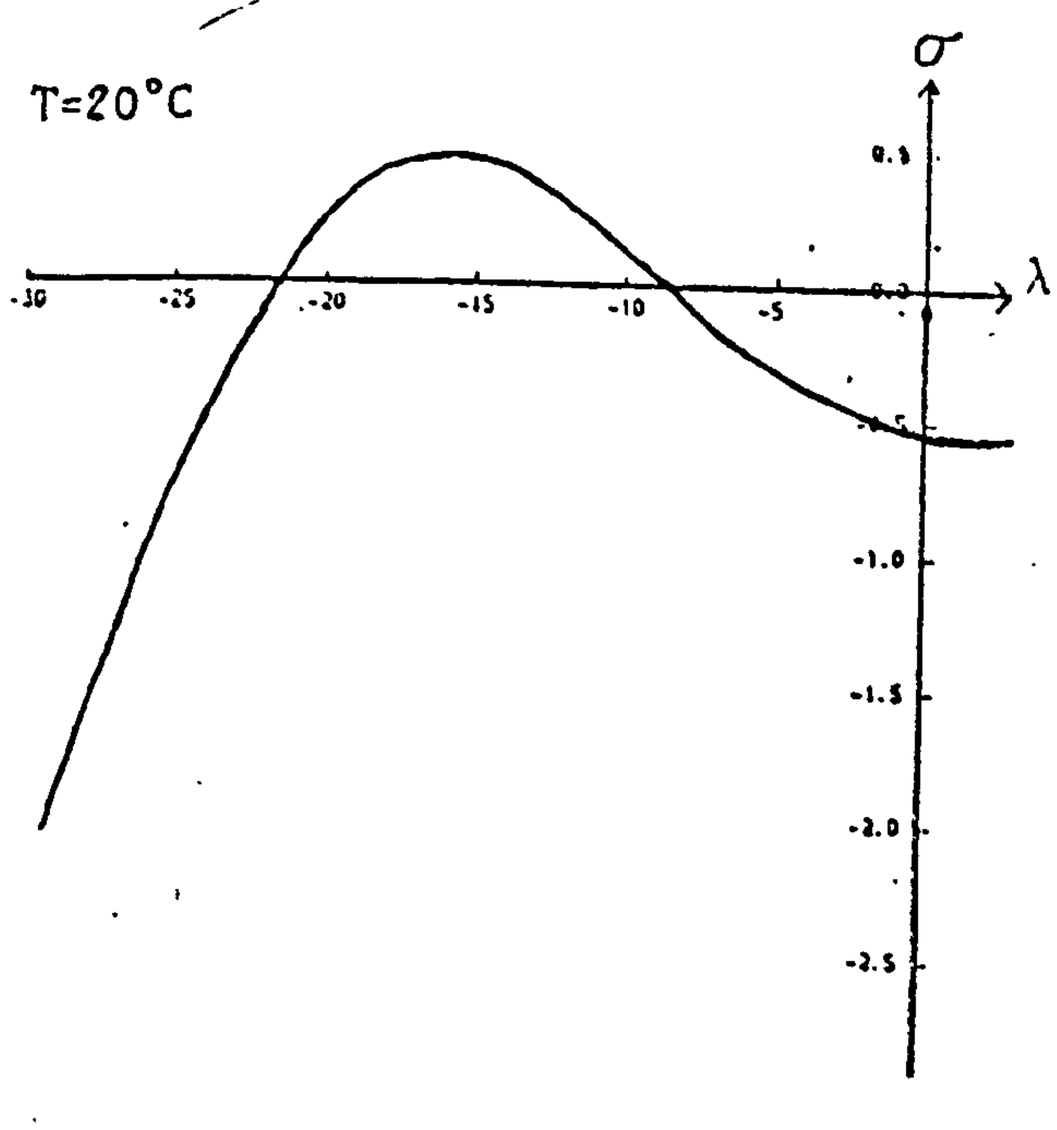

Figure IV.1.1. The real part $\sigma(\lambda,T)$ of the complex eigenvalues of $\frac{d\gamma}{du}(0,\lambda,T)$ plotted against λ.

crosses the imaginary axis twice, transversally. This confirms the results of Hassard [12] for temperatures a $6.3^{o}C$ and $0.^{o}C$.

Therefore, for $T < 28.5^{o}C$, the equations HH satisfy the hypotheses of the Hopf bifurcation theorem [20], [13]. This establishes the existence of two families of periodic solutions bifurcating from the equilibrium $(0,\lambda,T)$ at the points where the eigenvalues are purely imaginary. If we apply the reduction of Ch. II to equations HH at these points, the reduced germ $r(\gamma) = xa(x^2,\lambda)$ will be $\mathbb{Z}_2$ equivalent to one of the germs (III. 1.1).

The last assertion can be verified computing the derivatives a_u and a_λ of the reduced germ, at the two points $(0,\lambda_1)$ and $(0,\lambda_2)$ $(\lambda_1 > \lambda_2)$ where the eigenvalues of $d_u\gamma$ cross the imaginary axis.

The formulae in Appendix 1, relating derivatives of γ to those of a, were used to write a FORTRAN program that computes $a_u(0,\lambda_i,T)$, using the analytical expressions for the derivatives of γ. The eigenvector c of $d_u\gamma$ corresponding to the eigenvalue θi (see III.1) was normalized so as to have 1 as its first component. Therefore the bifurcation diagrams become λ × amplitude graphs in the V direction, i.e., in the direction of the only variable that can be observed in experiments. This choice also has the advantage of allowing comparison with the results of other authors.

Some of the results are shown in Table IV.1.2.

The other derivative, a_λ, satisfies

$$a_\lambda = \frac{-d\theta}{d\lambda}(\lambda,T)$$

and therefore a_λ is non-zero at both $(0,\lambda_1)$ and $(0,\lambda_2)$ for low (< 28.85) temperatures. Comparing with case(III.1.1) we have $\delta = 1$ at $(0,\lambda_1)$ and $\delta = -1$ at $(0,\lambda_2)$.

At the first bifurcation point $(0,\lambda_2)$, the derivative a_u is always positive. In the language of Chapter III, $\varepsilon = +1$, $\delta = -1$. At $(0,\lambda_1)$, and for $T < 28.853^oC$ we have $a_u < 0$ and $\varepsilon = -1$ $\delta = \pm 1$. Therefore, both periodic solution branches grow towards the right, as shown in Fig. IV.1.3. This is the same result obtained by Rinzel and Miller (cf. Fig. IV.1.4).

As T grows, however, $a_u(0,\lambda_1)$ changes sign (Table IV.1.2) so that $\varepsilon = -1$ and the second periodic solution branch grows towards the left, as indicated in Fig. IV.1.3b. The change in the bifurcation diagrams is analogous to the crossing of the hysteresis variety H_0 (II. 4.8).

For some temperature T_c the λ-parametrized curves of complex eigenvalues must be tangent to the imaginary axis - the graph of the real parts of the eigenvalues, plotted against λ always has a maximum (Fig. IV.1.1), and this maximum changes sign between those temperatures.

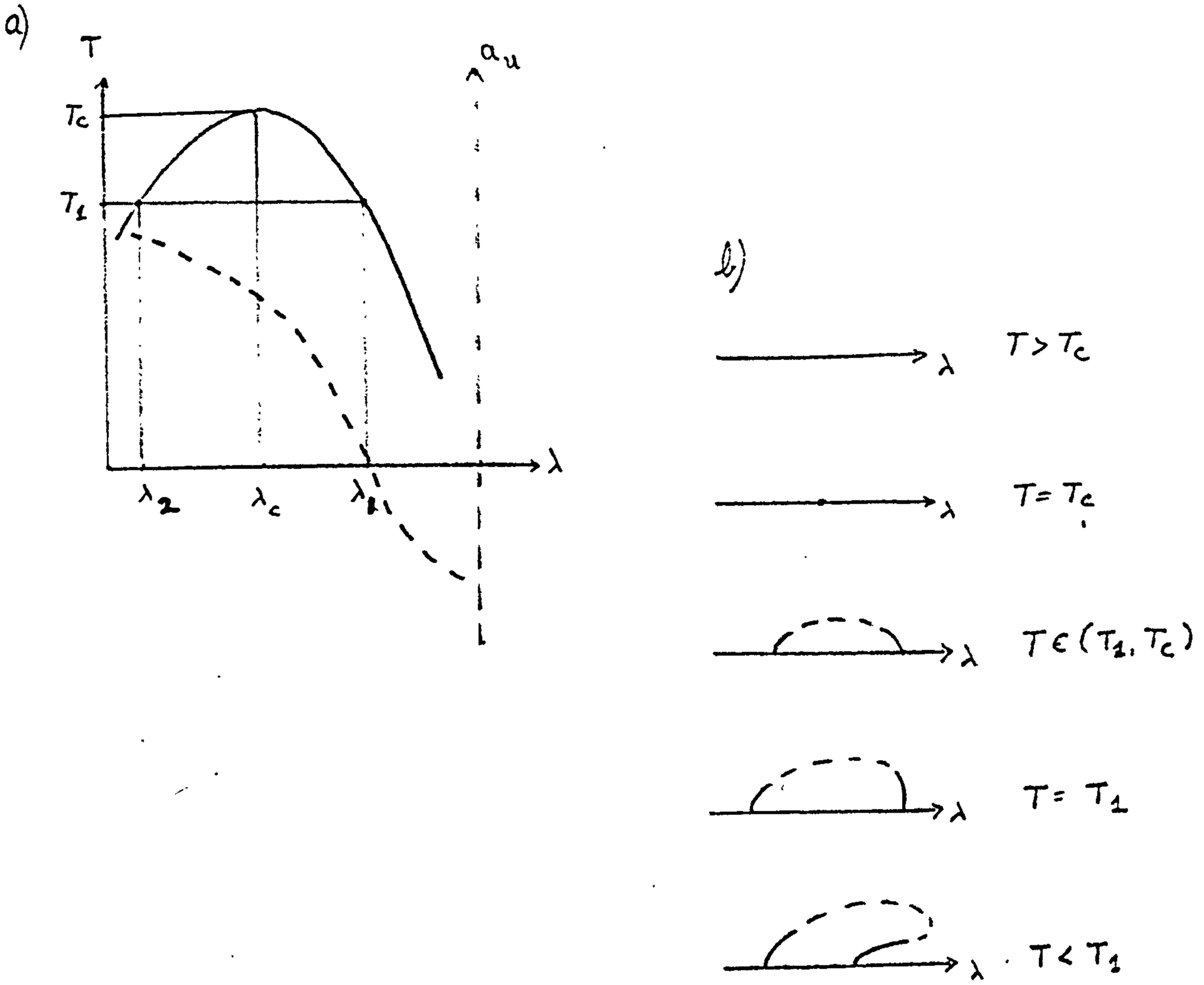

Figure IV.1.3. Bifurcation diagrams for the Hodgkin and Huxley equations:

(a) Schematic representation of $T(\lambda)$ = temperature where there is a Hopf bifurcation at λ (solid line), and $a_u(0,\lambda,T(\lambda))$ (dashed line).

(b) Corresponding bifurcation diagrams, with x standing for amplitude. Dashed lines correspond to hypothetical joining.

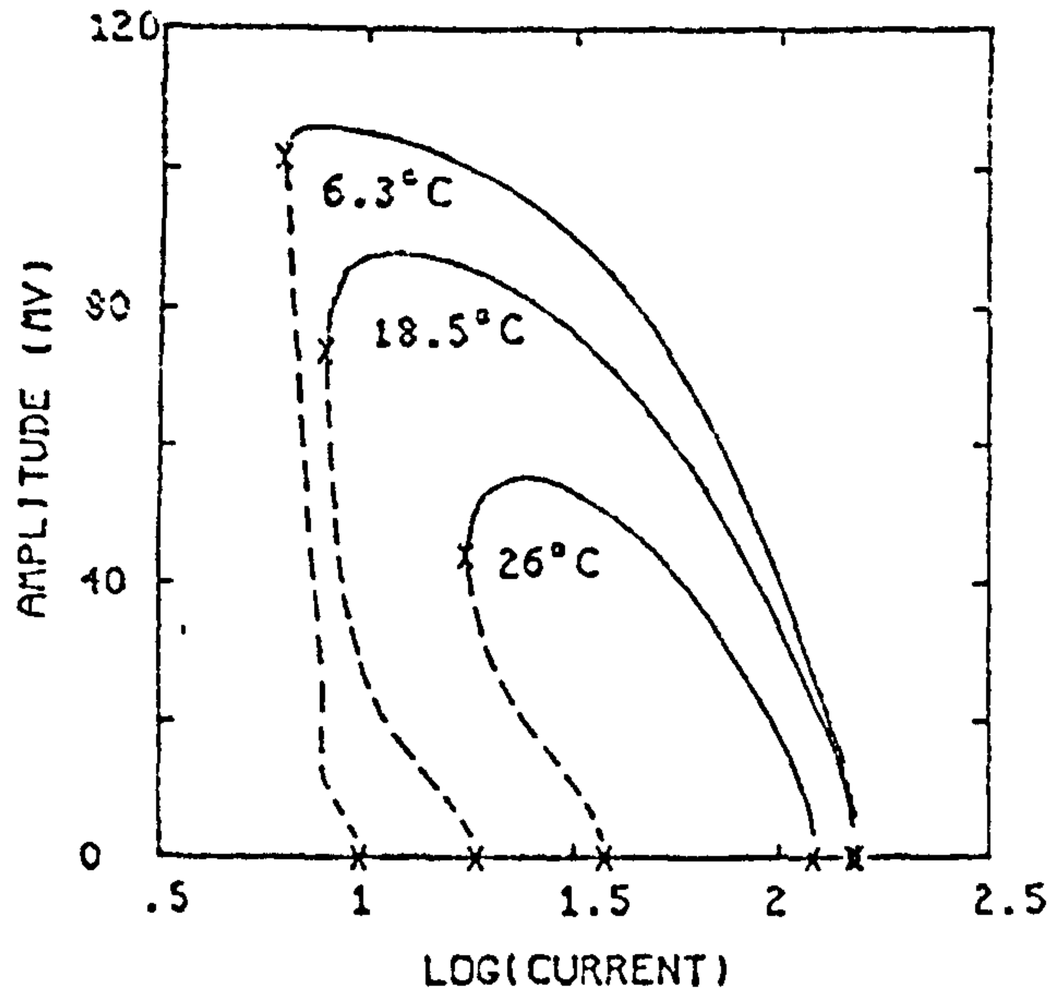

Figure IV.1.4. Amplitude (V) of periodic solutions of H1 as functions of applied current (I) for three temperatures. Dashed portions correspond to unstable limit cycles. Points of Hopf bifurcation and knees on amplitude curves are indicated by ×. Reproduced from [25].

There is only one value of λ, say λ_c, for which $d_u\gamma(0,\lambda_c,T_c)$ has purely imaginary eigenvalues, and, at this point $(0,\lambda_c,T_c)$, Hopf's hypothesis of transverse crossing is violated, and $a_\lambda = 0$. The analysis above does not apply at T_c, as well as at the temperature T_1 where $a_u(\lambda_1,0)$ changes sign. The problem is more degenerate at these two points.

TABLE IV. 1.2

	λ	$I(\lambda)$	$T(\lambda)$	$a_u \times 10^4$	
λ_1	-12.07	39.08	26.322	-42.59	
	-14.40	56.43	28.288	-20.59	
	-15.56	67.00	28.763	- 7.16	
	-16.14	72.80	28.851	- 0.33	
	-16.16	73.00	28.853	- 0.10	$a_u = 0$
	-16.22	73.62	28.855	0.60	
	-16.26	74.04	28.8566	1.06	
	-16.32	74.67	28.8579	1.75	
	-16.38	75.30	28.8580	2.44	maximum
λ_2	-16.46	76.15	28.8566	3.61	
	-18.08	95.03	28.339	20.11	
	-20.02	122.14	26.085	32.17	

$T(\lambda)$ = temperature where there is a Hopf bifurcation at

$I(\lambda)$ = stimulus intensity

a_u = $a_u(0,\lambda,T(\lambda))$

2. HUNTING FOR AN ORGANIZING CENTRE

If no further degeneracies are present at the temperature T_c where the two Hopf bifurcation points coalesce, then HH will be contact equivalent, after reduction, to one of the germs (III.1.2). The point $(0,\lambda_c,T_c)$ is called an *organizing centre* [26], [28] for the system HH - its local dynamics determines the behaviour of the periodic solution branch. In a neighbourhood of the organizing centre, we can think of HH as part of the unfolding of (III.1.2), with the temperature T playing the rôle of an unfolding parameter. Last section's discussion of the direction of bifurcation, and an inspection of Fig. III.1.2, shows that we are in case $\varepsilon\delta = 1$. Thus we have established that *if the derivative* $a_{\lambda\lambda}(0,\lambda_c,T_c)$ *is nonzero, then there is a neighbourhood of* $(0,\lambda_c,T_c)$ *in* $\mathbb{R}^3$ *where* $r(\gamma)$ is (III.1.2) *with* $\varepsilon\delta = 1$, *up to a* $\mathbb{Z}_2$*-invariant change of coordinates.*

An analogous discussion applies to the other degeneracy, viz. $a_u(0,\lambda_1,T_1) = 0$. This time the least degenerate candidate for an organizing centre is the germ (III.1.3) with $\varepsilon\delta = 1$. This germ has a single periodic solution branch, and for negative values of the unfolding parameter α, a characteristic knee appears in this branch, following the change of sign in a (cf. Fig. III.1.3). Therefore, *if* $a_{uu}(0,\lambda_2,T_1) \neq 0$, *then* $r(\gamma)$ *is* $\mathbb{Z}_2$*-contact equivalent, at* $(0,\lambda_1,T_1)$, *to* (III.1.3) *with* $\varepsilon\delta = 1$.

The point $(0,\lambda_2,T_1)$ is thus a second organizing centre for HH. The change of sign of a_u helps to explain why the same knee appears in Rinzel and Miller's picture (cf. Fig. IV. 1.4). This analysis, however, applies only to a neighbourhood of $(0,\lambda_2,T_1)$ not containing the second, non-degenerate, Hopf bifurcation point $(0,\lambda_2)$ present at the same temperature T_1.

In this way we have plausibly found two organizing centres for the Hodgkin and Huxley equations, each one of them accounting for one of the characteristics of the bifurcation diagrams observed by Rinzel and Miller, and reproduced in Fig. IV. 1.4. The fact that we have a single periodic solution branch undergoing two Hopf bifurcations is explained by the local analysis at $(0,\lambda_c,T_c)$, whereas the study of the equations at the point $(0,\lambda_2,T_1)$ explains the bend in the diagrams.

The other two characteristics that can be predicted from the analysis above are more difficult to establish numerically, viz. the absence of periodic orbits for temperatures higher than T_c, and the absence of the knee for $T \in (T_1,T_c)$. This last property would be quite conspicuous but for the tiny range of temperatures to which it applies, contained in the interval (28.853, 28.859). However, Rinzel and Miller observed that: "The dashed curves [for the knees on amplitude-versus-current bifurcation curves] are not quite complete, *due to a numerical*

deterioration in our knee-finding scheme at the highest temperatures. Nevertheless we are confident that they coalesce with the solid curves [for Hopf bifurcation points] at 28.85°C. This, of course, corresponds to the narrowing and collapse of the amplitude curve [...] onto the horizontal axis at $I = 75\ \mu A/cm^2$ for this limiting temperature. *Above this temperature no periodic solutions to the* HH *equations with constant* I *arise through Hopf bifurcation*." [25] (our italics)

3. THE PERTURBED HODGKIN AND HUXLEY EQUATIONS

In an attempt to bring the two organizing centres together into a highly degenerate point, we perturbed the equations HH, by varying the values of the average ion permeabilities g_{Na} and $\bar{g}_K$. The numerical proximity of the two points in question suggests this procedure as a natural way of studying the transition from one local behaviour to the other. The more degenerate organizing centre thus obtained is called a *hidden organizing centre*, since the local dynamics of the perturbed equations around this point contains all the information about the change in the direction of bifurcation discussed in the preceding sections. A more detailed account of hidden organizing centres can be found in [26] or in [28]

Variations in the average ion permeabilities $\bar{g}_{ion}$ did not change the pattern of two Hopf bifurcations below a critical temperature $T_c(\bar{g}_{ion})$ and a single one at T_c, very much like Fig. IV. 1.1. Figure IV. 3.1 shows $a_u(0, \lambda_c(\bar{g}_{Na}), T_c(\bar{g}_{Na}))$ for several values of average sodium permeability. For each value of $\bar{g}_{Na}$, the critical point $(\lambda_c(\bar{g}_{Na}), T_c(\bar{g}_{Na}))$ was determined as the maximum of the curve:

(3.1) $T(\lambda, \bar{g}_{Na})$ = temperature for which there is a Hopf bifurcation at λ. The curve $T(\lambda, 120)$ is shown as a solid line in Fig. IV. 1.3a.

A search by the golden section [23] was carried out to determine the maximum of $T(\lambda, \bar{g}_{Na})$ for 10 different values of $\bar{g}_{Na}$. Around $\bar{g}_{Na}$ = 80 the computations of the eigenvalues seem to break down. For $\bar{g}_{Na} \in [85, 130]$, the procedure was repeated with increasing precision in the initial guess, until the computed values of a_u agreed to within three significant figures in several successive computations. The result is that *for some value* $\bar{g}$ *of* $\bar{g}_{Na}$ *between* 105 *and* 110, i.e. *within* 10% *of the original value of* 120, *there is a single generalized Hopf bifurcation at* $(0, \lambda_c(\bar{g}), T_c(\bar{g}))$, *with*

$$a_u(0, \lambda_c(\bar{g}), T_c(\bar{g})) = 0.$$

This is our hidden organizing centre.

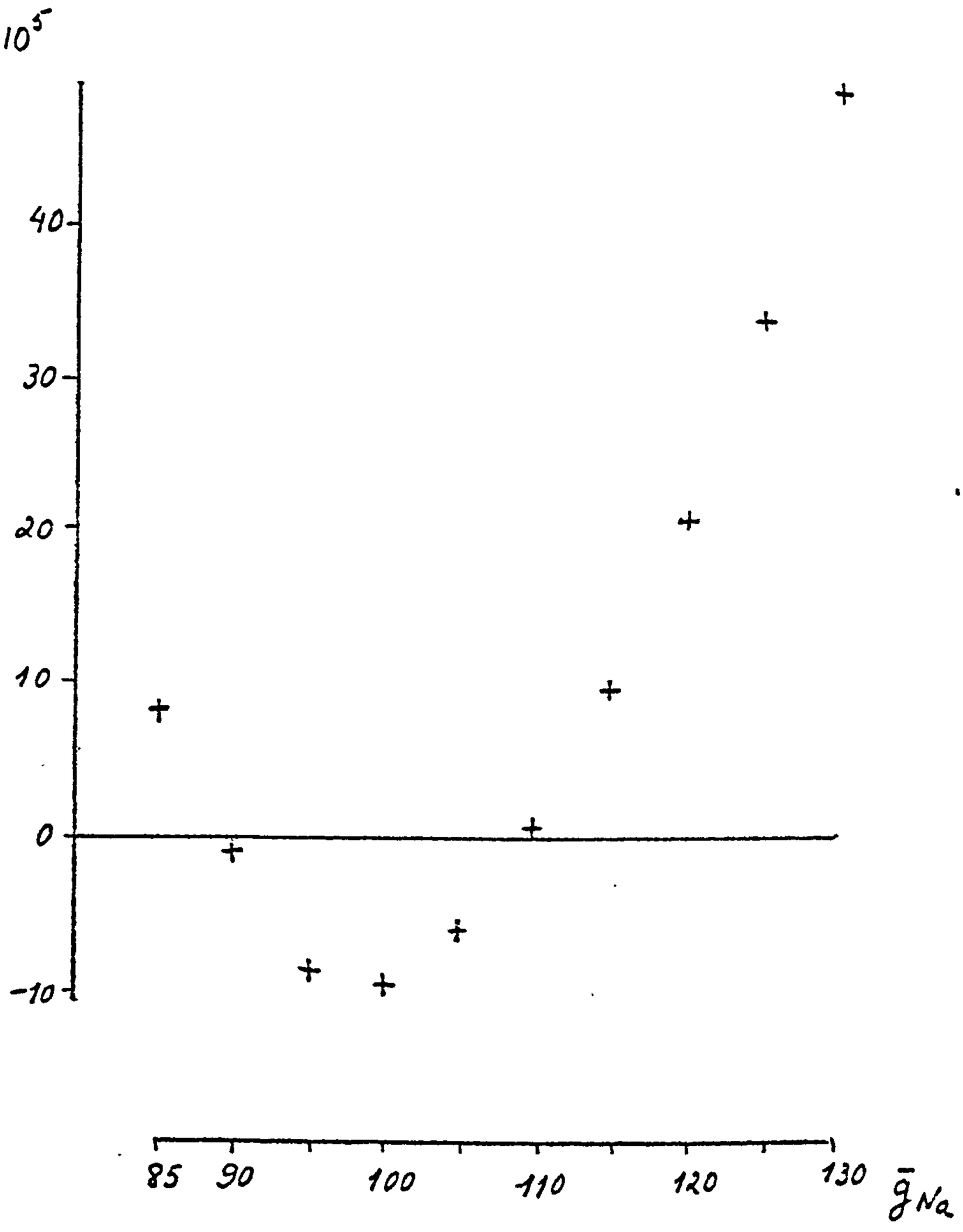

Fig. IV.3.1 $a_u(0, \lambda_c(\bar{g}_{Na}), T_c(\bar{g}_{Na}))$ for the perturbed Hodgkin and Huxley equations

Since the two Hopf bifurcation points coalesce at $(0, \lambda_c(\bar{g}), T_c(\bar{g}))$, we also have

$$a_\lambda(0, \lambda_c(\bar{g}), T_c(\bar{g})) = 0.$$

The conditions $a_u = a_\lambda = 0$ are satisfied by the 1-parameter family of germs (III.2.1). It is easy to see that any germ satisfying these conditions is abutted by the family (III.2.1), and therefore has modality > 1. All the germs described in Section III.2 are in this case, and in this sense the family (III.2.1) is the simplest possible candidate for the hidden organizing centre. If this is the case, we can presumably expect to have case (III.2.3) with $b < 0$, by comparison of the bifurcation diagrams in Figs. III.2.2, III.2.3 and those of Figs. IV. 1.3, IV. 1.4. Nevertheless it is impossible to decide rigorously which of the cases $b = -1$, $b < -1$ or $-1 < b < 0$ takes place, without computing the derivatives a_{uu}, $a_{u\lambda}$, $a_{\lambda\lambda}$ and estimating the modal parameter

$$b = \frac{a_{u\lambda}}{|a_{uu} \cdot a_{\lambda\lambda}|^{\frac{1}{2}}} .$$

Assuming this computation can be carried out successfully (as it is in the next section), and if no further degeneracy is present, we can visualize HH as a surface on $\mathbb{R}^3$ (α-β-b space) fibred by the T-parametrized curves corresponding to fixed values of $\bar{g}_{Na}$. The two zeros of the graph in Fig. IV. 3.1 will correspond to curves that go through the organizing centre (0,0,b). As $\bar{g}_{Na}$ is moved away from these two values, the curve moves to a position where it crosses

the varieties B_0 and H_0 at two different temperatures.

4. THE MODAL PARAMETER

We computed the second order derivatives a_{uu}, $a_{u\lambda}$, $a_{\lambda\lambda}$, and the modal parameter b for the Hodgkin and Huxley equations at $(0, \lambda_c(\bar{g}_{Na}), T_c(\bar{g}_{Na}))$, for values of g_{Na} near those where $a_u(0, \lambda_c(\bar{g}_{Na}), T_c(\bar{g}_{Na}))$ changes sign. The method used was the same for computing a_u - see appendices. Table IV. 4.1 contains the results of these calculations.

TABLE IV. 4.1

$\bar{g}_{Na}$	εb	$\varepsilon\phi$	germ in Chap. III.
115	-11.40	+1	
110	-12.69	+1	III.2.3
105	-16.92	+1	
90	6.93	-1	III.2.2
85	4.15	-1	

Table IV. 4.1 - Preliminary estimates of parameters for HH.

For $\bar{g}_{Na}$ around 110 we have found, as expected, $b < 0$, $\varepsilon\delta = \text{sign}(a_{uu}.a_{\lambda\lambda}) = +1$. We are in case III.2.3, with $b < -1$.

In this case, the set of values of λ for which periodic solutions exist, must contain an interval of infinite length (cf. Fig. III.2.3) for all choices of α and β. All the bifurcation diagrams of Section 1 appear, followed by a branch of periodic solutions whose amplitude is bounded away from zero. Such a branch can be easily missed in a numerical analysis, since it is not produced by a classical Hopf bifurcation.

The presence of this periodic solution branch implies that the linearly stable solution $u \equiv 0$ looses asymptotic stability. In this case, small perturbations of the equilibrium solution can have marked consequences, even if it is impossible to reach the stable periodic orbits. For a discussion of an analogous case, see the first chapter of [13].

At the second zero of a_u, however, we have $b > 0$ and $\varepsilon\delta = 1$, i.e. case (III.2.2). The bifurcation diagrams for this germ (Fig. III.2.2) are different from those described in Section 1. Moreover, there is no way to move continuously inside the family (III.2.1), from $\varepsilon\delta = 1$ to $\varepsilon\delta = -1$. This might be an indication of the presence of some further degeneracy.

IV. 5. ERRORS

In Chapter III we gave explicit criteria (from [6]) for determining whether a given $\mathbb{Z}_2$-equivalent germ $xa(x^2,\lambda)$ is $\mathbb{Z}_2$-equivalent to one of the cases listed. Each equivalence

class of germs with codimension ≤ 3 is characterized by a set of non-zero derivatives of the germ a (non-degeneracy condition), and by a set of derivatives that equal zero. In all cases we also need to know the sign of the non-zero derivatives.

All the information we have about HH, after reduction, is a numerical estimate of its derivatives. So far we were concerned with derivatives that are zero at special points. In the case of a_u we have shown that it changes sign as $\bar{g}_{Na}$ is varied, and therefore that it is zero at some point, if we make the assumption that a_u depends continuously on $\bar{g}_{Na}$.

For the derivative a_λ we used its expression in terms of the eigenvalues of γ, in order to obtain a zero. This time we had to assume, besides the continuity of the eigenvalues of γ with respect to λ and T, their differentiability in λ and the continuity in T, of their λ-derivative. These assumptions are justified, since γ is C^∞ in the range discussed, and the reduction process preserves differentiability.

Checking the non-degeneracy conditions is a more delicate task, since we cannot expect to obtain zero as the result of a computation. This poses the problem of deciding whether a small number is to be interpreted as a badly computed zero or as a small but non-zero value.

We tackled this problem by the same method used to study the zeros, viz. to observe the variation in the computed numbers as we change the values of some of the parameters appearing in HH. The expressions in Appendix 1, for the first and second order derivatives of a reduced germ were evaluated, for HH, at 10 values of $\bar{g}_{Na}$ in the interval [85, 130]. For each choice of $\bar{g}_{Na}$ the procedure was repeated along the curve $T(\lambda,\bar{g}_{Na})$ (3.1) for values of λ near the maximum, $\lambda_c(\bar{g}_{Na})$, of each curve. Thus, each choice of (λ,T) corresponds to a Hopf bifurcation point, and the computed expressions could still be interpreted as derivatives of $r(\gamma)$. Some results are shown in Figs. IV. 5.1 to IV. 5.5.

Yet another reason for evaluating the derivatives of $r(\gamma)$ at several points along $T(\lambda)$ (3.1), is the difficulty in determining accurately the maximum of $T(\lambda)$, since the search by the golden section converges very slowly in λ. Faster algorithms could not be used because they required extra information about $T(\lambda)$ that we did not have, usually the derivatives. The repetition of the calculations for several values of λ appeared thus as the simplest way of overcoming the error introduced by the lack of accuracy in the calculation of λ_c. Moreover, as we are never computing the derivatives at the organizing centre, but near it, it is important to establish the consequences, for the final result, of small variations in λ.

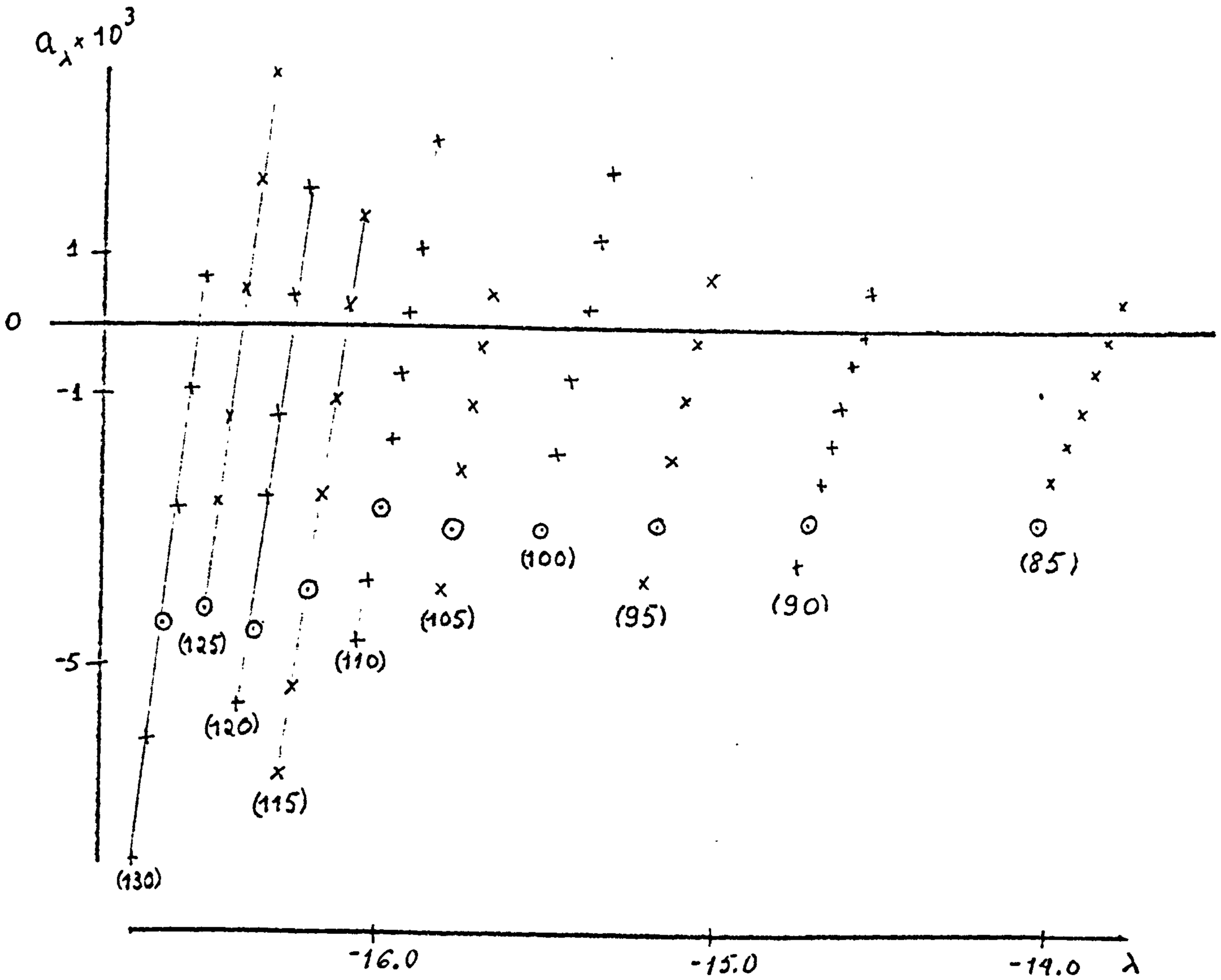

Fig. IV. 5.1 Variation of a_λ along the curve $T(\lambda, \bar{g}_{Na})$ the results of a first iteration on the search by the golden section are marked ⊙, and $\bar{g}_{Na}$ is indicated in brackets. Figures IV.5.2 to IV.5.5 use the same values of $\lambda, \bar{g}_{Na}$ and T.

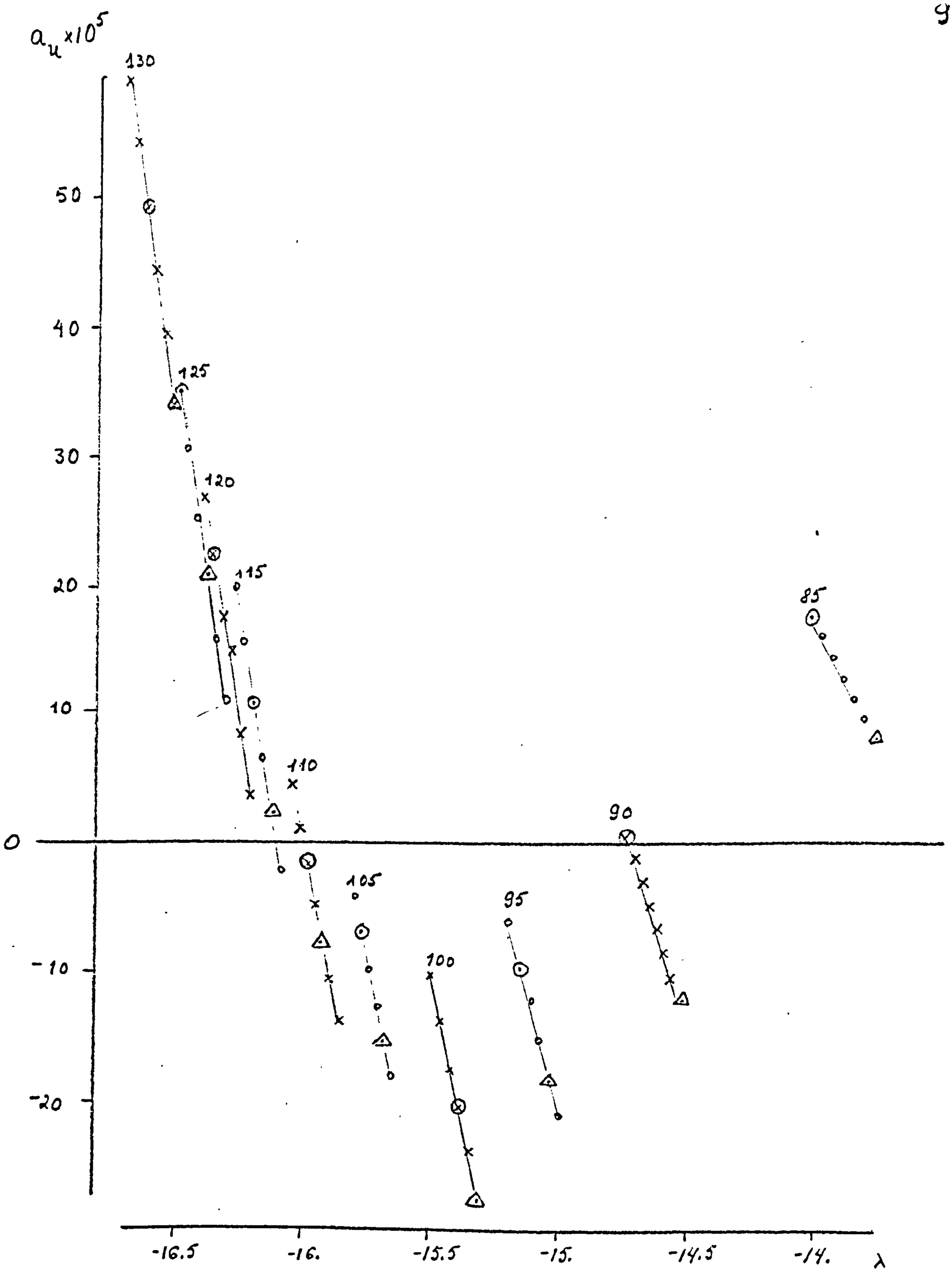

Fig. IV.5.2 Variation of a_u along $T(\lambda, \bar{g}_{Na})$. Conventions and data as in Fig. IV. 5.1. The minimum of $|a_\lambda|$ is also indicated as Δ

Figure IV.5.1 shows the values of a_λ, computed directly from the formulae in Appendix 1, when λ is perturbed from the critical value λ_c. For these calculations $T(\lambda)$ was evaluated with a prescribed maximum error of 10^{-3}. In most cases the actual error in T was less than 10^{-4} and the real part of the complex eigenvalue of $d_u\gamma$ was less than 10^{-5}.

At the point $\underset{\sim}{\lambda}$ where $T(\lambda)$ assumes its largest value, for the λ's tested, a_λ is always negative. If λ_0 is the first value of λ where $a_\lambda(\lambda_0, T_c(\lambda_0)) > 0$, in this computation we have, for all the $\bar{g}_{Na}$'s tested, $|\lambda_0 - \underset{\sim}{\lambda}| < .02$ which is less than .2% of λ_c.

The values λ_0 and λ_c were used as initial data for a search by the golden section, and after increasing dramatically the accuracy in the computation of $T(\lambda)$ it was possible to improve this result. An estimate of λ_c with $a_\lambda(\lambda_c, T(\lambda_c)) < 10^{-4}$ was obtained requiring around 40 iterations of $T(\lambda)$, and about the same number of iterations for the search by the golden section.

The derivative $a_u(\lambda, T(\lambda), \bar{g}_{Na})$ was computed for the same values of λ and $\bar{g}_{Na}$ used for the results in Fig. IV.5.1, and with the same accuracy in the calculation of $T(\lambda)$. Figures IV.5.2 and IV.3.1 can be compared to check that the features discussed in Section 3 are not affected by an error of .2% in λ.

For the other second order derivatives, the consequences of variations in λ are even less marked than for a_u and a_λ - see Figs. IV.3.3, IV.3.4 and IV.3.5, where we also indicate the results of the more accurate computations described above.

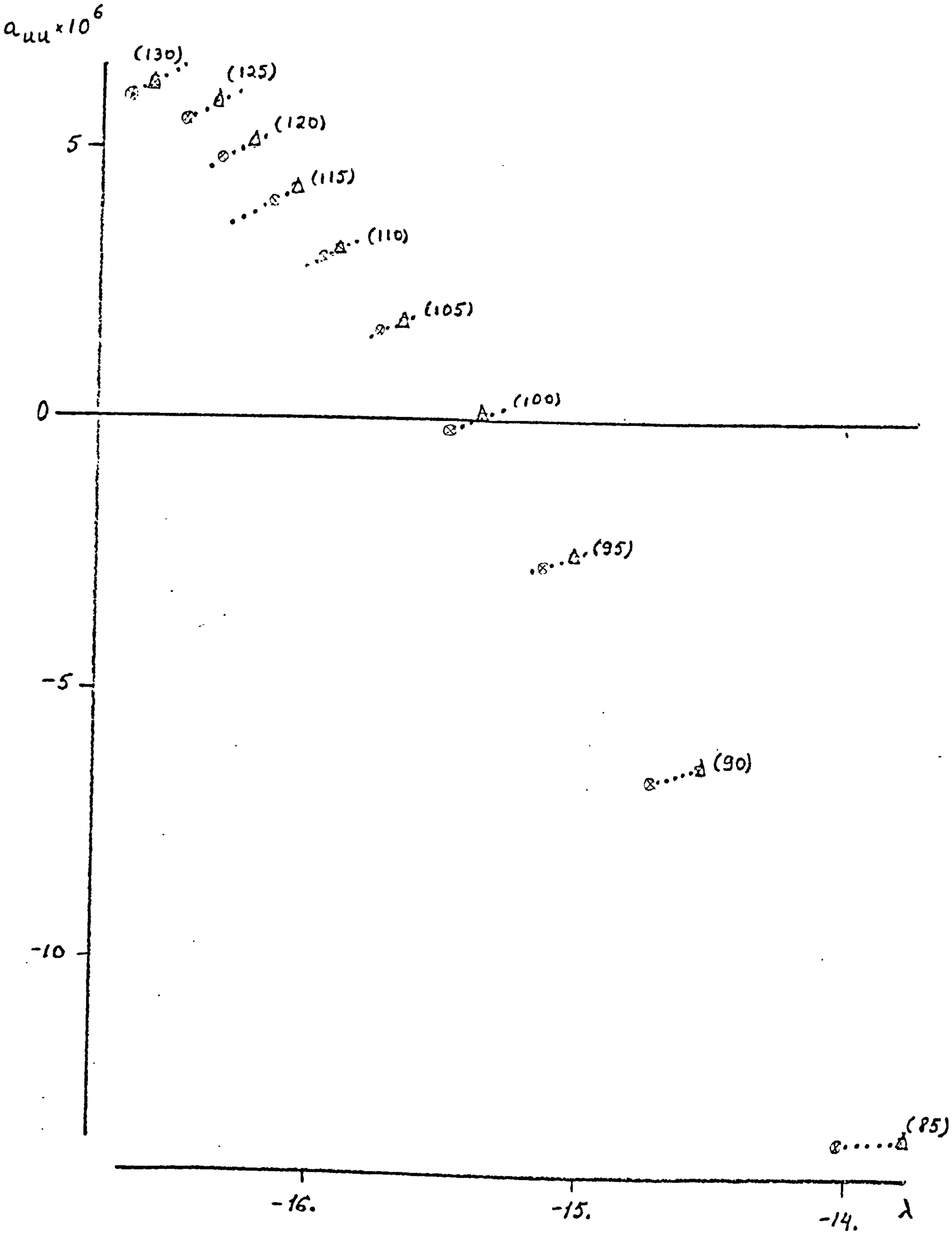

Fig. IV.5.3 Variation of a_{uu} along $T(\lambda, \bar{g}_{Na})$. Conventions and data as in Fig. IV. 5.2.

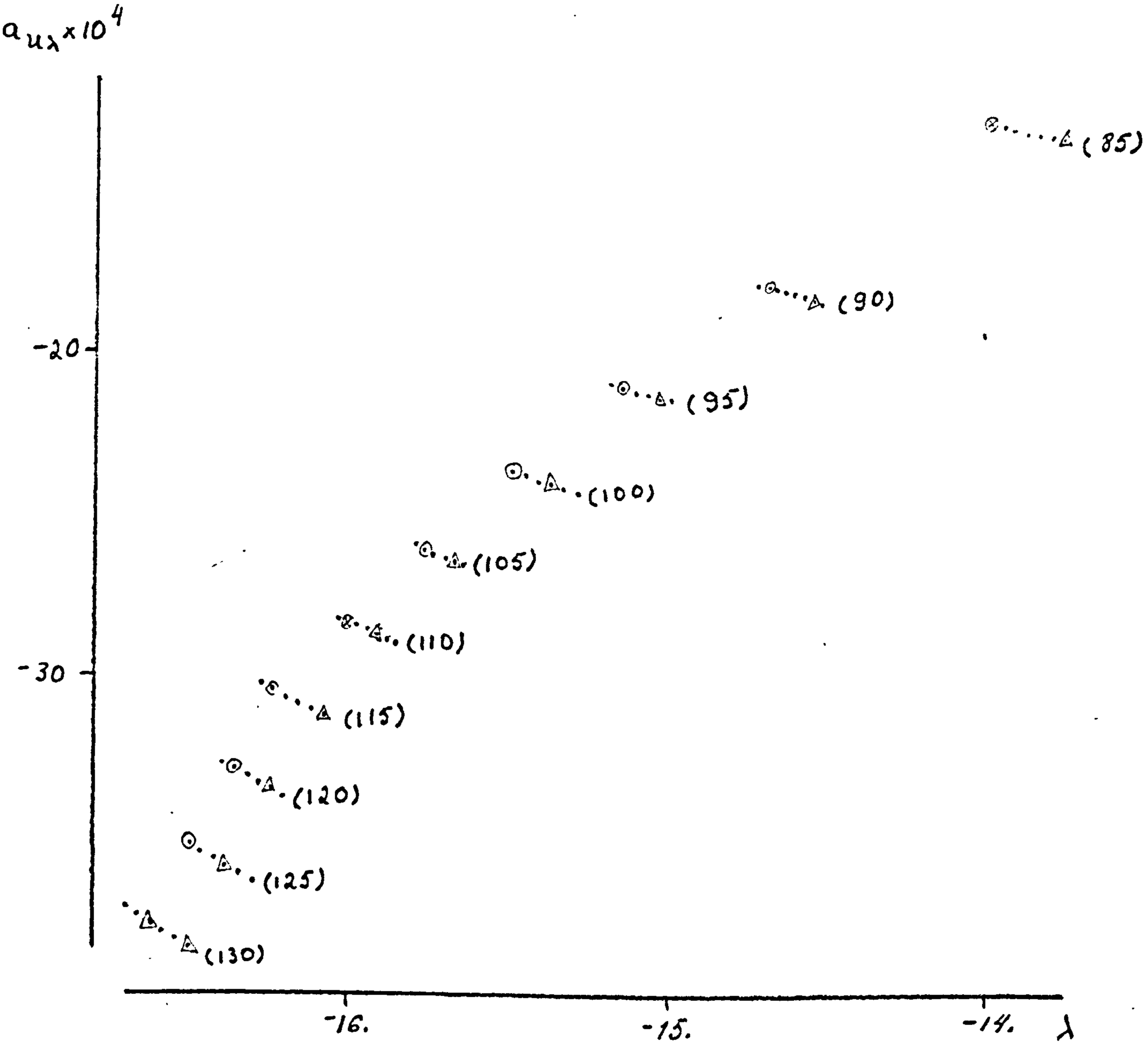

Fig. IV. 5.4 Variation of $a_{u\lambda}$ along $T(\lambda, \bar{g}_{Na})$. Conventions and data as in Fig. IV. 5.2

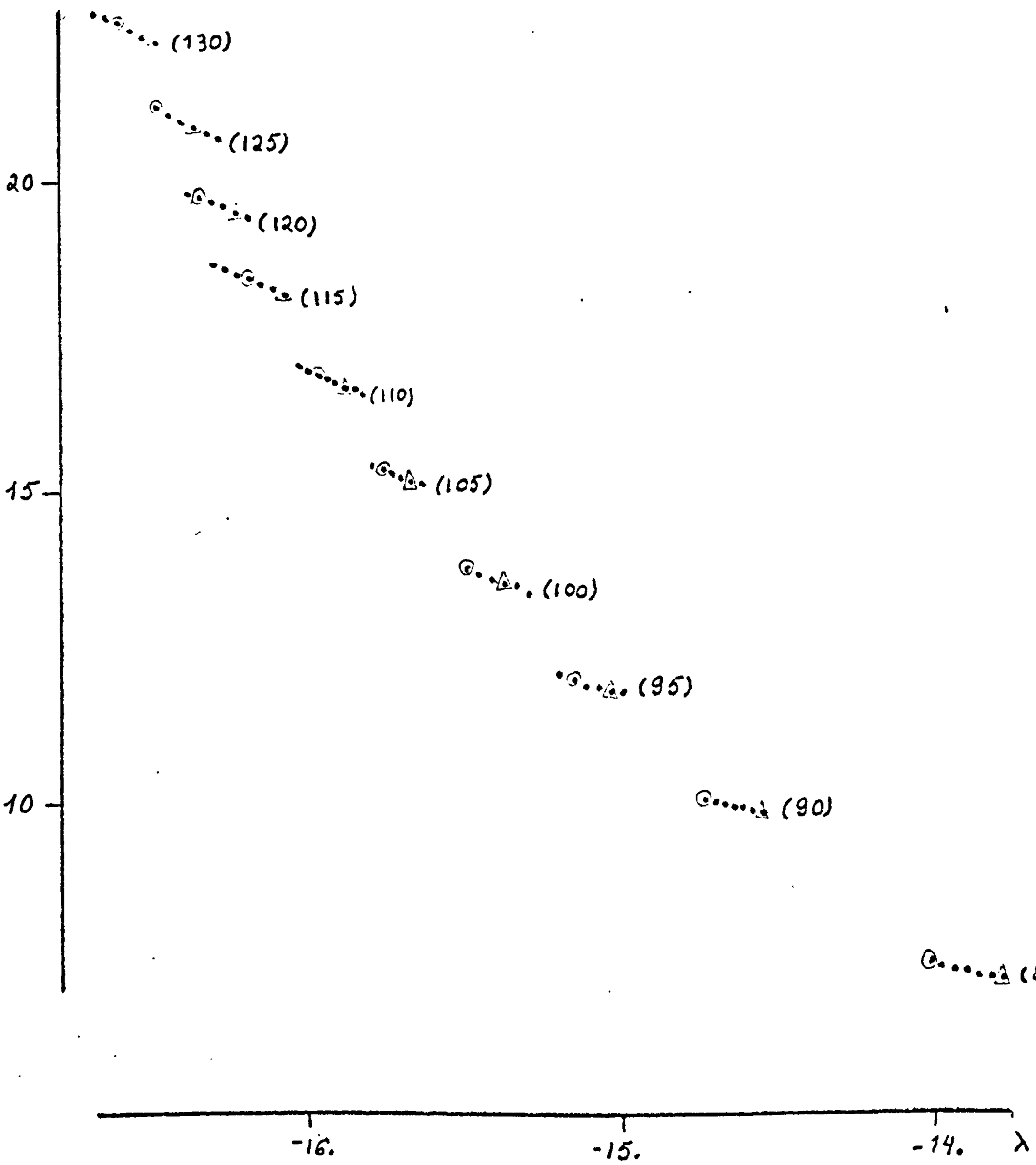

Fig. IV. 5.5 Variation of $a_{\lambda\lambda}$ along $T(\lambda, \bar{g}_{Na})$. Conventions and data as in Fig. IV. 5.2.

CHAPTER V : DISCUSSION

1. CONCLUSION

The hidden organizing centre for the Hodgkin and Huxley equations has the following characteristics:

Temperature $T_c \in [25.°, 26.6°]$

(1.1) Average sodium permeability $g_c \in [100\ ,\ 110\ ]$

Bifurcation parameter $\lambda_c \in [-16.1, -15.5]$

$$a_u(0,\lambda_c) = a_\lambda(0,\lambda_c)$$

$$a_{uu}(0,\lambda_c) > 0;\ a_{u\lambda}(0,\lambda_c) < 0;\ a_{\lambda\lambda}(0,\lambda_c) > 0$$

Therefore HH is equivalent, after reduction, to one of the germs (III.2.3) with $\varepsilon\phi = +1$, $\varepsilon b = B \in [-17, -12]$. As temperature varies, the perturbed HH equations follow a path in the unfolding of (III.2.3) through the origin $\alpha = \beta = 0$ (Fig. V.1.1a) and we obtain, for low temperatures, a periodic solution branch, similar to that of Fig. IV.1.1b, followed by a branch that does not appear through a classical Hopf bifurcation. These isolated branches are known in the literature as *isolas*. For temperatures above T_c, only the isola is present.

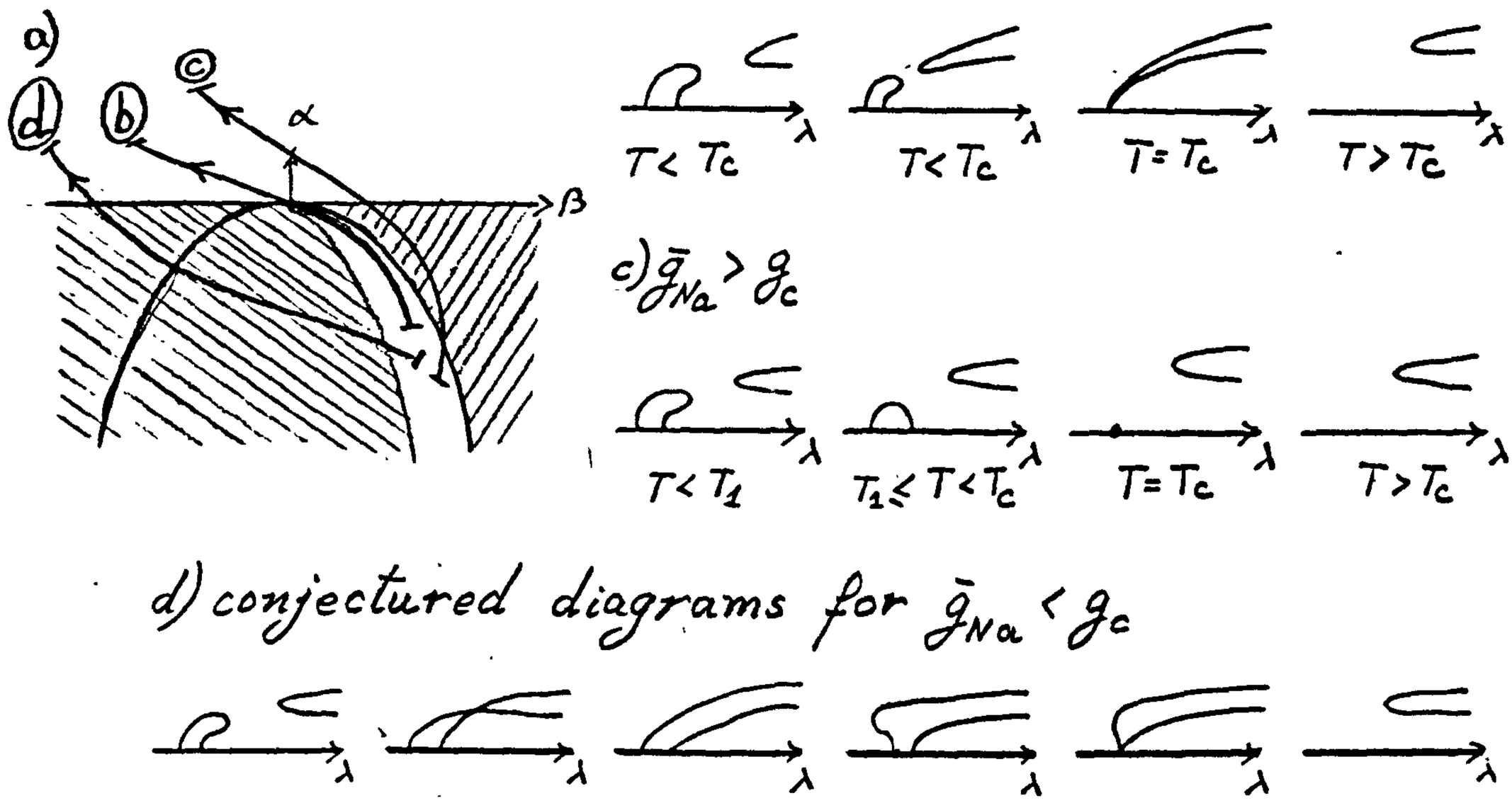

Fig. V.1.1a Equations HH, seen as a T-parametrized curve for each $\bar{g}_{Na}$, on the unfolding of (III.2.3). b), c) and d) bifurcation diagrams along the curves indicated in a).

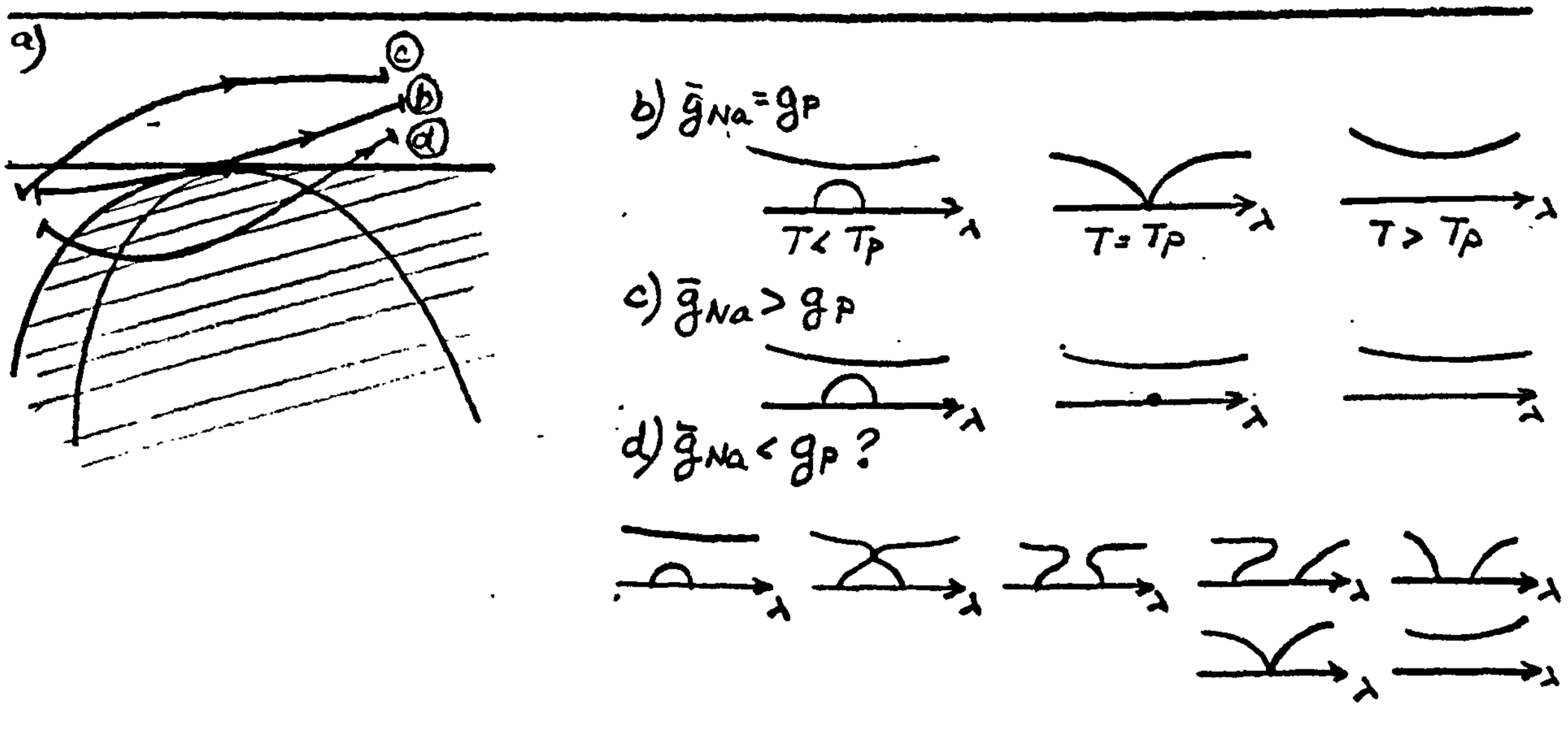

Fig. V.1.2a The Hodgkin and Huxley equations, for $\bar{g}_{Na}$ near g_p, represented as paths on the unfolding of (III.2.2). b), c) and d) bifurcation diagrams for the paths in a).

For the unperturbed equations, with $\bar{g}_{Na} > g_c$, the T-parametrized path moves away from the origin, and therefore it must go through one of the shaded areas of Fig. V.1.1a. Diagrams are as in Fig. V.1.1c, since we can exclude those of Fig. V.1.1d by comparing them to our data on the direction of bifurcation (IV.1). This completes the description of periodic solutions of HH, with $\bar{g}_{Na} > 110$.

At the second zero of a_u, the data are:

(1.2) Average sodium permeability $g_p \in [85, 90]$

Temperature $T_p \in [13.^o, 18.5^o]$

Bifurcation parameter $\lambda_p \in [-15., -13.8]$

$a_u(0,\lambda_p) = a_\lambda(0,\lambda_p) = 0$

$a_{uu}(0,\lambda_p) < 0$; $a_{u\lambda}(0, \ _p) < 0$; $a_{\lambda\lambda}(0,\lambda_p) > 0$.

This is case (III.2.2) with B ϵ [4., 7.] and $\varepsilon\delta = -1$ (see Fig. V.1.2). Thus, as $\bar{g}_{Na}$ decreases, the perturbed Hodgkin and Huxley equations undergo a transition from case (III.2.3) to case (III.2.2). This type of transition, which must be via B = ∞, not 0, was discussed in connection with the unimodal germs (III.2.7) and (III.2.8). Indeed if we could perturb the zero of a_{uu} and the hidden organizing centre into a single point, the result would be $\mathbb{Z}_2$ equivalent to (III.2.8), with the characteristics:

(1.3) $a_u = a_\lambda = a_{uu} = 0$

$a_{u\lambda} < 0$, sign $(a_{u\lambda}) = \delta = -1$

$a_{\lambda\lambda} > 0$, sign $(a_{\lambda\lambda}) = \phi = +1$

ε = sign a_{uuu}.

If ε= -1, the germs (III.2.2) and (III.2.3) abutt (III.2.8) as follows:

(1.4) $\gamma > 0$ - (III.2.2) with $B = \frac{1}{2\sqrt{|\gamma|}} > 0$

$\gamma < 0$ - (III.2.3) with $B = \frac{-1}{2\sqrt{|\gamma|}} < -1$

An inspection of Fig. III.2.8 shows that in this case, the isola discussed above opens into a periodic orbit present for all values of λ within some *uniform* (in the unfolding

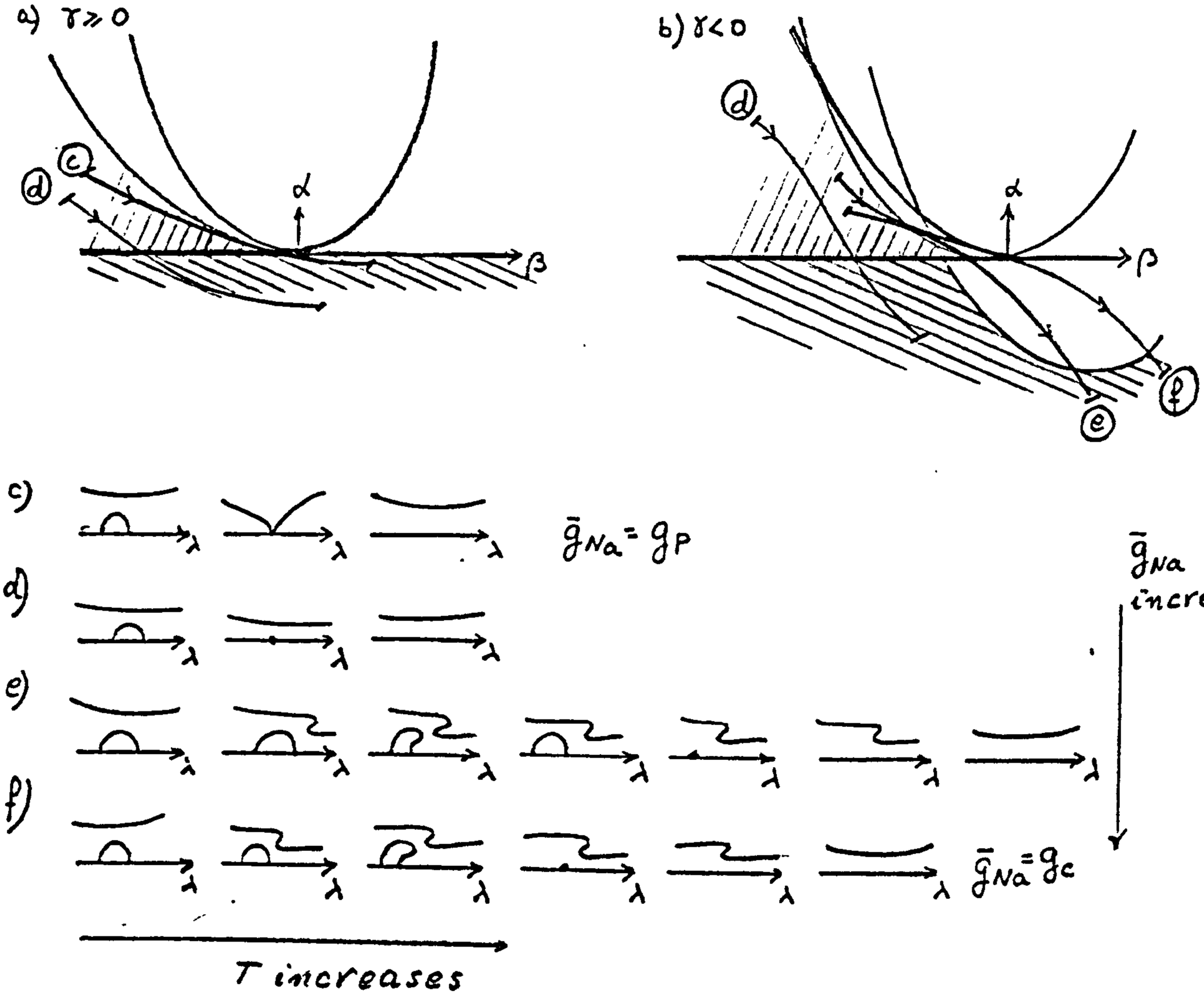

Fig. V.1.3 The perturbed HH equations as a family of T-parametrized curves on the unfolding of (III.2.8), $\varepsilon\phi = -1$. a) and b) curves on α-β-γ-space. Notice that areas with similar shading are connected in $\mathbb{R}^3 - \Sigma$. c), d), e) and f) Bifurcation diagrams for the curves in a) and b), as possible representation for the HH equations. Diagrams for the unperturbed equations are similar to those in e).

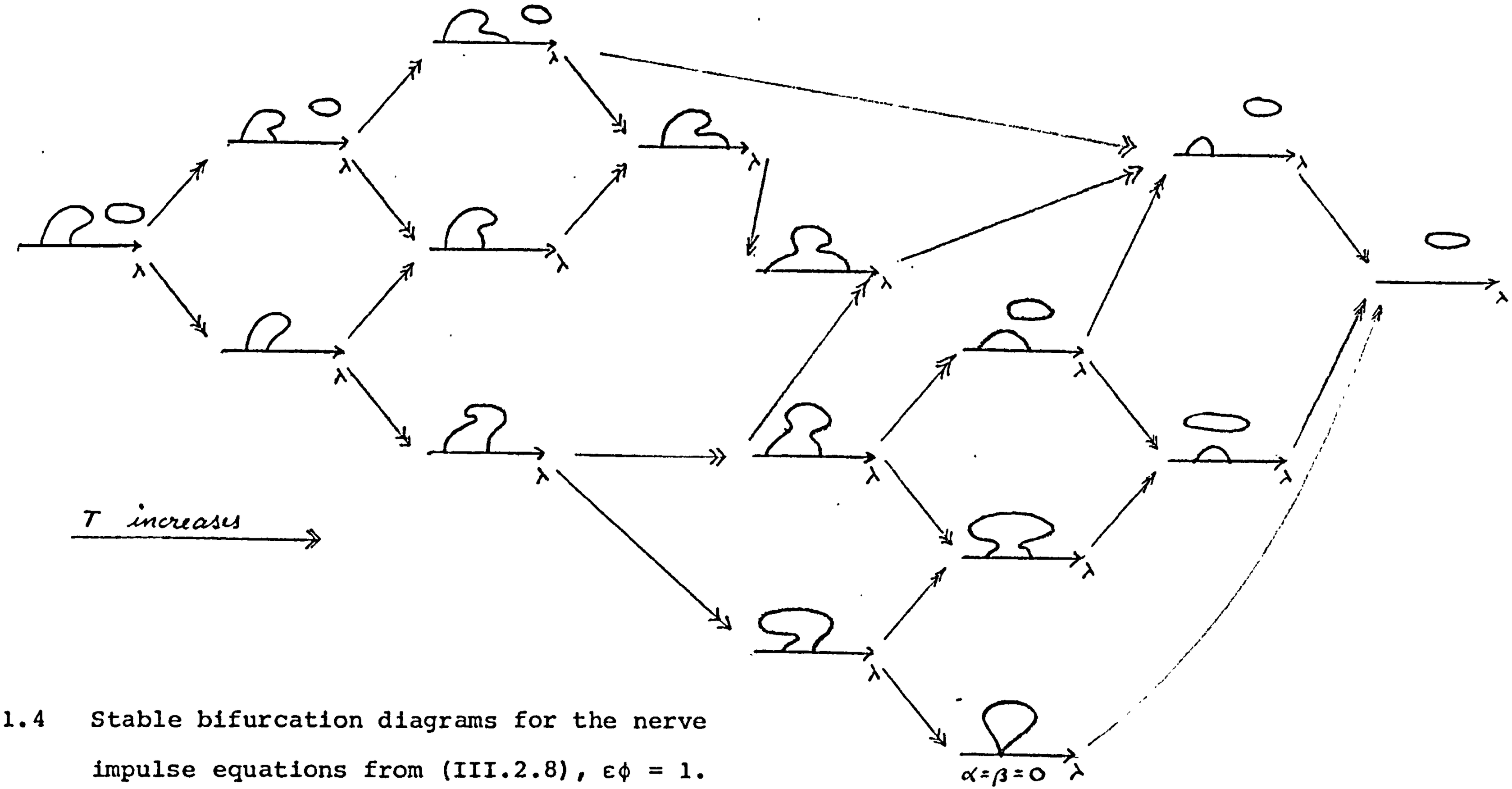

Fig. V.1.4 Stable bifurcation diagrams for the nerve impulse equations from (III.2.8), $\varepsilon\phi = 1$.

parameter) interval. Otherwise the bifurcation diagrams are the same, as can be seen in Fig. V.1.3.

For $\varepsilon = \pm 1$ the transition from (III.2.2) to (III.2.3) is

(1.5) $\gamma > 0$ - (III.2.3) with $B = -\frac{1}{2\sqrt{|\gamma|}} < -1$

$\gamma < 0$ - (III.2.2) with $B = \frac{1}{2\sqrt{|\gamma|}} > 0$

In this case periodic solutions are present only in a limited range of values of λ. There are several diagrams exhibiting a second knee, as found numerically by Rinzel and Miller (cf. Figs. III.2.9 and IV.1.4). The most striking feature, however, is the presence, for $\gamma < 0$, of diagrams with a knee on the left hand side, in unavoidable way (see Fig. V.1.4). Although the unperturbed HH equations do not exhibit this behaviour, it was observed in experiments on squid axons bathed in low Ca seawater [11].

2. ORGANIZATION BY DEGENERACY

A $\mathbb{Z}_2$-equivariant germ has different bifurcation diagrams depending on whether the germ is studied on its own or seen as part of the unfolding of a more degenerate (i.e. higher codimension) germ. The presence of a degeneracy close by is extra information about the germ and this is reflected in the diagrams we obtain for it.

A simple example was discussed in Chapter IV. If a system $\dot{v} = F(v,\lambda)$ has two classical Hopf bifurcations at $\lambda_1 < \lambda_2$, with the same direction of bifurcation, there is no *a priori* reason why the two periodic solution branches ought to meet. The proximity of a degeneracy, in this case a change in the direction of bifurcation, together with the coalescence of the two bifurcation points, makes the analysis "more global". It shows that the apparent lack of information about the periodic solution branches away from the bifurcation points is an artifact of local analysis.

The same discussion applies to members of the one parameter family (III.2.1) when compared to (III.2.6) ($\varepsilon\delta = 1$, $B = \pm 1$) or to (III.2.7) and (III.2.8) ($B \to \pm \infty$). The bifurcation diagrams for the organizing centre of the germs (III.2.1) appear either "capped off" or with an extra branch, when viewed as part of the unfolding of the higher codimension cases. Moreover, the stable perturbations of the more degenerate germ are *not* just the union of diagrams obtained by perturbing the modal parameter first and then unfolding the new germ. This point is made particularly clear in the discussion of the unfolding of (III.2.8). This is part of the rationale for studying perturbed problems and looking for a hidden organizing centre. The results of the

perturbation analysis would be relevant even if we knew (and it is not the case) that those parameter values are never assumed in practice.

3. EXPERIMENTS

In this section we explore the asymptotic stability of bifurcation diagrams for the nerve impulse equations and compare our predictions with experimental results on nerve cells. A classical Hopf bifurcation is characterized by the fact that as the amplitude of the periodic solution branch tends to zero (when it approaches the bifurcation point) its period tends to $2\pi/\theta_0$. Thus, when the bifurcation point $(0,\lambda_o)$ is asymptotically stable, a stable branching point may be observed in experiments as a threshold value of the control parameter λ for the onset of repetitive behaviour with period close to $2\pi/\theta_0$. This is the case for equations HH (unperturbed) at temperatures T $\in$ (28.853, 28.859, as well as at the branching point on the right hand side of Rinzel and Miller's (Fig. IV.1.4) diagrams.

Many of the diagrams obtained for the reduced Hodgkin and Huxley equations have a stable fold connected to a stable branching point as in Fig. V.3.1a. below:

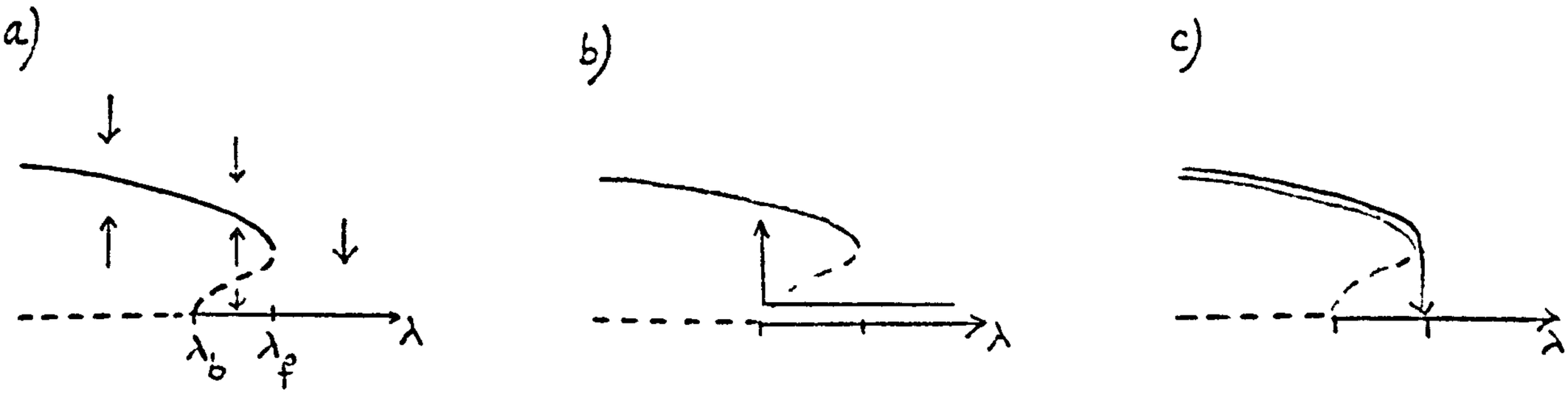

Fig. V.3.1.

where the solid lines stand for asymptotically stable solutions, and the dotted lines for asymptotically unstable ones. Vertical arrows in (a) indicate the direction of the flow.

For each λ in the *overlap* range $[\lambda_b, \lambda_f]$ two asymptotically stable solutions coexists, and the unstable solution forms a separatrix for their basins of attraction on the centre manifold at λ (see II.5). When the system is in a steady state and λ is decreased past λ_b the equilibrium $(0,\lambda)$ becomes unstable, and the system tends towards the stable periodic solution (Fig. V.3.1b). If λ is then increased again, the periodic solution branch remains stable, until it disappears at $\lambda = \lambda_f > \lambda_b$, and the system returns to the steady state (Fig. V.3.1c). This type of behaviour is called hysteresis. It can be observed in voltage clamp experiments where the stimulating current I is varied, as a larger threshold value $I = -f(\lambda_b)$ for the initiation of repetitive firing (I increases) than for its termination, as I decreases, at $I = -f(\lambda_f)$. (Recall that $\lambda = f^{-1}(-I)$ is a decreasing function.)

Besides turning all diagrams back to front, the change of variables of Section IV.0 has the effect of transforming the curve

$$V_* = f(-I);\ J_* = j_\infty(V_*),\ J = M,N,H$$

into the straight line v = m = n = h = 0. Thus a bifurcation diagram like Fig.V.3.1 will have the aspect shown in Fig. V.3.2a.

If the stimulating current I is varied slowly (compared to the period $2\pi/\theta_o$ of the solution branch), then the hysteresis loop of Fig. V.3.2b is a good description of a voltage clamp experiment. In most cases, however, the stimulus is increased abruptly to its new value, as a current step (Fig. V.3.3). When I is increased discontinuously (Fig. V.3.3a and b) so does the voltage V, but the membrane conductances M, N, H are not instantaneously affected. The system is pushed away from equilibrium, and therefore the threshold value of I, for the initiation of repetitive firing should be lower for a suddenly applied stimulus than for stimulation that increases slowly.

Under those circumstances an axon will show different responses, depending not only on stimulus intensity, but also on the way this intensity is attained. The presence of hysteresis will also have the effect of stabilizing the cell's response to fluctuations of the stimulus near the threshold. A system exhibiting a classical Hopf bifurcation without hysteresis will be thrown in and out of repetitive firing by small variations in I (see [25]).

As a rule, giant squid axons bathed in sea water do not exhibit maintained repetitive firing in a current clamp experiment. In most cases the axon fires one or more times under constant stimulation, and then returns to equilibrium.

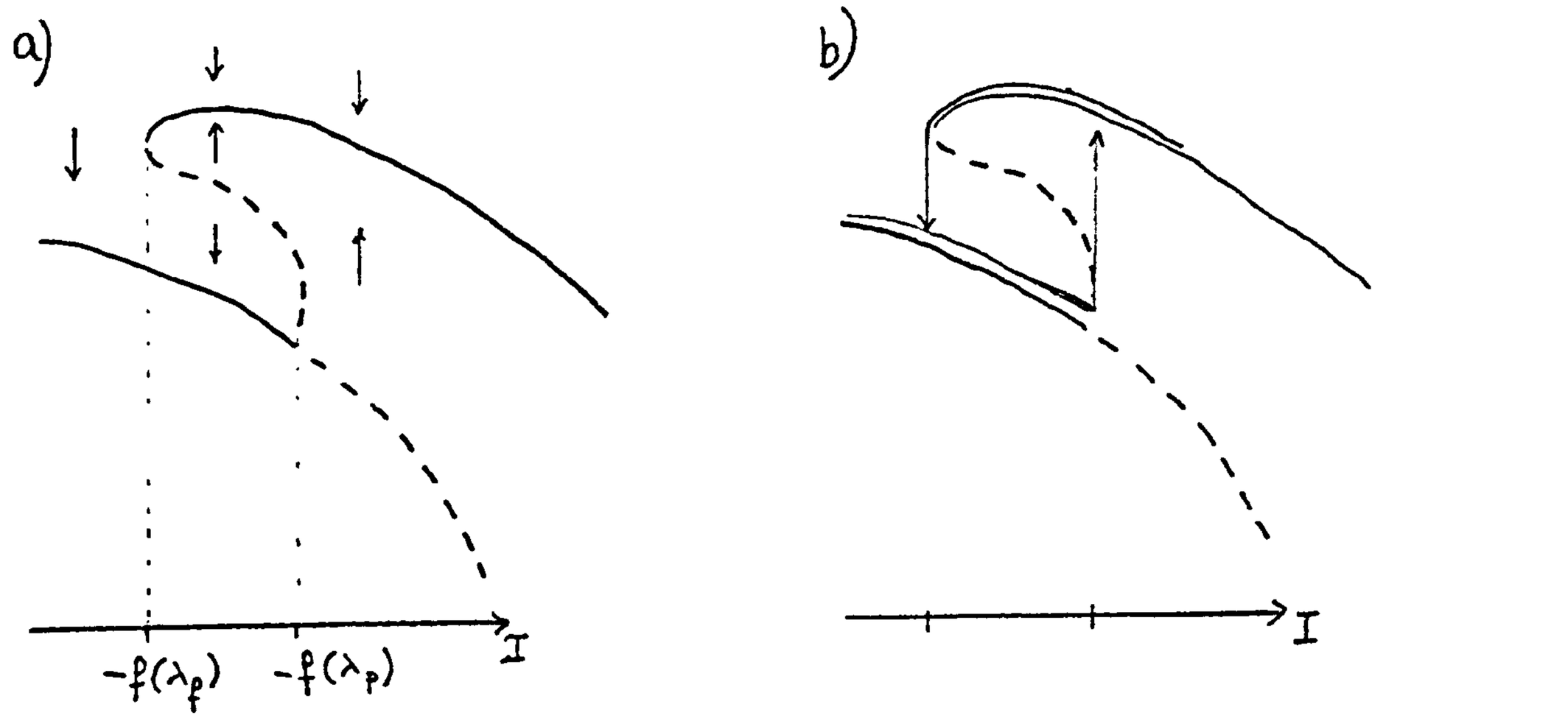

Fig. V.3.2 Bifurcation diagrams and hysteresis for the Hodgkin and Huxley equations.

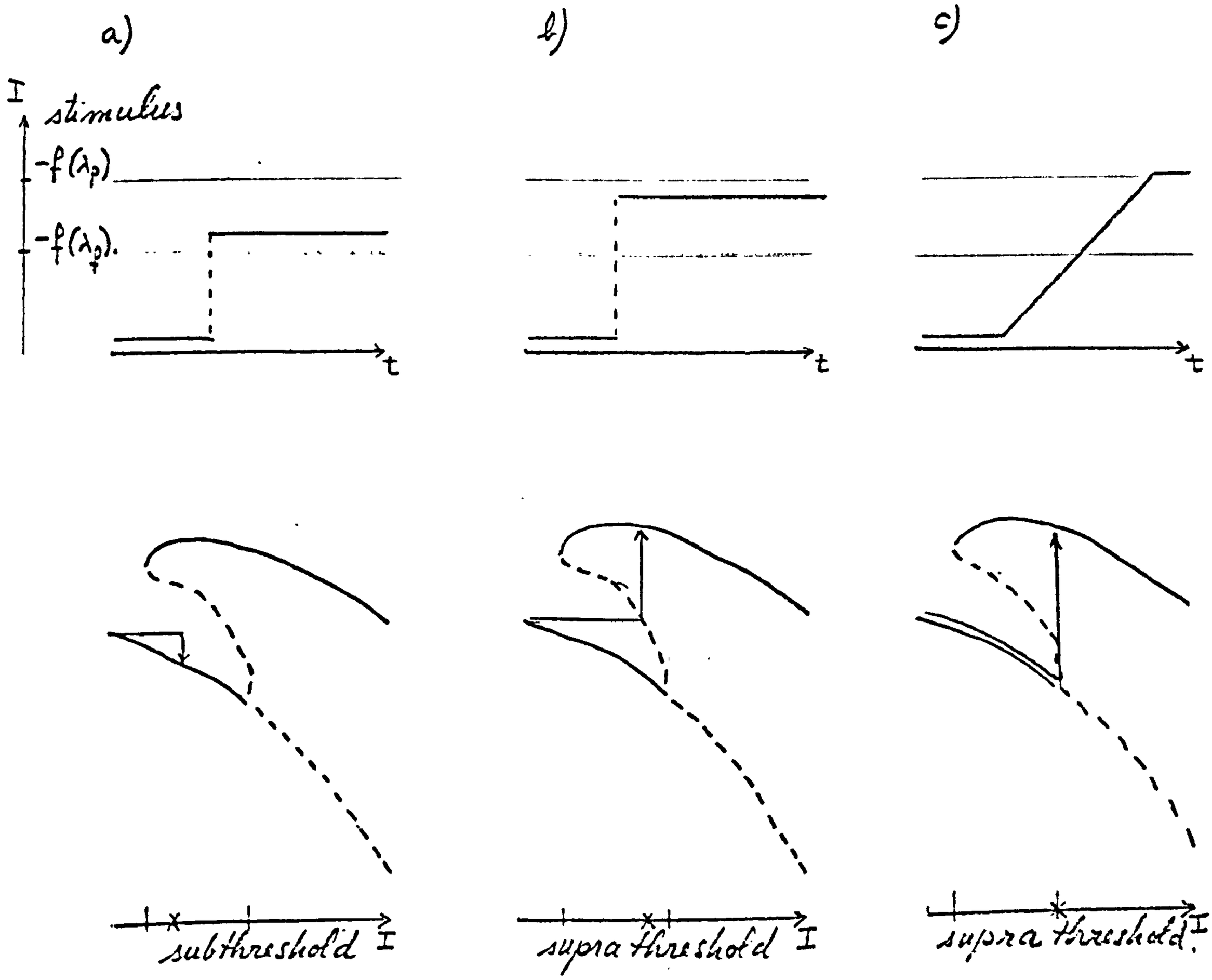

Fig. V.3.3 Threshold variations for nerve impulse equations, according to type of stimulus.

When bathed in low Ca sea water, however, squid axons will fire repetitively in response to an adequate current step [1] [11]. Guttman et al [11] found that in this experimental setting the axons exhibit a sharp threshold of minimum current intensity for repetitive firing, with a nonzero critical firing frequency. The threshold value is different, depending on the way the stimulus varies: it is lower for a suddenly applied stimulus than for a continuously increasing ramp of current. Once repetitive firing is established it can be terminated by both depolarizing (increase in I) or hyperpolarizing (decrease in I) shocks of appropriate intensity. We reproduce here two oscilloscope recordings from [11] of an axon's response to a step stimulus (Fig. V.3.4a and b).

Hysteresis and high intensity cut-off are elegantly demonstrated by the experiment of Fig. V.3.4c and d. Notice that hysteresis takes place at *both* ends of the periodic solution branch. For the unperturbed Hodgkin and Huxley equations at fixed temperature, the periodic solution remains asymptotically stable as it shrinks into the steady state (see Fig. V.1.1c) and therefore HH exhibits only one hysteresis loop. The experimental results of Guttman et al [11] are in qualitative agreement with our description of the perturbed equations (see Figs. V.1.1d and V.1.4).

Similar results were obtained by Jalife and Antzelevitch [21] on isolated pacemaker cells of mammals. They found that

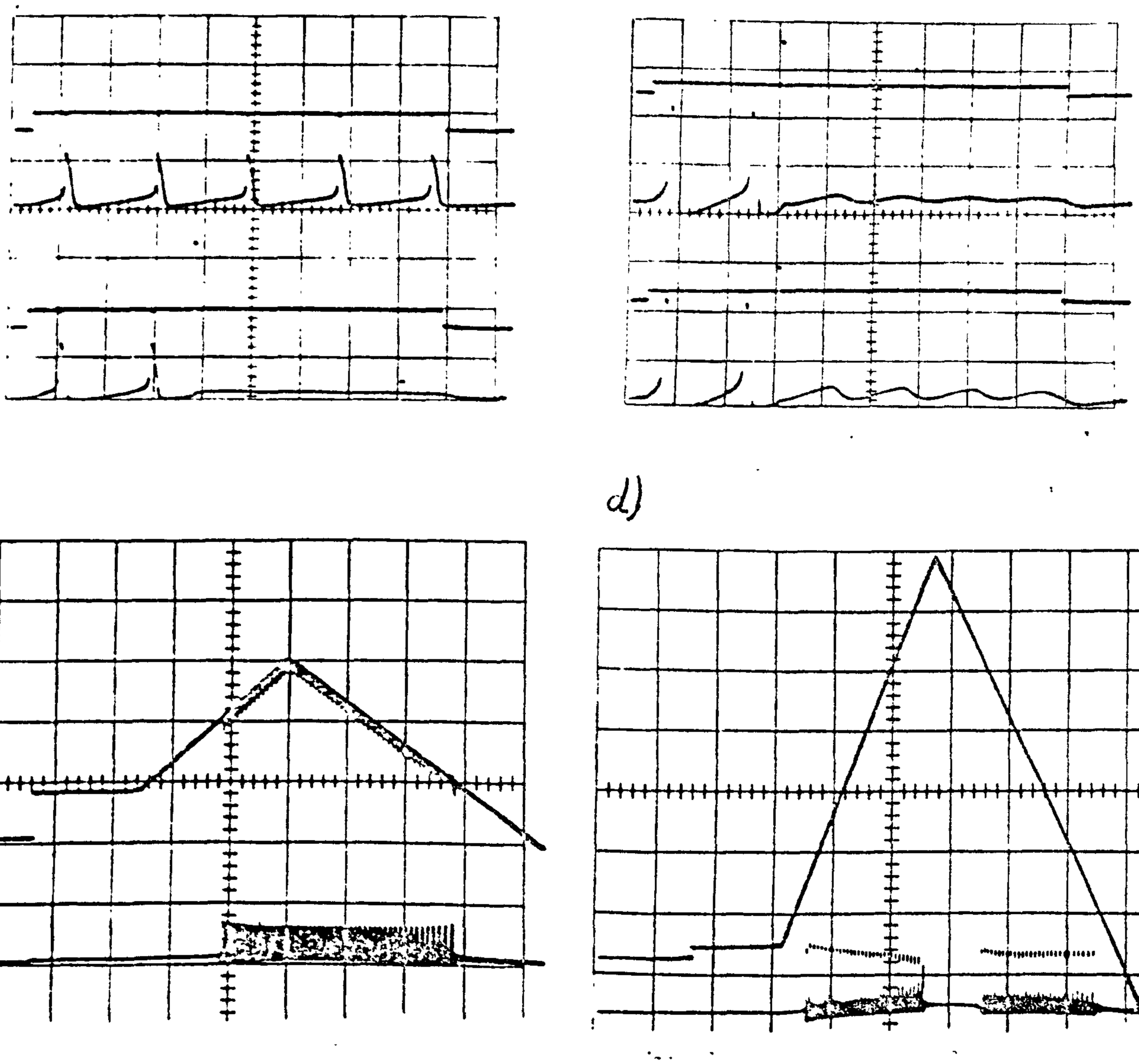

Fig. V.3.4 Annihilation of repetitive firing of space-clamped squid axon. a and b - step stimulus, c and d, continuous stimulus. Note the subthreshold oscillations in a and b, and hysteresis at commencement and at cut-off in c and d.

Calibration:

a)	100 mV/div	2μA/div	2msec/div at	22.3°C
b)	50	5	2	22.0
c)	100	1	50	22.0
d)	50	2	50	20.2

Reproduced from [11].

the spontaneous activity of those cells could be abolished by both depolarizing and hyperpolarizing shocks. The same results were obtained numerically by Best [2] in a simulation of a pacemaker that used a modified version of HH. Unfortunately threshold stimuli for terminating and reinstating repetitive firing were not compared in the experiments nor in the simulations.

For the pacemaker cells the presence of hysteresis provides a simple mechanism for the triggering on and off of repetitive firing by a brief stimulus. If in the absence of stimulus the cell is in the overlap range of the hysteresis loop, repetitive firing (or its absence) would be maintained withoutthe need of constant external stimulation. The same mechanism could be present in other types of excitable tissue, like time keeping neurones or stretch receptors.

Yet another feature of the bifurcation diagrams we obtain for HH is the presence of isolas. As we have already remarked these solutions of HH have not been previously described. At first sight the isolas seem unimportant to the problem of control of repetitive firing of nerve cells, because they cannot be reached by moving continuously from the asymptotically stable equilibrium. It is not possible to obtain any information about the position of isolas in $V \times M \times N \times H \times \lambda$-space with the methods used here, as these solutions do not arise through a classical Hopf bifurcation. It would be interesting to obtain a numerical tracing of these solutions since they define the boundary of the steady-state's

basin of attraction on the centre manifold. All we know is the isola meets the constant solution $x = 0$ at $\bar{g}_{Na} = g_c$, $T = T_c$. If, for the unperturbed equations, it lies close to equilibrium and within physiologically meaningful range, then the steady state has a very small basin of attraction. In this case the system may be perturbed into maintained repetitive activity by, for instance, an accumulation of ions in periaxonal space that modified the membrane permeability, or by the presence of exciting/inhibiting substances.

When a perturbation is not large enough to push the variables into the isola, the system returns to equilibrium with damped oscilations. This has the functional interpretation of increasing the duration of subthreshold synaptic (or external) input. In this way the presence of isolas may be responsible for subthreshold oscilations (see [29]).

At low temperatures ($< 0^{o}C$) our analysis of unperturbed HH breaks down: the eigenvalues of $d_u\gamma(0,\lambda_c)$ go through the origin (i.e. $\sigma(\lambda_c) = \theta(\lambda_c) = 0$ in II.0) and the Liapunov-Schmidt reduction can no longer be applied to γ. It may be possible to obtain similar results using another reduction process, like the Centre Manifold Theorem. In the proximity of a zero eigenvalue, however, the problem is likely to exhibit an entirely different behaviour.

Finally, the qualitative analysis carried out here does not eliminate the need for numerical tracings of the periodic solutions of HH. The methods we use necessarily lose important information about the geometry of periodic orbits, and the way they are embedded in $\mathbb{R}^5$. This information is necessary to explain certain experimental results like the fact that the annihilation of repetitive firing depends not only on stimulus intensity and temporal distribution, but also on the phase where it is applied, observed both by [11] and [21].

It is not usual to look for periodic solutions numerically without having some reason to expect them to exist. A good example is provided by the isolas in Hodgkin and Huxley equations - they may be present and yet have been missed (quite naturally) by numerical tracings. What the method tells us is which type of periodic solution branch to look for, and where to look for it, in a numerical study. It also shows that the Hodgkin and Huxley equations, regarded as a family of biological problems, are capable of explaining some of the complex repetitive behaviour of excitable tissues.

APPENDIX 1

We present here the formulae from [6] that we used to compute the derivatives of the reduced germ

$$r(\gamma) = xa(x^2, \lambda).$$

In [6] it is assumed that time has been rescaled so as to have $\pm i$ as the purely imaginary eigenvalue of $d_u\gamma(0,\lambda_0)$. We do not make this assumption here, and consequently the imaginary eigenvalue $\theta_o i$ appears in the formulae. We also indicate in each case the FORTRAN subroutine that evaluates the formulae, as well as the correspondence between names of variables in the two appendices.

(A1.1) Notation

We indicate as

$$\gamma^k : \mathbb{R}^n \times \mathbb{R}^n \times \ldots \times \mathbb{R}^n \longrightarrow \mathbb{R}^n$$

the symmetric k-linear form defined by

$$\gamma^k(v_1,\ldots,v_k) = [d_u^k\gamma\ (0,\lambda_o)]\cdot(v_1,\ldots,v_K)\cdot$$

Recall that $A = \gamma^1 = d_u\gamma(0,\lambda_o)$.

Similarly we define

$$\gamma^{k,\ell}\ \mathbb{R}^{n\times k} \longrightarrow \mathbb{R}^n$$

as $$\gamma^{k,\ell}(v_1,\ldots,v_k) = [d_u^k \frac{\partial^\ell \gamma}{\partial \lambda^\ell}\ (0,\lambda_o)]\cdot(v_1,\ldots,v_K)$$

In (II.2) we obtain bifurcation equations in component form

$$f_1(x,0;\lambda,\tau) = xp(x^2;\lambda,\tau) = 0$$

$$f_2(x,0;\lambda,\tau) = xq(x^2;\lambda,\tau) = 0.$$

Writing $u = x^2$, we denote by $p_{jk\ell}$ and $q_{jk\ell}$ the coefficients in the Taylor expansions of p and q:

$$p(x;\lambda,\tau) \sim \Sigma\, p_{jk\ell}\, u^j(\lambda-\lambda_o)^k\tau^\ell$$

$$q(x;\lambda,\tau) \sim \Sigma\, q_{jk\ell}\, u^j(\lambda-\lambda_o)^k\tau^\ell$$

where

$$p_{jk\ell} = \frac{1}{(2j+1)!k!\,\ell!}\;\frac{\partial^{2j+1+k+\ell} f_1(0,0;\lambda_o,0)}{\partial x^{2j+1}\partial\lambda^k\partial\tau^\ell}$$

$$q_{jk\ell} = \frac{1}{(2j+1)!k!\,\ell!}\;\frac{\partial^{2j+1+k+\ell} f_2(0,0;\lambda_o,0)}{\partial x^{2j+1}\partial\lambda^k\partial\tau^\ell}$$

In the FORTRAN subroutines of Appendix 2 the coefficients $p_{jk\ell}$ and $q_{jk\ell}$ appear as variables XPjkℓ, XQjkℓ. (for instance XP100, XQ100) and are evaluated by the subroutines P2 in the module UM.

The derivatives of a at the bifurcation point $(0,\lambda_o)$ are denoted:

derivative		variable in Appendix 2 (subroutine VSOP)
a_u	$= \frac{\partial a}{\partial u}(0,\lambda_o)$	DAZ
a_λ	$= \frac{\partial a}{\partial \lambda}(0,\lambda_o)$	DAL
a_{uu}	$= \frac{1}{2}\frac{\partial^2 a}{\partial u^2}(0,\lambda_o)$	DAZZ
$a_{u\lambda}$	$= \frac{\partial^2 a}{\partial u \partial \lambda}(0,\lambda_o)$	DAZL
$a_{\lambda\lambda}$	$= \frac{1}{2}\frac{\partial^2 a}{\partial \lambda^2}(0,\lambda_o)$	DALL

A1.2. We also indicate by c and d the eigenvectors of A and A^t respectively, corresponding to the eigenvalues $\theta_o i$, $-\theta_o i$ resp. (see II.1) and by * the complex scalar product of two vectors. Recall that c and d were chosen to satisfy d*c = 2, and that $d_u\gamma(0,\lambda)$ has complex eigenvalues

$$\sigma(\lambda) \pm i\theta(\lambda)$$

satisfying

$$\sigma(0) = 0, \theta(0) = \theta_o > 0.$$

A1.3. The derivatives of a are given by:

$$a_\lambda = p_{010} = -\frac{1}{2}\,\mathrm{Re}\,[\gamma^{1,1}(c)*d] = -\sigma'(\lambda_o)$$

$$a_u = p_{100} = -\frac{1}{4}\,\mathrm{Re}\,[\beta*d]$$

where $\beta = \gamma^{2,0}(a_o,c) + \gamma^{2,0}(a_2,\bar{c}) + \frac{1}{4}\gamma^{3,0}(c,c,\bar{c})$

β appears as the variable OB in the subroutines PQ100 and A1.

$$a_{uu} = \rho_{200} + p_{101}\, q_{100}$$

where

$$q_{100} = -\frac{1}{4}\ \mathrm{Im}\ [\beta * d]$$

$$p_{101} = \frac{1}{6}\ \mathrm{Re}\ [\gamma^{2,0}(f_2, \bar{c}) * d]$$

$$p_{200} = -\frac{1}{4!}\ \mathrm{Re}\ [\alpha * d]$$

and

$$\alpha = \frac{1}{2}\gamma^{2,0}(b_o, c) + \frac{1}{2}\gamma^{2,0}(b_2, \bar{c}) + 2\gamma^{2,0}(a_o, a_1) +$$

$$+ 2\gamma^{2,0}(\bar{a}_2, a_2) + 2\gamma^{2,0}(\bar{a}_1, a_2) + \frac{3}{2}\gamma^{3,0}(a_o, a_o, c) +$$

$$+ 3\gamma^{3,0}(a_2, \bar{a}_2, c) + 3\gamma^{3,0}(a_o, a_2, \bar{c}) +$$

$$+ \frac{1}{2}\gamma^{3,0}(\bar{a}_1, c, c) + \gamma^{3,0}(a_1, c, \bar{c}) + \frac{1}{2}\gamma^{3,0}(a_3, \bar{c}, \bar{c}) +$$

$$+ \frac{1}{4}\gamma^{4,0}(\bar{a}_2, c, c, c) + \frac{3}{4}\gamma^{4,0}(a_o, c, c, \bar{c}) +$$

$$+ \frac{3}{4}\gamma^{4,0}(a_2, c, \bar{c}, \bar{c}) + \frac{1}{16}\gamma^{5,0}(c, c, c, \bar{c}, \bar{c})$$

$$a_{u\lambda} = p_{110} + p_{101}\, q_{010}$$

where p_{101} is given above and

$$q_{010} = -\frac{1}{2}\ \mathrm{Im}\ [\gamma^{1,1}(c)*d]$$

$$p_{110} = -\frac{1}{2}\ \mathrm{Re}\ [\eta*d]$$

where

$$\eta = \frac{1}{3}\ \gamma^{1,1}(a_1) + \gamma^{2,0}(h_1,a_o) + \gamma^{2,0}(\bar{h}_1,a_2) +$$

$$+ \frac{1}{2}\ [\gamma^{2,0}(h_2,\bar{c}) + \gamma(h_o,c) + \gamma^{2,1}(a_o,c) + \gamma^{2,1}(a_2,\bar{c}) +$$

$$+ \frac{1}{2}\ \gamma^{3,0}(\bar{h}_1,c,c) + \gamma^{3,0}(h_1,c,\bar{c}) + \frac{1}{4}\ \gamma^{3,1}(c,c,\bar{c})]$$

$$a_{\lambda\lambda} = p_{020} = -\mathrm{Re}\ [(\gamma^{1,1}(h_1) + \frac{1}{4}\ \gamma^{1,2}(c))\ *\ d]$$

and if $a_\lambda = 0$ then $a_{\lambda\lambda} = -\frac{1}{2}\ \sigma'(\lambda_o)$.

The vectors a_i, b_i, f_i and h_i are obtained as solutions of the equations below. On the left hand side we indicate the name of the subroutine in the group P1 of the module UM (see Appendix 2) that computes each one of them, followed by the variable name in brackets. The identity matrix in $\mathbb{C}^4$ is denoted I.

AO(QAO) $\qquad Aa_o = -\frac{1}{2}\ \gamma^{2,0}(c,\bar{c})$

A2(QA2) $\qquad [A-2i\theta_o I]a_2 = -\frac{1}{4}\ \gamma^{2,0}(c,c)$

A1(QA1) $\qquad \begin{cases} [A-i\theta_o I]a_1 = \frac{3}{4}\ (\beta*d)c - \frac{3}{2}\ \beta \\ a_1*d = 0 \end{cases}$

A3(QA3) $\qquad [A-3i\theta_o I]a_3 = -\frac{3}{2}\ \gamma^{2,0}(a_2,c) - \frac{1}{8}\ \gamma^{3,0}(c,c,c).$

BO(QBO) $\quad Ab_o = -2\gamma^{2,0}(a_1,\bar{c}) - 2\gamma^{2,0}(\bar{a}_1,c)$

$$-6\gamma^{2,0}(a_2,\bar{a}_2) - 3\gamma^{2,0}(a_0,a_0) - 3\gamma^{3,0}(a_o,c,\bar{c})$$

$$- \frac{3}{2}\gamma^{3,0}(a_2,\bar{c},\bar{c}) - \frac{3}{2}\gamma^{3,0}(\bar{a}_2,c,c) \quad - \frac{3}{8}\gamma^{4,0}(c,c,\bar{c},\bar{c})$$

B2(QB2) $\quad [A-2i\theta_o I]b_2 = -2\gamma^{2,0}(a_1,c)-2\gamma^{2,0}(a_3,\bar{c})-6\gamma^{2,0}(a_o,a_2) -$

$$- \frac{3}{2}\gamma^{3,0}(a_o,c,c) - 3\gamma^{3,0}(a_2,c,\bar{c}) - \frac{1}{4}\gamma^{4,0}(c,c,c,\bar{c})$$

F2(QF2) $\quad [A-2i\theta_o I]f_2 = 2i\theta_o a_2$

HUM (PH1) $\quad \begin{cases} [A-2i\theta_o I]h_1 = \frac{1}{2}[(\gamma^{1,1}(c)*d)\frac{c}{2} - \gamma^{1,1}(c)] \\ h_1 * d = 0 \end{cases}$

HO(PHO) $\quad Ah_o = -\gamma^{1,1}(a_o) - \frac{1}{2}\gamma^{2,1}(c,\bar{c}) - 2\,\mathrm{Re}\,\gamma^{2,0}(h_1,\bar{c})$

H2(PH2) $\quad [A-2i\theta_o I]h_2 = -\gamma^{1,1}(a_2) - \gamma^{2,0}(h_1,c) - \frac{1}{4}\gamma^{2,1}(c,c)$

A1.4 In (II.1) we remark that the normalization of the eigenvectors c,d with $d * c = 2$ is not sufficient to determine c and d. Indeed, for any complex number $K \neq 0$, the vectors

$$\underset{\sim}{c} = Kc \qquad\qquad \underset{\sim}{d} = \frac{d}{\bar{K}}$$

satisfy the conditions in A1.2. When we compute the first order derivatives of the reduced germ $a(u,\lambda)$ using the new pair of eigenvalues, we get:

$$\underset{\sim}{a}_\lambda = -\frac{1}{2}\,\mathrm{Re}\,[\gamma^{1,1}(\underset{\sim}{c}) * \underset{\sim}{d}] = \frac{K}{K}\,a_\lambda = a_\lambda$$

whereas

$$\underset{\sim}{a}_u = -\frac{1}{4}\,[\underset{\sim}{\beta} * \underset{\sim}{d}] = |k|^2 a_u$$

since

$$\underset{\sim}{a}_o = -\frac{1}{2}\,A^{-1}(\gamma^{2,0}(\underset{\sim}{c},\bar{\underset{\sim}{c}})) = k\bar{k}\,a_o$$

$$\underset{\sim}{a}_2 = -\frac{1}{4}\,[A-2i\theta_o I]^{-1}\,(\gamma^{2,0}(\underset{\sim}{c},\underset{\sim}{c})) = k^2 a_2$$

$$\underset{\sim}{\beta} = \gamma^{2,0}(\underset{\sim}{a}_o,\underset{\sim}{c}) + \gamma^{2,0}(\underset{\sim}{a}_2,\bar{\underset{\sim}{c}}) + \frac{1}{4}\,\gamma^{3,0}(\underset{\sim}{c},\underset{\sim}{c},\bar{\underset{\sim}{c}}) =$$

$$= K^2\bar{K}\beta.$$

In most calculations this difference is unimportant, since the sign of a_u remains unchanged. However, since we want to study the variation in a_u as the parameters in HH are perturbed, we have normalized the vectors c to have 1 as their first component. (i.e. c is 1 in the direction v). In this way the bifurcation diagrams we obtain can be interpreted as qualitative graphs in the direction of the only variable that can be measured experimentally. Moreover this choice allowed us to compare our first order results to the numerical results of [12].

APPENDIX 2

We present here the listing of the subroutines that were used to compute the derivatives of $\gamma(u,\lambda,T)$ after reduction, at the maximum of the curve $T(\lambda)$ (IV.3.1).

The subroutines are divided in four groups: subroutines for multilinear algebra (LINEAR), for the computation of derivatives of γ (BIBLIOTECA), and two independent modules for evaluation of the maximum of $T(\lambda)$ (ZERO), and for the calculation of the formulae in Appendix 1 (UM). Subroutines FO2AFF and FO2AGF are NAG subroutines for the calculation of complex eigenvalues and eigenvectors. Subroutines FO4ADF (also NAG) solves a system of linear equations.

One main program is presented as an example of how the subroutines are put together. It computes the derivatives of $r(\gamma)$ with increasing accuracy in the calculation of the maximum of $T(\lambda)$, in the intervals $\lambda \in$ [ALO, AL1], $T \in$ [TO,T1], read from DADOS.

Communication between the two modules (ZERO and UM) is made via a common block; /ZERO/ given by:

COMMON / ZERO / AL, T, GK, GNA

corresponds to: λ, T, $\bar{g}_k$, $\bar{g}_{Na}$

The other two common blocks for the module UM are:

COMMON/UM/ PC(4,4), QC(4), QCB(4), QD(4), QDB(4)

A(4,4), EIG(2), TETA

variable:

PC(J,1)	eigenvector for EIG(1) $\in \mathbb{R}$
PC(J,2)	eigenvector for EIG(2) $\in \mathbb{R}$
PC(J,3)	eigenvector for $-i\theta$
PC(J,4) = QC(J)	eigenvector for $i\theta$,
QC(J)	c (II.1)
QCB(J)	$\bar{c}$
QD(J)	d (II.1)
QDB(J)	$\bar{d}$
A(I,J)	$A = d_u\gamma(0,\lambda,T)$ (II.1)
EIG(I)	Real eigenvalues of A
TETA	$\theta(\lambda)$ = Im (imaginary eigenvalue of A) > 0

All variables are computed by subroutine PREPAR, except for A, computed by MARIA. (both from BIBLIOTECA).

COMMON/DERI/QFM11, QFM12, QFQ, QFC

QFS, QFM21, QFT, QFM31.

This block contains the partial derivatives of γ(IV.0) needed for the formulae in Appendix 1. They are given by:

variable		subroutine
QFS(I,J,K)	$\frac{\partial^2 \gamma^I}{\partial x_I \partial x_J}$ (0,λ)	PAR2
QFT(I,J,K,L)	$\frac{\partial^3 \gamma^I}{\partial x_J \partial x_K \partial x_L}$(0,λ)	PAR3
QFQ(I,J,K,L,M)	$\frac{\partial^4 \gamma^I}{\partial x_J \partial x_K \partial x_L \partial x_M}$(0,λ)	PAR4
QFC(I,J,K,L,M,N)	$\frac{\partial^5 \gamma^I}{\partial x_J \partial x_K \partial x_L \partial x_M \partial x_N}$(0,λ)	PAR5
QFM11(I,J)	$\frac{\partial^2 \gamma^I}{\partial \lambda \partial x_J}$(0,λ)	MIX11
QFM12(I,J)	$\frac{\partial^3 \gamma^I}{\partial \lambda^2 \partial x_J}$(0,λ)	MIX12
QFM21(I,J,K)	$\frac{\partial^3 \gamma^I}{\partial \lambda \partial x_J \partial x_K}$(0,λ)	MIX21
QFM31(I,J,K,L)	$\frac{\partial^4 \gamma^I}{\partial \lambda \partial x_J \partial x_K \partial x_L}$(0,λ)	MIX31

Where $\gamma = (\gamma^1, \gamma^2, \gamma^3, \gamma^4)$

and $(x_1, x_2, x_3, x_4) = (v, m, n, h)$

and all subroutines are in the group BIBLIOTECA

In order to compute these derivatives we use the results of subroutine INFI (from BIBLIOTECA), that computes: (see IV.0).

$$XA(I,J) = \frac{d^{J-1}\alpha_i}{d\lambda^{J-1}}(\lambda)$$

$$XB(I,J) = \frac{d^{J-1}\beta_i}{d\lambda^{J-1}}(\lambda)$$

$$XINF(I,J) = \frac{d^{J-1}i_\infty}{d\lambda^{J-1}}(\lambda)$$

where I = 2, 3, 4

corresponds
to: i = m, n, h

The remaining variables were defined in Appendix 1.

SUBROUTINE TITLES

ZERO
- TETA
- TLMEL
- NNACCI

UM
- ANTES
- DERIVA
- VSOP
- PREPAR

UM/P1
- A0
- A1
- A2
- A3
- B0
- B2
- F2
- H0
- HUM
- H2

UM/P2
- P020
- P101
- P110
- P200
- PQ010
- PQ100

BIBLIOTECA
- MARIA
- INFI
- PAR2
- PAR3
- PAR4
- PAR5
- MIX11
- MIX12
- MIX21
- MIX31

LINEAR
- DERIF1
- DERIF2
- DERIF3
- DERIF4
- DERIF5
- CONDIC

MAIN PROGRAM

NOVO/DADOS

ZERO

SUBROUTINES THAT COMPUTE THE MAXIMUM OF THE CURVE T(λ)

TETA COMPUTES THE REAL PART OF THE COMPLEX EIGENVALUES OF A

TLMEL COMPUTES THE FUNCTION T(λ) - SEE IV.3

NNACCI COMPUTES THE MAXIMUM OF T(λ) USING A SEARCH BY THE GOLDEN SECTION

```
      SUBROUTINE TETA(AL,TE,GK,GNA,TERE,ITH,MER)

      REAL A(4,4),RR(4),RI(4)
      INTEGER INT(4)
      MER=0
      CALL MARIA(AL,TE,GK,GNA,A)
      CALL F02AFF(A,4,4,RR,RI,INT,MER)
      IF(MER.NE.0)RETURN
      DO 1 I=1,4
        IF(RI(I).LT..0001)GO TO 1
        TERE=RR(I)
        I=5
        IF(TERE.GT.0)GO TO 2
        ITH=-1
        GO TO 1
2       ITH=1
1       CONTINUE
      RETURN
      END
```

```
      SUBROUTINE TLMEL(AL,TP,TG,TNEW,GK,GNA,NIT,NI,EI,EROU,ETOU,FLAG)

      INTEGER FLAG(6)
      FLAG(1)=0
      FLAG(2)=0
      T0=TP
      T1=TG
      CALL TETA(AL,T0,GK,GNA,THR0,I0,MER)
      IF(MER.NE.0)GO TO 90
      CALL TETA(AL,T1,GK,GNA,THR1,I1,MER)
      IF(MER.NE.0)GO TO 100
      IF(I0.EQ.I1)GO TO 80
      NI=0
   10   ALF=(T1+T0)*.5
        CALL TETA(AL,ALF,GK,GNA,THRALF,IALF,MER)
        IF(MER.NE.0)GO TO 110
        NI=NI+1
      IF(IALF.EQ.I1)GO TO 30
      T0=ALF
      I0=IALF
      THR0=THRALF
      GO TO 40
   30   T1=ALF
        I1=IALF
        THR1=THRALF
   40 IF(NI.GE.NIT)GO TO 60
      IF(ABS(THR0).GT.EI.OR.ABS(THR1).GT.EI)GO TO 10
   60   ETOU=ABS(T1-T0)
        IF(ABS(THR0).LT.ABS(THR1))GO TO 70
        TNEW=T1
        EROU=THR1
        RETURN
   70 TNEW=T0
      EROU=THR0
      RETURN
C*    THE REAL PART DOES NOT CHANGE SIGN
   80   FLAG(1)=I0
        RETURN
C*    FAILURE IN TETA
   90 WRITE(6,301)T0
      GO TO 120
  100 WRITE(6,302)T1
      GO TO 120
  110 WRITE(6,303)ALF
  120 WRITE(6,305)AL,GK,GNA,MER
      FLAG(2)=MER
      RETURN
  301 FORMAT(2X,'T0=',F18.10,'DEGREES')
  302 FORMAT(2X,'T1=',F18.10,'DEGREES')
  303 FORMAT(2X,'ALF=',F18.10,'DEGREES')
  304 FORMAT(2X,'FAILURE IN TETA INSIDE TLMEL FOR TEMPERATURE ABOVE')
  305 FORMAT(2X,'AL=',F18.10,2X,'GK=',F7.2,2X,'GNA=',F7.2,2X,'MER=',I4)
      END
```

```
      SUBROUTINE NNACCI(X0,X1,T0,T1,ERIN,EROUT,NIN,NOUT,FLAG)
      COMMON/ZERO/XLAM,XT,GK,GNA
      REAL ERIN(6),EROUT(6)
      INTEGER NIN(4),NOUT(4),FLAG(6)
      NIT=NIN(1)
      EI=ERIN(1)
      NOUT(2)=0
      NOUT(3)=0
      DELTA1=-(1.-SQRT(5.))/2.
      DELTA2=DELTA1*DELTA1
      ALF=X0+DELTA2*(X1-X0)
      BET=X0+DELTA1*(X1-X0)
C*    INITIAL  BLOCK
  1     CALL TLMEL(X0,T0,T1,F0,GK,GNA,NIT,IOUT,EI,E0,ET0,FLAG)
        IF(FLAG(1).NE.0)GO TO 1000
        IF(FLAG(2).NE.0)RETURN
        NOUT(1)=MAX0(IOUT,NOUT(1))
        CALL TLMEL(X1,T0,T1,F1,GK,GNA,NIT,IOUT,EI,E1,ET1,FLAG)
        IF(FLAG(1).NE.0)GO TO 1000
        IF(FLAG(2).NE.0)RETURN
        NOUT(1)=MAX0(IOUT,NOUT(1))
        CALL TLMEL(ALF,T0,T1,FA,GK,GNA,NIT,IOUT,EI,EA,ETA,FLAG)
        IF(FLAG(1).NE.0)GO TO 1000
        IF(FLAG(2).NE.0)RETURN
        NOUT(1)=MAX0(IOUT,NOUT(1))
        CALL TLMEL(BET,T0,T1,FB,GK,GNA,NIT,IOUT,EI,EB,ETB,FLAG)
        IF(FLAG(1).NE.0)GO TO 1000
        IF(FLAG(2).NE.0)RETURN
        NOUT(1)=MAX0(IOUT,NOUT(1))
      IF(NOUT(2).GE.NIN(2))GO TO 21
C*    REDUCTION OF INTERVAL IN T
  2     VAR=(AMIN1(F0,FA,FB,F1)-T0)/FLOAT(NOUT(2)+2)
        T0=AMAX1(T0,AMIN1(FA,FB,F0,F1)-VAR)
        T1=AMIN1(T1,(AMAX1(FA,FB,F0,F1)+2.*T1)/3.)
```

```
C*      CENTRAL BLOCK
        IF(FA.GT.FB)GO TO 10
        X0=ALF
        F0=FA
        E0=EA
        ET0=ETA
        ALF=BET
        FA=FB
        EA=EB
        ETA=ETB
        BET=X0+DELTA1*(X1-X0)
        CALL TLMEL(BET,T0,T1,FB,GK,GNA,NIT,IOUT,EI,EB,ETB,FLAG)
        IF(FLAG(1).NE.0)GO TO 1000
        IF(FLAG(2).NE.0)RETURN
        NOUT(1)=MAX0(IOUT,NOUT(1))
        GO TO 20
10      X1=BET
        F1=FB
        E1=EB
        ET1=ETB
        BET=ALF
        FB=FA
        EB=EA
        ETB=ETA
        ALF=X0+DELTA2*(X1-X0)
        CALL TLMEL(ALF,T0,T1,FA,GK,GNA,NIT,IOUT,EI,EA,ETA,FLAG)
        IF(FLAG(1).NE.0)GO TO 1000
        IF(FLAG(2).NE.0)RETURN
        NOUT(1)=MAX0(IOUT,NOUT(1))
20        NOUT(2)=NOUT(2)+1
          IF(NOUT(2).LE.NIN(2).AND.(X1-X0).GE.ERIN(3))GO TO 2
```

```
C*      SUCCESSFUL RETURN
   21   EROUT(2)=AMAX1(F0,F1,FA,FB)-AMIN1(F0,F1,FA,FB)
        EROUT(3)=X1-X0
        IF(FA.GT.FB)GO TO 40
          XT=FB
          EROUT(1)=EB
          EROUT(4)=ETB
          XLAM=BET
          RETURN
  40    XT=FA
        XLAM=ALF
        EROUT(1)=EA
        EROUT(4)=ETA
        RETURN
C*      EXPANSION OF INTERVAL IN T
 1000   VAR=(T1-T0)/FLOAT(NIN(1))
        NOUT(3)=NOUT(3)+1
        IF(NOUT(3).GT.NIN(2))GO TO 1002
        IF(FLAG(1).LT.0)GO TO 1001
        T1=T1+VAR
        FLAG(1)=0
        GO TO 1
 1001     T0=T0-VAR
          FLAG(1)=0
          GO TO 1
C*      TOO MANY EXPANSIONS  -  ERROR MESSAGES
 1002   WRITE(6,100)T0,T1
        WRITE(6,200)X0,X1,GK,GNA
        WRITE(6,300)NOUT(2),NOUT(3)
        FLAG(3)=4
        RETURN
  100   FORMAT(//2X,'TOO MANY EXPANSIONS , T0=',F8.4,2X,'T1=',F8.4)
  200   FORMAT(2X,'AL0=',F9.4,2X,'AL1=',F9.4,2X,'K=',F6.1,2X,'NA=',F6.1)
  300   FORMAT(2X,I4,'ITERATIONS',5X,I4,'EXPANSIONS')
        END
```

UM

SUBROUTINES THAT EVALUATE THE FORMULAE IN APPENDIX 2
THE VARIABLES AL,T,GK,GNA ENTER AS THE COMMON BLOCK /ZEPO/.
THE SUBROUTINES ARE DIVIDED IN THREE GROUPS:

UM SUBROUTINES THAT EVALUATE THE DERIVATIVES OF γ , AND CALL THE OTHER TWO GROUPS

ANTES: CALLS ALL OTHER SUBROUTINES IN THE GROUP
DERIVA: CALLS SUBROUTINES IN THE GROUP BIBLIOTECA. ESTABLISHES THE COMMON BLOCK /DERI/
VSOP: CALLS GROUPS P1 AND P2. OUTPUTS ERROR MESSAGES FROM NAG SUBROUTINES.

P1 SUBROUTINES THAT EVALUATE THE SECOND GROUP OF FORMULAE IN APPENDIX 1

P2 SUBROUTINES THAT COMPUTE TERMS IN THE TAYLOR EXPANSION OF P (SEE APPENDIX 1)

UM

```
      SUBROUTINE ANTES(DAZ,DAL,DAZZ,DAZL,DALL,MER)

      IMPLICIT COMPLEX(O,P,Q)
      COMMON/ZERO/AL,T,GK,GNA
      REAL XA(4,7),XB(4,7),XINF(4,7)
      COMMON/DERI/QFM11(4,4),QFM12(4,4),QFQ(4,4,4,4,4),QFC(4,4,4,4,4,4)
      COMMON/DERI/QFS(4,4,4),QFM21(4,4,4),QFT(4,4,4,4),QFM31(4,4,4,4)
      COMMON/UM/PC(4,4),QC(4),QCB(4),QD(4),QDB(4)
      COMMON/UM/A(4,4),EIG(2),TETA
        MER=0
        CALL MARIA(AL,T,GK,GNA,A)
        CALL PREPAR(A,QC,QD,TETA,PC,EIG,MER)
        IF(MER.NE.0)GO TO 1000
        DO 1 I=1,4
          QCB(I)=CONJG(QC(I))
     1    QDB(I)=CONJG(QD(I))
        LIM=7
        LINF=4
        CALL INFI(AL,XA,XB,XINF,LIM,LINF)
        CALL DERIVA(XA,XB,XINF)
        CALL VSOP(DAZ,DAL,DAZZ,DAZL,DALL,MER)
      RETURN
 1000 WRITE(6,2000)AL,T,GK,GNA
      WRITE(6,3000)MER
      RETURN
 2000 FORMAT(/15X,'AL=',F15.10,'T=',F15.10,'GK=',F4.1,'GNA=',F4.1)
 3000 FORMAT(2X,'FAILURE IN PREPAR, IN ANTES: MER=',I4/)
      END
```

```
SUBROUTINE DERIVA(XA,XB,XINF)

IMPLICIT COMPLEX(O,P,Q)
COMMON/ZERO/AL,T,GK,GNA
REAL XA(4,7),XB(4,7),XINF(4,7)
COMMON/DERI/QFM11(4,4),QFM12(4,4),QFQ(4,4,4,4,4),QFC(4,4,4,4,4,4)
COMMON/DERI/QFS(4,4,4),QFM21(4,4,4),QFT(4,4,4,4),QFM31(4,4,4,4)
CALL MIX11(AL,T,GK,GNA,XA,XB,XINF,QFM11)
CALL MIX12(AL,T,GK,GNA,XA,XB,XINF,QFM12)
CALL MIX21(AL,T,GK,GNA,XA,XB,XINF,QFM21)
CALL MIX31(AL,T,GK,GNA,XA,XB,XINF,QFM31)
CALL PAR2(AL,T,GK,GNA,XA,XB,XINF,QFS)
CALL PAR3(AL,T,GK,GNA,XA,XB,XINF,QFT)
CALL PAR4(AL,T,GK,GNA,XA,XB,XINF,QFQ)
CALL PAR5(AL,T,GK,GNA,XA,XB,XINF,QFC)
RETURN
END
```

```
      SUBROUTINE VSOP(DAZ,DAL,DAZZ,DAZL,DALL,MER)

      IMPLICIT COMPLEX(O,P,Q)
      COMMON/DERI/QFM11(4,4),QFM12(4,4),QFQ(4,4,4,4,4),QFC(4,4,4,4,4,4)
      COMMON/DERI/QFS(4,4,4),QFM21(4,4,4),QFT(4,4,4,4),QFM31(4,4,4,4)
      COMMON/UM/PC(4,4),QC(4),QCB(4),QD(4),QDB(4)
      COMMON/UM/A(4,4),EIG(2),TETA
      COMPLEX QA0(4),QA1(4),QA2(4),QA3(4),QB0(4),QB2(4)
      COMPLEX OB(4),QF2(4),PH0(4),PH1(4),PH2(4)
      MER=0
        CALL A0(QA0,MER)
      IF(MER.EQ.0)GO TO 1
      MER=MER+10
      WRITE(6,100)
      RETURN
    1   CALL A2(QA2,MER)
      IF(MER.EQ.0)GO TO 2
      MER=MER+20
      WRITE(6,200)
      RETURN
    2   CALL PQ100(QA0,QA2,OB,OUX,DAZ,XQ100)
        CALL A1(OB,QA1,MER)
      IF(MER.EQ.0)GO TO 3
      MER=MER+30
      WRITE(6,300)MER
      RETURN
    3   CALL A3(QA2,QA3,MER)
      IF(MER.EQ.0)GO TO 4
      MER=MER+40
      WRITE(6,400)
      RETURN
    4   CALL B0(QA0,QA1,QA2,QB0,MER)
      IF(MER.EQ.0)GO TO 5
      MER=MER+50
      WRITE(6,500)
      RETURN
    5   CALL B2(QA0,QA1,QA2,QA3,QB2,MER)
      IF(MER.EQ.0)GO TO 6
      MER=MER+60
      WRITE(6,600)
      RETURN
    6   CALL F2(QA2,QF2,MER)
      IF(MER.EQ.0)GO TO 7
      MER=MER+70
      WRITE(6,700)
      RETURN
    7   CALL HUM(PH1,MER)
      IF(MER.EQ.0)GO TO 8
      MER=MER+80
      WRITE(6,800)MER
      RETURN
```

```
8       CALL H0(QA0,PH1,PH0,MER)
      IF(MER.EQ.0)GO TO 9
      MER=MER+90
      WRITE(6,900)
      RETURN
9       CALL H2(QA2,PH1,PH2,MER)
      IF(MER.EQ.0)GO TO 10
      MER=MER+100
      WRITE(6,1000)
      RETURN
10    CALL PQ010(DAL,XQ010)
      CALL P020(PH1,DALL)
      CALL P101(QF2,XP101)
      CALL P110(QA0,QA1,QA2,PH0,PH1,PH2,XP110)
      CALL P200(QA0,QA1,QA2,QA3,QB0,QB2,XP200)
    DAZZ=XP200+XP101*XQ100
    DAZL=XP110+XP101*XQ010
    RETURN
100     FORMAT(//2X,'ERROR IN BIBLO/P1/A0')
200     FORMAT(//2X,'ERROR IN BIBLO/P1/A2')
300     FORMAT(//2X,'ERROR IN BIBLO/P1/A1    MER=',I4)
400     FORMAT(//2X,'ERROR IN BIBLO/P1/A3')
500     FORMAT(//2X,'ERROR IN BIBLO/P1/B0')
600     FORMAT(//2X,'ERROR IN BIBLO/P1/B2')
700     FORMAT(//2X,'ERROR IN BIBLO/P1/F2')
800     FORMAT(//2X,'ERROR IN BIBLO/P1/HUM    MER=',I4)
900     FORMAT(//2X,'ERROR IN BIBLO/P1/H0')
1000     FORMAT(//2X,'ERROR IN BIBLO/P1/H2')
        END
```

P1

```
      SUBROUTINE A0(QA0,MER)

      IMPLICIT COMPLEX(O,P,Q)
      REAL WK(4)
      COMPLEX PA(4,4),PP(4,1),PA0(4,1),QA0(4),PS(4)
      COMMON/DERI/QFM11(4,4),QFM12(4,4),QFQ(4,4,4,4,4),QFC(4,4,4,4,4,4)
      COMMON/DERI/QFS(4,4,4),QFM21(4,4,4),QFT(4,4,4,4),QFM31(4,4,4,4)
      COMMON/UM/PC(4,4),QC(4),QCB(4),QD(4),QDB(4)
      COMMON/UM/A(4,4),EIG(2),TETA
      CALL DERIF2(QFS,QC,QCB,PS)
      DO 2 I=1,4
        PP(I,1)=PS(I)*CMPLX(-.5,0.)
        DO 2 J=1,4
    2     PA(I,J)=CMPLX(A(I,J),0.)
      MER=0
      CALL F04ADF(PA,4,PP,4,4,1,PA0,4,WK,MER)
      IF(MER.NE.0)RETURN
      DO 3 I=1,4
    3   QA0(I)=PA0(I,1)
      RETURN
      END
```

```
      SUBROUTINE A1(OB,QA1,MER)

      IMPLICIT COMPLEX(O,P,Q)
      COMPLEX QA1(4),QV(4),OB(4)
      COMMON/UM/PC(4,4),QC(4),QCB(4),QD(4),QDB(4)
      COMMON/UM/A(4,4),EIG(2),TETA
      DO 1 I=1,4
1     QV(I)=1.5*OB(I)
      MER=0
      CALL CONDIC(PC,TETA,EIG,QV,QA1,MER)
      RETURN
      END
```

```
      SUBROUTINE A2(QA2,MER)

      IMPLICIT COMPLEX(O,P,Q)
      COMMON/DERI/QFM11(4,4),QFM12(4,4),QFQ(4,4,4,4,4),QFC(4,4,4,4,4,4)
      COMMON/DERI/QFS(4,4,4),QFM21(4,4,4),QFT(4,4,4,4),QFM31(4,4,4,4)
      COMMON/UM/PC(4,4),QC(4),QCB(4),QD(4),QDB(4)
      COMMON/UM/A(4,4),EIG(2),TETA
      REAL WK(4)
      COMPLEX QA2(4),OU(4),PA2(4,1),PE(4,1),OA(4,4)
      CALL DERIF2(QFS,QC,QC,OU)
      DO 1 I=1,4
        PE(I,1)=OU(I)*CMPLX(-.25,0.)
        OA(I,I)=CMPLX(0.,-2.*TETA)
        DO 1 J=1,4
1         OA(I,J)=OA(I,J)+CMPLX(A(I,J),0.)
      MER=0
      CALL F04ADF(OA,4,PE,4,4,1,PA2,4,WK,MER)
      IF(MER.NE.0)RETURN
      DO 2 I=1,4
2       QA2(I)=PA2(I,1)
      RETURN
      END
```

```
      SUBROUTINE A3(QA2,QA3,MER)

      IMPLICIT COMPLEX(O,P,Q)
      COMMON/DERI/QFM11(4,4),QFM12(4,4),QFQ(4,4,4,4,4),QFC(4,4,4,4,4,4)
      COMMON/DERI/QFS(4,4,4),QFM21(4,4,4),QFT(4,4,4,4),QFM31(4,4,4,4)
      COMMON/UM/PC(4,4),QC(4),QCB(4),QD(4),QDB(4)
      COMMON/UM/A(4,4),EIG(2),TETA
      COMPLEX QA2(4),QA3(4),OK(4),OL(4)
     1 COMPLEX PA(4,4),PS(4,1),PE(4,1)
     2 REAL WK(4)
     3 CALL DERIF2(QFS,QA2,QC,OK)
     4 CALL DERIF3(QFT,QC,QC,QC,OL)
     5 DO 1 I=1,4
     6   PA(I,I)=CMPLX(0.,-3.*TETA)
     7   PE(I,1)=CMPLX(-1.5,0.)*OK(I)
     8   PE(I,1)=PE(I,1)-CMPLX(.125,0.)*OL(I)
     9   DO 1 J=1,4
    10 1   PA(I,J)=PA(I,J)+CMPLX(A(I,J),0.)
    11   MER=0
    12   CALL F04ADF(PA,4,PE,4,4,1,PS,4,WK,MER)
    13   IF(MER.NE.0)RETURN
    14   DO 2 I=1,4
    15 2  QA3(I)=PS(I,1)
    16   RETURN
    17   END
```

```
      SUBROUTINE B0(QA0,QA1,QA2,QB0,MER)

      IMPLICIT COMPLEX(O,P,Q)
      COMMON/DERI/QFM11(4,4),QFM12(4,4),QFQ(4,4,4,4,4),QFC(4,4,4,4,4,4)
      COMMON/DERI/QFS(4,4,4),QFM21(4,4,4),QFT(4,4,4,4),QFM31(4,4,4,4)
      COMMON/UM/PC(4,4),QC(4),QCB(4),QD(4),QDB(4)
      COMMON/UM/A(4,4),EIG(2),TETA
      REAL WK(4)
      COMPLEX QA0(4),QA1(4),QA2(4),QB0(4),Q2A(4)
      COMPLEX OI(4),OJ(4),OK(4),OL(4),OM(4),ON(4)
      COMPLEX PA(4,4),PE(4,1),PS(4,1)
      DO 1 I=1,4
        Q2A(I)=CONJG(QA2(I))
        DO 1 J=1,4
1       PA(I,J)=CMPLX(A(I,J),0.)
      CALL DERIF2(QFS,QA1,QCB,OI)
      CALL DERIF3(QFT,QA2,QCB,QCB,OJ)
      CALL DERIF2(QFS,QA0,QA0,OK)
      CALL DERIF2(QFS,QA2,Q2A,OL)
      CALL DERIF3(QFT,QA0,QC,QCB,OM)
      CALL DERIF4(QFQ,QC,QC,QCB,QCB,ON)
      DO 2 I=1,4
        PE(I,1)=CMPLX(4.*REAL(OI(I))+3.*REAL(OJ(I)),0.)
        PE(I,1)=CMPLX(3.,0.)*(OK(I)+OM(I))+PE(I,1)
        PE(I,1)=CMPLX(6.,0.)*OL(I)+PE(I,1)
2       PE(I,1)=CMPLX(-.375,0.)*ON(I)-PE(I,1)
      MER=0
      CALL F04ADF(PA,4,PE,4,4,1,PS,4,WK,MER)
      IF(MER.NE.0)RETURN
      DO 3 I=1,4
3       QB0(I)=PS(I,1)
      RETURN
      END
```

```
      SUBROUTINE B2(QA0,QA1,QA2,QA3,QB2,MER)

      IMPLICIT COMPLEX(O,P,Q)
      COMMON/DERI/QFM11(4,4),QFM12(4,4),QFQ(4,4,4,4,4),QFC(4,4,4,4,4,4)
      COMMON/DERI/QFS(4,4,4),QFM21(4,4,4),QFT(4,4,4,4),QFM31(4,4,4,4)
      COMMON/UM/PC(4,4),QC(4),QCB(4),QD(4),QDB(4)
      COMMON/UM/A(4,4),EIG(2),TETA
      REAL WK(4)
      COMPLEX QA0(4),QA1(4),QA2(4),QA3(4),QB2(4)
      COMPLEX OU(4),OV(4),OW(4),OX(4),OY(4),OZ(4)
      COMPLEX PA(4,4),PE(4,1),PS(4,1)
      CALL DERIF2(QFS,QA1,QC,OU)
      CALL DERIF2(QFS,QA3,QCB,OV)
      CALL DERIF2(QFS,QA0,QA2,OW)
      CALL DERIF3(QFT,QA0,QC,QC,OX)
      CALL DERIF3(QFT,QA2,QC,QCB,OY)
      CALL DERIF4(QFQ,QC,QC,QC,QCB,OZ)
      DO 2 I=1,4
        PE(I,1)=CMPLX(2.,0.)*(OU(I)+OV(I))
        PE(I,1)=CMPLX(6.,0.)*OW(I)+PE(I,1)
        PE(I,1)=CMPLX(1.5,0.)*OX(I)+PE(I,1)
        PE(I,1)=CMPLX(3.,0.)*OY(I)+PE(I,1)
        PE(I,1)=CMPLX(-.25,0.)*OZ(I)-PE(I,1)
        PA(I,I)=CMPLX(0.,2.*TETA)
        DO 2 J=1,4
 2        PA(I,J)=CMPLX(A(I,J),0.)-PA(I,J)
      CALL F04ADF(PA,4,PE,4,4,1,PS,4,WK,MER)
      IF(MER.NE.0)RETURN
      DO 3 I=1,4
 3      QB2(I)=PS(I,1)
      RETURN
      END
```

```
      SUBROUTINE F2(QA2,QF2,MER)

      IMPLICIT COMPLEX(O,P,Q)
      COMMON/UM/PC(4,4),QC(4),QCB(4),QD(4),QDB(4)
      COMMON/UM/A(4,4),EIG(2),TETA
      REAL WK(4)
      COMPLEX QA2(4),QF2(4),OA(4,4),OE(4,1),OS(4,1)
      DO 1 I=1,4
        OA(I,I)=CMPLX(0.,2.*TETA)
        OE(I,1)=OA(I,I)*QA2(I)
        DO 1 J=1,4
1       OA(I,J)=CMPLX(A(I,J),0.)-OA(I,J)
      MER=0
      CALL F04ADF(OA,4,OE,4,4,1,OS,4,WK,MER)
      IF(IFA.NE.0)RETURN
      DO 2 I=1,4
2         QF2(I)=OS(I,1)
      RETURN
      END
```

```
      SUBROUTINE H0(QA0,PH1,PH0,MER)

      IMPLICIT COMPLEX(O,P,Q)
      COMMON/DERI/QFM11(4,4),QFM12(4,4),QFQ(4,4,4,4,4),QFC(4,4,4,4,4,4)
      COMMON/DERI/QFS(4,4,4),QFM21(4,4,4),QFT(4,4,4,4),QFM31(4,4,4,4)
      COMMON/UM/PC(4,4),QC(4),QCB(4),QD(4),QDB(4)
      COMMON/UM/A(4,4),EIG(2),TETA
      REAL WK(4)
      COMPLEX QA0(4),PH1(4),PH0(4),OV(4),OX(4),OY(4)
      COMPLEX PA(4,4),PE(4,1),PS(4,1)
      CALL DERIF1(QFM11,QA0,OV)
      CALL DERIF2(QFS,PH1,QCB,OX)
      CALL DERIF2(QFM21,QC,QCB,OY)
      DO 2 I=1,4
        PE(I,1)=CMPLX(.5,0.)*OY(I)+OV(I)
        PE(I,1)=-PE(I,1)-CMPLX(2.*REAL(OX(I)),0.)
        DO 2 J=1,4
2         PA(I,J)=CMPLX(A(I,J),0.)
      CALL F04ADF(PA,4,PE,4,4,1,PS,4,WK,MER)
      IF(MER.EQ.0)RETURN
      DO 3 I=1,4
3       PH0(I)=PS(I,1)
      RETURN
      END
```

```
      SUBROUTINE HUM(PH1,MER)

      IMPLICIT COMPLEX(O,P,Q)
      COMMON/DERI/QFM11(4,4),QFM12(4,4),QFQ(4,4,4,4,4),QFC(4,4,4,4,4,4)
      COMMON/DERI/QFS(4,4,4),QFM21(4,4,4),QFT(4,4,4,4),QFM31(4,4,4,4)
      COMMON/UM/PC(4,4),QC(4),QCB(4),QD(4),QDB(4)
      COMMON/UM/A(4,4),EIG(2),TETA
      COMPLEX PH1(4),QV(4)
      CALL DERIF1(QFM11,QC,QV)
      DO 1 I=1,4
    1   QV(I)=CMPLX(.5,0.)*QV(I)
      CALL CONDIC(PC,TETA,EIG,QV,PH1,MER)
      IF(MER.NE.0)GO TO 1000
      MER=0
 1000 RETURN
      END
```

```
      SUBROUTINE H2(QA2,PH1,PH2,MER)

      IMPLICIT COMPLEX(O,P,Q)
      COMMON/DERI/QFM11(4,4),QFM12(4,4),QFQ(4,4,4,4,4),QFC(4,4,4,4,4,4)
      COMMON/DERI/QFS(4,4,4),QFM21(4,4,4),QFT(4,4,4,4),QFM31(4,4,4,4)
      COMMON/UM/PC(4,4),QC(4),QCB(4),QD(4),QDB(4)
      COMMON/UM/A(4,4),EIG(2),TETA
      REAL WK(4)
      COMPLEX QA2(4),PH1(4),PH2(2),OV(4),OX(4),OY(4)
      COMPLEX PA(4,4),PE(4,1),PS(4,1)
      CALL DERIF1(QFM11,QA2,OV)
      CALL DERIF2(QFS,PH1,QC,OX)
      CALL DERIF2(QFM21,QC,QC,OY)
      DO 1 I=1,4
        PE(I,1)=CMPLX(.25,0.)*OY(I)
        PE(I,1)=-PE(I,1)-OV(I)-OX(I)
        PA(I,I)=CMPLX(0.,2.*TETA)
        DO 1 J=1,4
1         PA(I,J)=CMPLX(A(I,J),0.)-PA(I,J)
      MER=0
      CALL F04ADF(PA,4,PE,4,4,1,PS,4,WK,MER)
      IF(MER.NE.0)RETURN
      DO 2 I=1,4
2       PH2(I)=PS(I,1)
      RETURN
      END
```

P2

```
      SUBROUTINE P020(PH1,DALL)

      IMPLICIT COMPLEX(O,P,Q)
      COMMON/DERI/QFM11(4,4),QFM12(4,4),QFQ(4,4,4,4,4),QFC(4,4,4,4,4,4)
      COMMON/DERI/QFS(4,4,4),QFM21(4,4,4),QFT(4,4,4,4),QFM31(4,4,4,4)
      COMMON/UM/PC(4,4),QC(4),QCB(4),QD(4),QDB(4)
      COMMON/UM/A(4,4),EIG(2),TETA
      COMPLEX OV(4),OU(4),PH1(4)
      CALL DERIF1(QFM11,PH1,OV)
      CALL DERIF1(QFM12,QC,OU)
      DO 1 I=1,4
        OU(I)=CMPLX(.25,0.)*OU(I)+OV(I)
1       OX=OX-OU(I)*QDB(I)
      DALL=REAL(OX)
      RETURN
      END
```

```
      SUBROUTINE P101(QF2,XP101)

      IMPLICIT COMPLEX(O,P,Q)
      COMMON/DERI/QFM11(4,4),QFM12(4,4),QFQ(4,4,4,4,4),QFC(4,4,4,4,4,4)
      COMMON/DERI/QFS(4,4,4),QFM21(4,4,4),QFT(4,4,4,4),QFM31(4,4,4,4)
      COMMON/UM/PC(4,4),QC(4),QCB(4),QD(4),QDB(4)
      COMMON/UM/A(4,4),EIG(2),TETA
      COMPLEX QF2(4),OU(4)
      CALL DERIF2(QFS,QF2,QCB,OU)
      DO 2 I=1,4
    2   OS=OS-OU(I)*QDB(I)
      XP101=.25*REAL(OS)
      RETURN
      END
```

```
      SUBROUTINE P110(QA0,QA1,QA2,PH0,PH1,PH2,XP110)

      IMPLICIT COMPLEX(O,P,Q)
      COMMON/DERI/QFM11(4,4),QFM12(4,4),QFQ(4,4,4,4,4),QFC(4,4,4,4,4,4)
      COMMON/DERI/QFS(4,4,4),QFM21(4,4,4),QFT(4,4,4,4),QFM31(4,4,4,4)
      COMMON/UM/PC(4,4),QC(4),QCB(4),QD(4),QDB(4)
      COMMON/UM/A(4,4),EIG(2),TETA
      COMPLEX QA0(4),QA1(4),QA2(4),PH0(4),PH1(4),PHB(4),PH2(4)
      COMPLEX QGA(4),OA(4),OB(4),OC(4),OD(4),OE(4),OF(4)
      DO 1 I=1,4
    1   PHB(I)=CONJG(PH1(I))
      CALL DERIF2(QFS,PH1,QA0,OA)
      CALL DERIF2(QFS,PHB,QA2,OB)
      CALL DERIF2(QFS,PH2,QCB,OC)
      CALL DERIF2(QFS,PH0,QC,OD)
      CALL DERIF3(QFT,PHB,QC,QC,OE)
      CALL DERIF3(QFT,PH1,QC,QCB,OF)
      DO 2 I=1,4
        QGA(I)=(OC(I)+OD(I)+OF(I))*CMPLX(.5,0.)
        QGA(I)=QGA(I)+OA(I)+OB(I)
    2   QGA(I)=QGA(I)+OE(I)*CMPLX(.25,0.)
      CALL DERIF1(QFM11,QA1,OA)
      CALL DERIF2(QFM21,QA0,QC,OB)
      CALL DERIF2(QFM21,QA2,QCB,OC)
      CALL DERIF3(QFM31,QC,QC,QCB,OD)
      DO 3 I=1,4
        QGA(I)=QGA(I)+OA(I)/CMPLX(3.,0.)
        OB(I)=OB(I)+OC(I)+CMPLX(.25,0.)*OD(I)
        QGA(I)=QGA(I)+OB(I)*CMPLX(.5,0.)
    3   OS=OS-QGA(I)*QDB(I)
      XP110=.5*REAL(OS)
      RETURN
      END
```

```
      SUBROUTINE P200(QA0,QA1,QA2,QA3,QB0,QB2,XP200)

      IMPLICIT COMPLEX(O,P,Q)
      COMMON/DERI/QFM11(4,4),QFM12(4,4),QFQ(4,4,4,4,4),QFC(4,4,4,4,4,4)
      COMMON/DERI/QFS(4,4,4),QFM21(4,4,4),QFT(4,4,4,4),QFM31(4,4,4,4)
      COMMON/UM/PC(4,4),QC(4),QCB(4),QD(4),QDB(4)
      COMMON/UM/A(4,4),EIG(2),TETA
      COMPLEX QA0(4),QA1(4),QA2(4),QA3(4),P1(4),P2(4)
      COMPLEX OA(4),OB(4),OC(4),OD(4),OE(4),OF(4),OG(4)
      COMPLEX QB0(4),QB2(4)
      DO 1 I=1,4
        P1(I)=CONJG(QA1(I))
    1   P2(I)=CONJG(QA2(I))
      CALL DERIF3(QFT,QA0,QA0,QC,OA)
      CALL DERIF3(QFT,QA2,P2,QC,OB)
      CALL DERIF3(QFT,QA0,QA2,QCB,OC)
      CALL DERIF3(QFT,P1,QC,QC,OD)
      CALL DERIF3(QFT,QA1,QC,QCB,OE)
      CALL DERIF3(QFT,QA3,QC,QCB,OF)
      DO 2 I=1,4
        OG(I)=CMPLX(3.,0.)*(OB(I)+OC(I)+CMPLX(.5,0.)*OA(I))
        OG(I)=OG(I)+CMPLX(.5,0.)*(OD(I)+OF(I))
    2   OG(I)=OG(I)+OE(I)
      CALL DERIF2(QFS,QA0,QA1,OA)
      CALL DERIF2(QFS,P2,QA3,OB)
      CALL DERIF2(QFS,P1,QA2,OC)
      CALL DERIF4(QFQ,P2,QC,QC,QC,OD)
      CALL DERIF4(QFQ,QA0,QC,QC,QCB,OE)
      CALL DERIF4(QFQ,QA2,QC,QCB,QCB,OF)
      DO 3 I=1,4
        OG(I)=OG(I)+CMPLX(2.,0.)*(OA(I)+OB(I)+OC(I))
        OG(I)=OG(I)+CMPLX(.25,0.)*OD(I)
    3   OG(I)=OG(I)+CMPLX(.75,0.)*(OE(I)+OF(I))
      CALL DERIF2(QFS,QB0,QC,OA)
      CALL DERIF2(QFS,QB2,QCB,OB)
      CALL DERIF5(QFQ,QC,QC,QC,QCB,QCB,OC)
      DO 4 I=1,4
        OG(I)=OG(I)+CMPLX(.5,0.)*(OA(I)+OB(I))
        OG(I)=OG(I)+CMPLX(.0625,0.)*OC(I)
    4   OUX=OUX-OG(I)*QDB(I)
      XP200=REAL(OUX)/24.
      RETURN
      END
```

```
      SUBROUTINE PQ010(XP010,XQ010)

      IMPLICIT COMPLEX(O,P,Q)
      COMMON/DERI/QFM11(4,4),QFM12(4,4),QFQ(4,4,4,4,4),QFC(4,4,4,4,4,4)
      COMMON/DERI/QFS(4,4,4),QFM21(4,4,4),QFT(4,4,4,4),QFM31(4,4,4,4)
      COMMON/UM/PC(4,4),QC(4),QCB(4),QD(4),QDB(4)
      COMMON/UM/A(4,4),EIG(2),TETA
      COMPLEX OU(4)
      CALL DERIF1(QFM11,QC,OU)
      OX=CMPLX(0.,0.)
      DO 1 I=1,4
    1   OX=OX-OU(I)*QDB(I)*CMPLX(.5,0.)
      XP010=REAL(OX)
      XQ010=AIMAG(OX)
      RETURN
      END
```

```
      SUBROUTINE PQ100(QA0,QA2,OB,OUX,XP100,XQ100)

      IMPLICIT COMPLEX(O,P,Q)
      COMMON/DERI/QFM11(4,4),QFM12(4,4),QFQ(4,4,4,4,4),QFC(4,4,4,4,4,4)
      COMMON/DERI/QFS(4,4,4),QFM21(4,4,4),QFT(4,4,4,4),QFM31(4,4,4,4)
      COMMON/UM/PC(4,4),QC(4),QCB(4),QD(4),QDB(4)
      COMMON/UM/A(4,4),EIG(2),TETA
      COMPLEX OB(4),OS(4),OT(4),QA0(4),QA2(4)
      CALL DERIF2(QFS,QC,QA0,OB)
      CALL DERIF2(QFS,QCB,QA2,OS)
      CALL DERIF3(QFT,QC,QC,QCB,OT)
      OUX=CMPLX(0.,0.)
      DO 2 I=1,4
        OB(I)=OB(I)+OS(I)+CMPLX(.25,0.)*OT(I)
2       OUX=OUX+QD(I)*CONJG(OB(I))
      XP100=-.25*REAL(OUX)
      XQ100=.25*AIMAG(OUX)
      RETURN
      END
```

```
      SUBROUTINE PREPAR(A,QC,QD,TETA,PC,EIG,MERDA)

      IMPLICIT COMPLEX(O,P,Q)
      INTEGER INT(4)
      REAL A(4,4),AA(4,4),AT(4,4),VR(4,4),VI(4,4)
      REAL RR(4),RI(4),EIG(2)
      COMPLEX PC(4,4),QC(4),QD(4)
      DO 1 I=1,4
      DO 1 J=1,4
      AA(I,J)=A(I,J)
    1 AT(I,J)=A(J,I)
      CALL F02AGF(AA,4,4,RR,RI,VR,4,VI,4,INT,IFA)
      IF(IFA.NE.0)GO TO 1000
      DO 2 I=1,4
      IF(RI(I).LT..001)GO TO 20
      TETA=RI(I)
      DO 3 J=1,4
      QC(J)=CMPLX(VR(J,I),VI(J,I))
    3 PC(J,4)=QC(J)
      GO TO 2
   20 IF(RI(I).GT.-.001)GO TO 30
      DO 4 J=1,4
    4 PC(J,3)=CMPLX(VR(J,I),VI(J,I))
      GO TO 2
   30 IF(EIG(1).NE.0.)GO TO 40
      EIG(1)=RR(I)
      DO 5 J=1,4
    5 PC(J,1)=CMPLX(VR(J,I),VI(J,I))
      GO TO 2
   40 EIG(2)=RR(I)
      DO 6 J=1,4
    6 PC(J,2)=CMPLX(VR(J,I),VI(J,I))
    2 CONTINUE
      DO 90 I=1,4
      RR(I)=0.
      RI(I)=0.
      DO 90 J=1,4
      VR(I,J)=0.
   90 VI(I,J)=0.
      CALL F02AGF(AT,4,4,RR,RI,VR,4,VI,4,INT,IFA)
      IF(IFA.NE.0)GO TO 1001
      DO 100 I=1,4
      IF(RI(I).GT.-.001)GO TO 100
      DO 110 J=1,4
  110 QD(J)=CMPLX(VR(J,I),VI(J,I))
  100 CONTINUE
      QR=CMPLX(0.,0.)
      DO 150 I=1,4
  150 QR=QR+QD(I)*CONJG(QC(I))
      IF(QR.EQ.0.)GO TO 1002
```

```
      DO 200 I=1,4
200   QD(I)=CMPLX(2.,0.)*QD(I)/QR
      MERDA=0
      RETURN
1001  MERDA=1
      RETURN
1000  MERDA=2
      RETURN
1002  MERDA=-1
      RETURN
      END
```

SUBROUTINES THAT COMPUTE THE PARTIAL DERIVATIVES OF σ (IV.0)

```
SUBROUTINE MARIA(AL,T,GK,GNA,A)

DIMENSION A(4,4)
FI=3.**(T/10.-.63)
YCM=EXP((AL/10.)+2.5)
XGM=((YCM-1.)**2)*10.
YAM=((1.-(2.5+AL/10.))*YCM-1.)/XGM
AM=(AL+25.)/(10.*(EXP(.1*(AL+25.))-1.))
YBM=(2./9.)*EXP(AL/18.)
BM=4.*(EXP(AL/18.))
XMINF=AM/(AM+BM)
XGN=(-1.+EXP(1.+(AL/10.)))**2
YAN=(-1.-(AL/10.)*EXP((AL/10.)+1.))/(100.*XGN)
AN=(AL+10.)/(100.*(EXP((AL/10.)+1.)-1.))
YBN=(.125/80.)*EXP(AL/80.)
BN=.125*EXP(AL/80.)
XNINF=AN/(AN+BN)
YAH=.0035*EXP(AL/20.)
YBH=-EXP((AL/10.)+3.)/(10.*((EXP((AL/10.)+3.)+1.)**2))
AH=.07*EXP(AL/20.)
BH=1./(1.+EXP((AL/10.)+3.))
XHINF=AH/(AH+BH)
A(3,2)=0
A(4,2)=0
A(4,3)=0
A(2,3)=0
A(2,4)=0
A(3,4)=0
A(1,1)=-GK*(XNINF**4)-GNA*(XMINF**3)*XHINF-.3
A(1,2)=-3.*GNA*(XMINF**2)*XHINF*(AL+115.)
A(1,3)=-GK*4.*(XNINF**3)*(AL-12.)
A(1,4)=-GNA*(XMINF**3)*(AL+115.)
A(2,1)=(YAM*(1.-XMINF)-YBM*XMINF)*FI
A(3,1)=(YAN*(1.-XNINF)-YBN*XNINF)*FI
A(4,1)=(YAH*(1.-XHINF)-YBH*XHINF)*FI
A(2,2)=-FI*(AM+BM)
A(3,3)=-FI*(AN+BN)
A(4,4)=-FI*(AH+BH)
RETURN
END
```

```
      SUBROUTINE INFI(AL,XA,XB,XINF,LIM,LINF)

      REAL XA(4,7),XB(4,7),XINF(4,7)
      IF(LIM.LT.LINF)LIM=LINF
      I=1
      V2=2.5+AL/10.
      E2=EXP(V2)
      F2=E2-1.
      XA(2,1)=V2/F2
      XB(2,1)=4.*EXP(AL/18.)
      V1=1.+AL/10.
      E1=EXP(V1)
      F1=E1-1.
      XA(3,1)=.1*V1/F1
      XB(3,1)=.125*EXP(AL/80.)
      XA(4,1)=.07*EXP(AL/20.)
      E3=EXP(3.+AL/10.)
      XB(4,1)=1./(1.+E3)
      IF(I.EQ.LIM)GO TO 1000
      I=I+1
      XA(2,2)=(F2-V2*E2)/(10.*(F2**2.))
      XB(2,2)=XB(2,1)/18.
      XA(3,2)=(F1-V1*E1)/(100.*(F1**2.))
      XB(3,2)=XB(3,1)/80.
      XA(4,2)=XA(4,1)/20.
      XB(4,2)=-E3*XB(4,1)*XB(4,1)/10.
      IF(I.EQ.LIM)GO TO 1000
      I=I+1
      GM=E2*(V2+2.+(V2-2.)*E2)
      XA(2,3)=GM/(100.*(F2**3.))
      XB(2,3)=XB(2,2)/18.
      GN=E1*(V1+2.+E1*(V1-2.))
      XA(3,3)=GN/(1000.*(F1**3.))
      XB(3,3)=XB(3,1)/6400.
      XA(4,3)=XA(4,1)/400.
      XB(4,3)=XB(4,1)*XB(4,1)*XB(4,1)*E3*(E3-1.)/100.
      IF(I.EQ.LIM)GO TO 1000
      I=I+1
      GGM=E2*(-V2-3.+E2*(E2*(3.-V2)-4.*V2))
      XA(2,4)=GGM/(1000.*(F2**4.))
      XB(2,4)=XB(2,3)/18.
      GGN=E1*(-V1-3.+E1*(E1*(3.-V1)-4*V1))
      XA(3,4)=GGN/(10000.*(F1**4.))
      XB(3,4)=XB(3,3)/80.
      XA(4,4)=XA(4,3)/20.
      XB(4,4)=(XB(4,1)**4.)*(4.*(E3**2.)-(E3**3.)-E3)/1000.
      IF(I.EQ.LIM)GO TO 1000
```

```
I=I+1
XA(2,5)=E2*(11.*V2-12.+E2*(V2-4.))
XA(2,5)=E2*(V2+4.+E2*(11.*V2+12.+XA(2,5)))
XA(2,5)=XA(2,5)/(F2*F2*F2*F2*F2)
XA(2,5)=XA(2,5)*.0001
XB(2,5)=XB(2,4)/18.
XA(3,5)=E1*(11.*V1-12.+E1*(V1-4.))
XA(3,5)=E1*(V1+4.+E1*(11.*V1+12.+XA(3,5)))
XA(3,5)=XA(3,5)/(F1*F1*F1*F1*F1)
XA(3,5)=XA(3,5)*.00001
XB(3,5)=XB(3,4)*.0125
XA(4,5)=XA(4,4)*.05
XB(4,5)=E3*(11.+E3*(E3-11.))
XB(4,5)=E3*(XB(4,5)-1.)*XB(4,1)*XB(4,1)
XB(4,5)=XB(4,5)*XB(4,1)*XB(4,1)*XB(4,1)*.0001
IF(I.EQ.LIM)GO TO 1000
I=I+1
XA(2,6)=E2*(-26.*V2+50.+E2*(-V2+5.))
XA(2,6)=E2*(-66.*V2+XA(2,6))
XA(2,6)=E2*(-26.*V2-50.+XA(2,6))
XA(2,6)=E2*(-V2-5.+XA(2,6))
XA(2,6)=XA(2,6)/(F2*F2*F2*F2*F2*F2)
XA(2,6)=XA(2,6)*.00001
XB(2,6)=XB(2,5)/18.
XA(3,6)=E1*(-26.*V1+50.+E1*(-V1+5.))
XA(3,6)=E1*(-66.*V1+XA(3,6))
XA(3,6)=E1*(-26.*V1-50.+XA(3,6))
XA(3,6)=E1*(-V1-5.+XA(3,6))
XA(3,6)=XA(3,6)/(F1*F1*F1*F1*F1*F1)
XA(3,6)=XA(3,6)*.000001
XB(3,6)=XB(3,5)*.0125
XA(4,6)=XA(4,5)*.05
XB(4,6)=E3*(-44.+E3*(26.-E3))
XB(4,6)=E3*(-1.+E3*(26.+XB(4,6)))
XB(4,6)=XB(4,6)*(XB(4,1)**6)*.00001
IF(I.EQ.LIM)GO TO 1000
```

```
1000 J=1
     AUXM=XA(2,1)+XB(2,1)
     XINF(2,1)=XA(2,1)/AUXM
     AUXN=XA(3,1)+XB(3,1)
     XINF(3,1)=XA(3,1)/AUXN
     AUXH=XA(4,1)+XB(4,1)
     XINF(4,1)=XA(4,1)/AUXH
     IF(J.EQ.LINF)RETURN
     J=J+1
     XINF(2,2)=(XA(2,2)*XB(2,1)-XA(2,1)*XB(2,2))/(AUXM*AUXM)
     XINF(3,2)=(XA(3,2)*XB(3,1)-XA(3,1)*XB(3,2))/(AUXN*AUXN)
     XINF(4,2)=(XA(4,2)*XB(4,1)-XA(4,1)*XB(4,2))/(AUXH*AUXH)
     IF(J.EQ.LINF)RETURN
     J=J+1
     XINF(2,3)=(XA(2,3)*XB(2,1)-XA(2,1)*XB(2,3))/AUXM
     XINF(2,3)=(XINF(2,3)-2.*(XA(2,2)+XB(2,2))*XINF(2,2))/AUXM
     XINF(3,3)=(XA(3,3)*XB(3,1)-XA(3,1)*XB(3,3))/AUXN
     XINF(3,3)=(XINF(3,3)-2.*(XA(3,2)+XB(3,2))*XINF(3,2))/AUXN
     XINF(4,3)=(XA(4,3)*XB(4,1)-XA(4,1)*XB(4,3))/AUXH
     XINF(4,3)=(XINF(4,3)-2.*(XA(4,2)+XB(4,2))*XINF(4,2))/AUXH
     IF(J.EQ.LINF)RETURN
     J=J+1
     RETURN
     END
```

```
      SUBROUTINE PAR2(AL,T,GK,GNA,XA,XB,XINF,QFS)

      IMPLICIT COMPLEX(O-Q)
      COMPLEX QFS(4,4,4)
      REAL XA(4,7),XB(4,7),XINF(4,7)
      FI=3.**(T/10.-.63)
      QFS(1,1,2)=CMPLX(-3.*GNA*(XINF(2,1)**2)*XINF(4,1),0.)
      QFS(1,1,3)=CMPLX(-4.*(XINF(3,1)**3.)*GK,0.)
      QFS(1,1,4)=CMPLX(-GNA*(XINF(2,1)**3.),0.)
      QFS(1,2,2)=CMPLX(-6.*GNA*XINF(2,1)*XINF(4,1)*(AL+115.),0.)
      QFS(1,2,4)=CMPLX(-3.*GNA*(XINF(2,1)**2.)*(AL+115.),0.)
      QFS(1,3,3)=CMPLX(-12.*(XINF(3,1)**2.)*(AL-12.)*GK,0.)
      DO 2 J=2,4
        QFS(J,1,1)=CMPLX(FI*(XA(J,3)-XINF(J,1)*(XA(J,3)+XB(J,3))),0.)
        QFS(J,1,J)=CMPLX(-FI*(XA(J,2)+XB(J,2)),0.)
2       QFS(J,J,1)=QFS(J,1,J)
      DO 1 J=2,4
        DO 1 K=1,J-1
1        QFS(1,J,K)=QFS(1,K,J)
      RETURN
      END
```

```
      SUBROUTINE PAR3(AL,T,GK,GNA,XA,XB,XINF,QFT)

      IMPLICIT COMPLEX(O,P,Q)
      COMPLEX QFT(4,4,4,4)
      REAL XA(4,7),XB(4,7),XINF(4,7)
      FI=3.**(T/10.-.63)
      QFT(1,1,2,2)=CMPLX(-6.*GNA*XINF(2,1)*XINF(4,1),0)
      QFT(1,1,2,4)=CMPLX(-3.*GNA*(XINF(2,1)**2.),0)
      QFT(1,1,3,3)=CMPLX(-12.*GK*(XINF(3,1)**2.),0)
      QFT(1,2,2,2)=CMPLX(-6.*GNA*XINF(4,1)*(AL+115.),0)
      QFT(1,2,2,4)=CMPLX(-6.*GNA*XINF(2,1)*(AL+115.),0)
      QFT(1,3,3,3)=CMPLX(-24.*GK*XINF(3,1)*(AL-12.),0)
      DO 1 J=2,4
        QFT(J,1,1,1)=CMPLX(FI*(XA(J,4)-XINF(J,1)*(XA(J,4)+XB(J,4))),0)
        QFT(J,1,1,J)=CMPLX(-FI*(XA(J,3)+XB(J,3)),0)
        QFT(J,1,J,1)=QFT(J,1,1,J)
1       QFT(J,J,1,1)=QFT(J,1,1,J)
       DO 2 J=1,4
        DO 2 K=1,4
         DO 2 L=1,4
         IF(L.LE.J.AND.J.LE.K)QFT(1,J,K,L)=QFT(1,L,J,K)
         IF(L.LE.K.AND.K.LE.J)QFT(1,J,K,L)=QFT(1,L,K,J)
         IF(J.LE.L.AND.L.LE.K)QFT(1,J,K,L)=QFT(1,J,L,K)
         IF(K.LE.L.AND.L.LE.J)QFT(1,J,K,L)=QFT(1,K,L,J)
         IF(K.LE.J.AND.J.LE.L)QFT(1,J,K,L)=QFT(1,K,J,L)
2     CONTINUE
      RETURN
      END
```

```
      SUBROUTINE PAR4(AL,T,GK,GNA,XA,XB,XINF,QFQ)

      IMPLICIT COMPLEX(O,P,Q)
      COMPLEX QFQ(4,4,4,4,4)
      REAL XA(4,7),XB(4,7),XINF(4,7)
      FI=3.**(T/10.-.63)
      VNA=AL+115.
      VK=AL-12.
        QFQ(1,1,2,2,2)=CMPLX(-6.*GNA*XINF(4,1),0.)
        QFQ(1,1,3,3,3)=CMPLX(-24.*GK*XINF(3,1),0.)
        QFQ(1,2,2,2,4)=CMPLX(-6.*GNA*VNA,0.)
        QFQ(1,3,3,3,3)=CMPLX(-24.*GK*VK,0.)
        DO 1 I=2,4
          AUX=(1.-XINF(I,1))*XA(I,5)-XINF(I,1)*XB(I,5)
          QFQ(I,1,1,1,1)=CMPLX(FI*AUX,0.)
          QFQ(I,1,1,1,I)=CMPLX(-FI*(XA(I,4)+XB(I,4)),0.)
          QFQ(I,1,1,I,1)=QFQ(I,1,1,1,I)
          QFQ(I,1,I,1,1)=QFQ(I,1,1,1,I)
1         QFQ(I,I,1,1,1)=QFQ(I,1,1,1,I)
        DO 2 I=2,3
          QFQ(1,I,1,I,I)=QFQ(1,1,I,I,I)
          QFQ(1,I,I,1,I)=QFQ(1,1,I,I,I)
2         QFQ(1,I,I,I,1)=QFQ(1,1,I,I,I)
        QFQ(1,2,2,4,2)=QFQ(1,2,2,2,4)
        QFQ(1,2,4,2,2)=QFQ(1,2,2,2,4)
        QFQ(1,4,2,2,2)=QFQ(1,2,2,2,4)
        P=CMPLX(-6.*GNA*XINF(2,1),0.)
        DO 3 I=1,4,3
          IF(I.EQ.1)J=4
          IF(I.EQ.4)J=1
          QFQ(1,2,2,I,J)=P
          QFQ(1,2,I,2,J)=P
          QFQ(1,2,I,J,2)=P
          QFQ(1,I,2,2,J)=P
          QFQ(1,I,2,J,2)=P
3         QFQ(1,I,J,2,2)=P
      RETURN
      END
```

```
      SUBROUTINE PAR5(AL,T,GK,GNA,XA,XB,XINF,QFC)

      IMPLICIT COMPLEX(O,P,Q)
      COMPLEX QFC(4,4,4,4,4,4)
      REAL XA(4,7),XB(4,7),XINF(4,7)
      FI=3.**(T/10.-.63)
      DO 1 I=2,4
        AUX=(1.-XINF(I,1))*XA(I,6)-XINF(I,1)*XB(I,6)
        QFC(I,1,1,1,1,1)=CMPLX(FI*AUX,0.)
        P=CMPLX(-FI*(XA(I,5)+XB(I,5)),0.)
        QFC(I,1,1,1,1,I)=P
        QFC(I,1,1,1,I,1)=P
        QFC(I,1,1,I,1,1)=P
        QFC(I,1,I,1,1,1)=P
1       QFC(I,I,1,1,1,1)=P
      P=CMPLX(-24.*GK,0.)
      QFC(1,1,3,3,3,3)=P
      QFC(1,3,1,3,3,3)=P
      QFC(1,3,3,1,3,3)=P
      QFC(1,3,3,3,1,3)=P
      QFC(1,3,3,3,3,1)=P
      P=CMPLX(-6.*GNA,0.)
      DO 2 I=1,4,3
        IF(I.EQ.1)J=4
        IF(I.EQ.4)J=1
        QFC(1,2,2,2,I,J)=P
        QFC(1,2,2,I,2,J)=P
        QFC(1,2,2,I,J,2)=P
        QFC(1,2,I,2,2,J)=P
        QFC(1,2,I,2,J,2)=P
        QFC(1,2,I,J,2,2)=P
        QFC(1,I,2,2,2,J)=P
        QFC(1,I,2,2,J,2)=P
        QFC(1,I,2,J,2,2)=P
2       QFC(1,I,J,2,2,2)=P
      RETURN
      END
```

```
      SUBROUTINE MIX11(AL,T,GK,GNA,XA,XB,XINF,QFM11)

      IMPLICIT COMPLEX(O,P,Q)
      COMPLEX QFM11(4,4)
      REAL XA(4,7),XB(4,7),XINF(4,7)
      FI=3.**(T/10.-.63)
      VNA=AL+115.
      VK=AL-12.
      DM1=3.*XINF(2,1)*XINF(2,1)*XINF(2,2)*XINF(4,1)
      DM1=DM1+(XINF(2,1)**3.)*XINF(4,2)
      DN1=4.*XINF(3,1)*XINF(3,1)*XINF(3,1)*XINF(3,2)
      QFM11(1,1)=CMPLX(-GNA*DM1-GK*DN1,0.)
      AUX=6.*XINF(2,1)*XINF(2,2)*XINF(4,1)
      AUX=VNA*(AUX+3.*XINF(2,1)*XINF(2,1)*XINF(4,2))
      QFM11(1,2)=CMPLX(-GNA*(AUX+3.*XINF(2,1)*XINF(2,1)*XINF(4,1)),0.)
      AUX=VK*12.*XINF(3,1)*XINF(3,1)*XINF(3,2)
      QFM11(1,3)=CMPLX(-GK*(AUX+4.*XINF(3,1)*XINF(3,1)*XINF(3,1)),0.)
      AUX=VNA*3.*XINF(2,1)*XINF(2,1)*XINF(2,2)
      QFM11(1,4)=CMPLX(-GNA*(AUX+XINF(2,1)*XINF(2,1)*XINF(2,1)),0.)
      DO 1 J=2,4
      QFM11(J,J)=CMPLX(-FI*(XA(J,2)+XB(J,2)),0.)
      OUX=CMPLX(FI*(XA(J,3)*(1.-XINF(J,1))-XB(J,3)*XINF(J,1)),0.)
1     QFM11(J,1)=QFM11(J,2)*CMPLX(XINF(J,2),0.)+OUX
      RETURN
      END
```

```
      SUBROUTINE MIX12(AL,T,GK,GNA,XA,XB,XINF,QFM12)

      IMPLICIT COMPLEX(O,P,Q)
      COMPLEX QFM12(4,4)
      REAL XA(4,7),XB(4,7),XINF(4,7)
      FI=3.**(T/10.-.63)
      VNA=AL+115.
      VK=AL-12.
      DM2=6.*XINF(2,1)*XINF(2,2)*XINF(2,2)*XINF(4,1)
      DM2=DM2+3.*XINF(2,1)*XINF(2,1)*XINF(2,3)*XINF(4,1)
      DM2=DM2+6.*XINF(2,1)*XINF(2,1)*XINF(2,2)*XINF(4,2)
      DM2=DM2+(XINF(2,1)**3.)*XINF(4,3)
      DN2=12.*XINF(3,1)*XINF(3,1)*XINF(3,2)*XINF(3,2)
      DN2=DN2+4.*(XINF(3,1)**3.)*XINF(3,3)
      QFM12(1,1)=CMPLX(-GNA*DM2-GK*DN2,0.)
      AUX=6.*(XINF(2,2)*XINF(2,2)+XINF(2,1)*XINF(2,3))*XINF(4,1)
      AUX=AUX+12.*XINF(2,1)*XINF(2,2)*XINF(4,2)
      AUX=VNA*(AUX+3.*XINF(2,1)*XINF(2,1)*XINF(4,3))
      AUX=AUX+12.*XINF(2,1)*XINF(2,2)*XINF(4,1)
      QFM12(1,2)=CMPLX(-GNA*(AUX+6.*XINF(2,1)*XINF(2,1)*XINF(4,2)),0.)
      AUX=VK*XINF(3,1)*(2.*XINF(3,2)*XINF(3,2)+XINF(3,1)*XINF(3,3))
       AUX=AUX+2.*XINF(3,1)*XINF(3,1)*XINF(3,2)
      QFM12(1,3)=CMPLX(-GK*12.*AUX,0.)
      AUX=2.*XINF(2,2)*XINF(2,2)+XINF(2,1)*XINF(2,3)
      AUX=VNA*AUX+2.*XINF(2,1)*XINF(2,2)
      QFM12(1,4)=CMPLX(-GNA*XINF(2,1)*3.*AUX,0.)
      DO 1 J=2,4
        QFM12(J,J)=CMPLX(-FI*(XA(J,3)+XB(J,3)),0.)
        AUX=-XINF(J,3)*(XA(J,2)+XB(J,2))
        AUX=AUX+(1.-XINF(J,1))*XA(J,4)
        AUX=FI*(AUX-XINF(J,1)*XB(J,4))
        QFM12(J,1)=CMPLX(2.*XINF(J,2),0.)*QFM12(J,J)
1       QFM12(J,1)=QFM12(J,1)+CMPLX(AUX,0.)
      RETURN
      END
```

```
      SUBROUTINE MIX21(AL,T,GK,GNA,XA,XB,XINF,QFM21)

      IMPLICIT COMPLEX(O,P,Q)
      COMPLEX QFM21(4,4,4)
      REAL XA(4,7),XB(4,7),XINF(4,7)
      FI=3.**(T/10.-.63)
      VNA=AL+115.
      VK=AL-12.
      AUX=2.*XINF(2,2)*XINF(4,1)+XINF(2,1)*XINF(4,2)
      QFM21(1,1,2)=CMPLX(-GNA*XINF(2,1)*3.*AUX,0.)
      QFM21(1,1,3)=CMPLX(-GK*12.*XINF(3,1)*XINF(3,1)*XINF(3,2),0.)
      QFM21(1,1,4)=CMPLX(-GNA*3.*XINF(2,1)*XINF(2,1)*XINF(2,2),0.)
      AUX=VNA*(XINF(2,2)*XINF(4,1)+XINF(2,1)*XINF(4,2))
      QFM21(1,2,2)=CMPLX(-GNA*6.*(AUX+XINF(2,1)*XINF(4,1)),0.)
      AUX=2.*XINF(2,2)*VNA+XINF(2,1)
      QFM21(1,2,4)=CMPLX(-GNA*3.*XINF(2,1)*AUX,0.)
      AUX=2.*XINF(3,2)*VK+XINF(3,1)
      QFM21(1,3,3)=CMPLX(-GK*12.*XINF(3,1)*AUX,0.)
       DO 1 J=2,4
        DO 1 K=1,J-1
    1 QFM21(1,J,K)=QFM21(1,K,J)
      DO 2 J=2,4
      OUX=CMPLX(FI*(XA(J,4)*(1.-XINF(J,1))-XB(J,4)*XINF(J,1)),0.)
      QFM21(J,1,J)=CMPLX(-FI*(XA(J,3)+XB(J,3)),0.)
      QFM21(J,1,1)=CMPLX(XINF(J,2),0.)*QFM21(J,1,J)+OUX
    2 QFM21(J,J,1)=QFM21(J,1,J)
      RETURN
      END
```

```
      SUBROUTINE MIX31(AL,T,GK,GNA,XA,XB,XINF,QFM31)

      IMPLICIT COMPLEX(O,P,Q)
      COMPLEX QFM31(4,4,4,4)
      REAL XA(4,7),XB(4,7),XINF(4,7)
      FI=3.**(T/10.-.63)
      VNA=AL+115.
      VK=AL-12.
      ZNA=-6.*GNA
      ZK=-24.*GK
        AUX=XINF(2,2)*XINF(4,1)+XINF(2,1)*XINF(4,2)
        QFM31(1,1,2,2)=CMPLX(ZNA*AUX,0.)
        QFM31(1,1,2,4)=CMPLX(ZNA*XINF(2,1)*XINF(4,1),0.)
        QFM31(1,1,3,3)=CMPLX(ZK*XINF(3,1)*XINF(3,2),0.)
        AUX=XINF(4,2)*VNA+XINF(4,1)
        QFM31(1,2,2,2)=CMPLX(ZNA*AUX,0.)
        AUX=XINF(2,2)*VNA+XINF(2,1)
        QFM31(1,2,2,4)=CMPLX(ZNA*AUX,0.)
        AUX=XINF(3,2)*VK+XINF(3,1)
        QFM31(1,3,3,3)=CMPLX(ZK*AUX,0.)
      DO 1 J=2,4
        QFM31(J,1,1,J)=CMPLX(-FI*(XA(J,4)+XB(J,4)),0.)
        OUX=CMPLX(FI*(XA(J,5)*(1.-XINF(J,1))-XB(J,5)*XINF(J,1)),0.)
        QFM31(J,1,1,1)=CMPLX(XINF(J,2),0.)*QFM31(J,1,1,J)+OUX
        QFM31(J,1,J,1)=QFM31(J,1,1,J)
1       QFM31(J,J,1,1)=QFM31(J,1,1,J)
       DO 2 J=1,4
        DO 2 K=1,4
         DO 2 L=1,4
         IF(L.LE.J.AND.J.LE.K)QFM31(1,J,K,L)=QFM31(1,L,J,K)
         IF(L.LE.K.AND.K.LE.J)QFM31(1,J,K,L)=QFM31(1,L,K,J)
         IF(J.LE.L.AND.L.LE.K)QFM31(1,J,K,L)=QFM31(1,J,L,K)
         IF(K.LE.L.AND.L.LE.J)QFM31(1,J,K,L)=QFM31(1,K,L,J)
         IF(K.LE.J.AND.J.LE.L)QFM31(1,J,K,L)=QFM31(1,K,J,L)
2     CONTINUE
      RETURN
      END
```

LINEAR

SUBROUTINES FOR MULTILINEAR ALGEBRA

SUBROUTINES DERIF I (I=1,2,3,4,5) EVALUATE A I-LINEAR MAP ON I VECTORS IN 4-DIMENSIONAL COMPLEX SPACE.

```
      SUBROUTINE DERIF1(Q1,PE,PS)

      IMPLICIT COMPLEX (O,P,Q)
      COMPLEX Q1(4,4),PE(4),PS(4)
      DO 1 I=1,4
      PS(I)=CMPLX(0.,0.)
      DO 1 J=1,4
    1 PS(I)=PS(I)+Q1(I,J)*PE(J)
      RETURN
      END
```

```
      SUBROUTINE DERIF2(QFS,QC,QD,PV)

      COMPLEX QFS(4,4,4),QC(4),QD(4),PV(4)
      DO 2 I=1,4
       PV(I)=CMPLX(0.,0.)
       DO 2 J=1,4
        DO 2 K=1,4
2     PV(I)=PV(I)+QFS(I,J,K)*QC(J)*QD(K)
      RETURN
      END
```

```
      SUBROUTINE DERIF3(QFT,QC,QD,QE,PS)

      COMPLEX QFT(4,4,4,4),QC(4),QD(4),QE(4),PS(4)
      DO 1 I=1,4
       PS(I)=CMPLX(0.,0.)
       DO 1 J=1,4
        DO 1 K=1,4
         DO 1 L=1,4
1     PS(I)=PS(I)+QFT(I,J,K,L)*QC(J)*QD(K)*QE(L)
      RETURN
      END
```

```
      SUBROUTINE DERIF4(QLN,P1,P2,P3,P4,OUT)

      IMPLICIT COMPLEX(O,P,Q)
      COMPLEX QLN(4,4,4,4,4)
      COMPLEX  P1(4),P2(4),P3(4),P4(4)
      COMPLEX OUT(4)
      DO 1 I=1,4
      OUT(I)=CMPLX(0.,0.)
      DO 1 J1=1,4
      DO 1 J2=1,4
      DO 1 J3=1,4
      DO 1 J4=1,4
1     OUT(I)=OUT(I)+QLN(I,J1,J2,J3,J4)*P1(J1)*P2(J2)*P3(J3)*P4(J4)
      RETURN
      END
```

```
      SUBROUTINE DERIF5(CL,P1,P2,P3,P4,P5,OUT)

      IMPLICIT COMPLEX(O,P,Q)
      COMPLEX CL(4,4,4,4,4,4)
      COMPLEX P1(4),P2(4),P3(4),P4(4),P5(4)
      COMPLEX OUT(4)
      DO 1 I=1,4
      OUT(I)=CMPLX(0.,0.)
      DO 1 J1=1,4
      DO 1 J2=1,4
      DO 1 J3=1,4
      DO 1 J4=1,4
      DO 1 J5=1,4
      QQ=P1(JI)*P2(J2)*P3(J3)*P4(J4)*P5(J5)
1     OUT(I)=OUT(I)+CL(I,J1,J2,J3,J4,J5)*QQ
      RETURN
      END

      SUBROUTINE CONDIC(PC,TETA,EIG,QV,QB,MER)

      IMPLICIT COMPLEX(O,P,Q)
      REAL EIG(2),WK(4)
      COMPLEX QV(4),QB(4),QH(3)
      COMPLEX QVV(4,1),QBB(4,1),PC(4,4),PP(4,4)
      MER=0
      DO 1 I=1,4
      QVV(I,1)=QV(I)
      DO 1 J=1,4
1     PP(I,J)=PC(I,J)
      CALL F04ADF(PP,4,QVV,4,4,1,QBB,4,WK,MER)
      IF(MER.NE.0)RETURN
      DO 2 I=1,2
2     QH(I)=-QBB(I,1)/CMPLX(EIG(I),0.-TETA)
      QH(3)=-QBB(3,1)*CMPLX(0.,.5/TETA)
      DO 3 J=1,4
      QB(J)=CMPLX(0.,0.)
      DO 3 I=1,3
3     QB(J)=QB(J)+QH(I)*PC(J,I)
      RETURN
      END
```

THIS SUBROUTINE SOLVES: $(A-i\theta_o I)QB = ((QV^* d)c - QV)$

FOR $QB^* d = 0$

MAIN PROGRAM

```
$RESET FREE SET AUTOBIND RESET LINEINFO SET ERRLIST
$BIND = FROM CATALOGO/=,*NAGF/=;
$RIND DADOS FROM NEW/DADOS;

      COMMON/ZERO/AL,T,GK,GNA
      REAL ERIN(6),EROUT(6)
      INTEGER NIN(4),NOUT(4),FLAG(6)
        INDIC=1
      WRITE(6,10)INDIC
        DO 1 J=1,4
        WRITE(6,20)J
        CALL DADOS(AL0,AL1,T0,T1,GK,GNA,INDIC)
            DO 3 K=1,4
              FLAG(K)=0
              ERIN(K)=10.**FLOAT(-J-2)
3             NIN(K)=J*5+15
              CALL NNACCI(AL0,AL1,T0,T1,ERIN,EROUT,NIN,NOUT,FLAG)
           WRITE(6,50)GK,GNA
           WRITE(6,100)AL0,AL1,AL
           WRITE(6,200)T0,T1,T
           WRITE(6,300)(ERIN(K),K=1,4),(EROUT(K),K=1,4)
           WRITE(6,400)(NIN(K),K=1,4),(NOUT(K),K=1,4)
        CALL ANTES(DAZ,DAL,DAZZ,DAZL,DALL,MER)
        IF(MER.EQ.0)GO TO 2
        WRITE(6,555)MER
        GO TO 1
2       WRITE(6,600)DAZ,DAL,MER
        WRITE(6,700)DAZZ,DAZL,DALL
        B=DAZL/SQRT(ABS(DAZZ*DALL))
        IF(DAZZ*DALL.GT.0)GO TO 4
        IPS=-1
        GO TO 1
4           IPS=1
1       WRITE(6,800)B,IPS
      STOP
10    FORMAT(1H1,5X,'BATO/',I3)
20    FORMAT(////I3,'-TH ATTEMPT')
50    FORMAT(////5X,'GK=',F6.1,'   GNA=',F6.1)
100   FORMAT(/3X,'AL0',G16.8,'  AL1',G16.8,'  AL',G16.8)
200   FORMAT(3X,'T0',G16.8,'  T1',G16.8,'  T',G16.8)
300   FORMAT(2X,'ERROS',/2X,'IN',4(G20.10,3X),/2X,'OUT',4(G20.10,3X)
400   FORMAT(/2X,'CONTADORES',/2X,'IN',4(3X,I5),/2X,'OUT',4(3X,I5))
500   FORMAT(/2X,'ERROR FLAGS',3(4X,I5))
555   FORMAT(//2X,'DANCOU TUDO NA SEGUNDA PARTE, MER=',I4)
600   FORMAT(///,2X,'DAZ=',G20.10,3X,'DAL=',G20.10,20X,'MER=',I4)
700   FORMAT(/,2X,'DAZZ=',G20.10,5X,'DAZL=',G20.10,5X,'DALL=',G20.10
800   FORMAT(/2X,'B=',G20.10,5X,'EPSILON=',I3)
        END
```

```
      SUBROUTINE DADOS(AL0,AL1,T0,T1,GK,GNA,IK)

C*      OBJECT CALLED NEW/DADOS
      IF(IK.EQ.10)GO TO 10
      IF(IK.EQ.9)GO TO 9
      IF(IK.EQ.8)GO TO 8
      IF(IK.EQ.7)GO TO 7
      IF(IK.EQ.6)GO TO 6
      IF(IK.EQ.5)GO TO 5
      IF(IK.EQ.4)GO TO 4
      IF(IK.EQ.3)GO TO 3
      IF(IK.EQ.2)GO TO 2
    1 AL0=-14.1
      AL1=-13.7
      T0=12.8
      T1=13.1
      GNA=85.
      GO TO 1000
    2 AL0=-14.8
      AL1=-14.5
      T0=18.
      T1=18.3
      GNA=90.
      GO TO 1000
    3 AL0=-15.2
      AL1=-15.
      T0=21.
      T1=21.5
      GNA=95.
      GO TO 1000
    4 AL0=-15.5
      AL1=-15.3
      T0=23.
      T1=23.5
      GNA=100.
      GO TO 1000
    5 AL0=-15.8
      AL1=-15.65
      T0=24.8
      T1=25.3
      GNA=105.
      GO TO 1000
    6 AL0=-16.1
      AL1=-15.8
      T0=26.3
      T1=26.7
      GNA=110.
      GO TO 1000
```

```
    7   AL0=-16.4
        AL1=-16.
        T0=27.6
        T1=27.9
        GNA=115.
        GO TO 1000
    8   AL0=-16.4
        AL1=-16.2
        T0=28.7
        T1=29.
        GNA=120.
        GO TO 1000
    9   AL0=-16.5
        AL1=-16.3
        T0=29.7
        T1=30.
        GNA=125.
        GO TO 1000
   10   AL0=-16.7
        AL1=-16.5
        T0=30.5
        T1=30.8
        GNA=130.
 1000   GK=36.
        RETURN
        END
```

REFERENCES

[1] Arvanitaki, A. (1939) Recherches sur la reponse oscillatoire locale de l'axone geant isolé de "Sepia" - Archs. int. Physiol. 49, 209-256.

[2] Best, E.N. (1979) Null space in the Hodgkin-Huxley equations. A critical test - Biophys. J. 27, 87-104.

[3] Carvalho, M.S.B. (1983) Dynamical Systems and game theory - Ph.D. thesis, Warwick.

[4] Chafee, N. (1968) The bifurcation of one or more closed orbit from an equilibrium point of an autonomous differential system - J. Diff. Eqs. 4, 661-679.

[5] Damon, J. The unfolding and determinacy theorems for subgroups of A and K - Arcata conference on singularities, to appear in A.M.S. Proc. Symp. Pure Maths.

[6] Golubitsky, M. and Langford, W.F. (1981) Classification and unfoldings of degenerate Hopf bifurcation germs - J. Diff. Eqs. 41, 375-415.

[7] Golubitsky, M. and Schaeffer, D. (1979) Imperfect bifurcation in the presence of symmetry - Comm. Math. Phys. 67, 205-232.

[8] Golubitsky, M. and Schaeffer, D. (1979) A theory for imperfect bifurcation via singularity theory - Comm. Pure Appl. Math. 32, 21-98.

[9] Golubitsky, M. and Schaeffer, D. Singularities and Groups in Bifurcation Theory (book) - in preparation.

[10] Griffith, J.S. (1971) Mathematical neurobiology-Academic Press, London.

[11] Guttman, R., Lewis, S. and Rinzel, J. (1980) Control of repetitive firing in squid axon membrane as a model for a neuroneoscillator - J. Physiol. 305, 377-395.

[12] Hassard, B.D. (1978) Bifurcation of periodic solutions of the Hodgkin-Huxley model for the squid giant axon, J. Theoret. Biol. 71, 401-420.

[13] Hassard, B.D., Kazarinoff, N.D. and Wan, Y-D (1981) Theory and applications of Hopf bifurcation - Cambridge University Press - Cambridge.

[14] Hodgkin, A.L. and Huxley, A.F. (1952) Currents carried by sodium and potassium ions through the membrane of the giant axon in Loligo - J. Physiol. 116, 449-472.

[15] Hodgkin, A.L. and Huxley, A.F. (1952) The components of membrane conductance in the giant axon of Loligo - J. Physiol. 116, 473-496.

[16] Hodgkin, A.L. and Huxley, A.F. (1952) The dual effect of membrane potential on sodium conductance in the giant axon of Loligo - J. Physiol. 116, 497-506.

[17] Hodgkin, A.L. and Huxley, A.F. (1952) A quantitative description of membrane current and its application to conduction and excitation in nerve - J. Physiol, 117, 500-544.

[18] Hodgkin, A.L., Huxley, A.F., and Katz, B. (1952) Measurement of Current-voltage relations in the membrane of the giant axon of Loligo - J. Physiol. 116, 424-448.

[19] Hodgkin, A.L., and Katz, B. (1952) The effects of sodium ions on the electrical activity of the giant axon of squid - J. Physiol. 108, 37-77.

[20] Hopf, E. (1942) Abzweigung einer periodischen Lösung von einer stationären Lösung eines Differentialsystems - Ber. Math. Kl. Säcks. Akad. Wiss. Leipzig 94, 3-22. English translation in [24].

[21] Jalife, J. and Antzelevitch, C. (1979) Phase resetting and Annihilation of Pacemaker Activity in Cardiae Tissue - Science 206, 695-697.

[22] Kelley, A. (1967) The stable, center-stable, center, center-unstable and unstable manifolds, J. Diff. Eqs. 3, 546-570.

[23] Luenberger, D.G. (1973) Introduction to linear and Non-linear programming - Addison Wesley.

[24] Marsden, J.E. and McGracken, M. (1976) The Hopf bifurcation and its applications - Appl. Math. Sciences vol 19 - Springer-Verlag - New York.

[25] Rinzel, J. and Miller, R.N. (1980) Numerical calculation of stable and unstable periodic solutions to the Hodgkin-Huxley equations - Math. Biosc. 49, 27-59.

[26] Schaeffer, D. (1980) Qualitative analysis of a model for boundary effects in the Taylor problem - Math. Proc. Camb. Phil. Soc. 87, 307-337.

[27] Schwarz, G. (1975) Smooth functions invariant under the action of a compact Lie group - Topology 14, 63-68.

[28] Zeeman, E.C. (1980) Bifurcation, catastrophe and turbulence, in "New directions in applied mathematics" Centenial conference, Case Western Reserve University - to appear in Springer Lecture Notes on mathematics.

[29] Hodgkin, A.L. (1938) The subthreshold potentials in a crustacean nerve fibre - Proc. Roy. Soc. London Ser. B - 842, vol 126, 87-121.